# INFORMATION TO USERS

This manuscript has been reproduced from the microfilm master. UMI films the text directly from the original or copy submitted. Thus, some thesis and dissertation copies are in typewriter face, while others may be from any type of computer printer.

**The quality of this reproduction is dependent upon the quality of the copy submitted.** Broken or indistinct print, colored or poor quality illustrations and photographs, print bleedthrough, substandard margins, and improper alignment can adversely affect reproduction.

In the unlikely event that the author did not send UMI a complete manuscript and there are missing pages, these will be noted. Also, if unauthorized copyright material had to be removed, a note will indicate the deletion.

Oversize materials (e.g., maps, drawings, charts) are reproduced by sectioning the original, beginning at the upper left-hand corner and continuing from left to right in equal sections with small overlaps.

Photographs included in the original manuscript have been reproduced xerographically in this copy. Higher quality 6" x 9" black and white photographic prints are available for any photographs or illustrations appearing in this copy for an additional charge. Contact UMI directly to order.

ProQuest Information and Learning
300 North Zeeb Road, Ann Arbor, MI 48106-1346 USA
800-521-0600

# INTRINSIC ELECTROPHYSIOLOGICAL PROPERTIES OF INTERSTITIAL CELLS OF CAJAL AND SMOOTH MUSCLE CELLS

by

JONATHAN CHEUK FUNG LEE, B.Sc

A Thesis

Submitted to the School of Graduate Studies

in Partial Fulfilment of the Requirements

for the Degree of Ph.D. in

Medical Sciences

McMaster University

DOCTORATE OF PHILOSOPHY (1999) McMASTER UNIVERSITY

MEDICAL SCIENCES Hamilton, Ontario

TITLE: Intrinsic electrophysiological properties of interstitial cells of cajal and smooth muscle cells

AUTHOR: Jonathan Cheuk Fung Lee, B.Sc. Honours (Memorial University)

SUPERVISOR: Dr. Jan D. Huizinga

NUMBER OF PAGES: xv, 214

# INTRINSIC ELECTROPHYSIOLOGICAL PROPERTIES OF INTERSTITIAL CELLS OF CAJAL AND SMOOTH MUSCLE CELLS

**Abstract**

The gastrointestinal (GI) tract is a hollow tubular organ that runs through the length of the central body. To move, mix, and compartmentalize ingesta through this tract, different patterns of motility are needed. This thesis is concerned with the myogenic control of motility through the pacemaker network of interstitial cells of Cajal (ICC) and the smooth muscle cells (SMC). Using patch clamp techniques, the electrophysiological properties of single ICC and SMC were examined. Previous research suggested the possibility of a specialized cell type generating the pacemaker slow wave potentials: the network of ICC that resides in the Auerbach's plexus region of the small intestine. An isolation procedure was developed and optimized to harvest single ICC that can survive short term culture and allow examination by patch clamp. Single cell patch clamp recordings demonstrated the presence of slow wave-like voltage oscillations driven by active current oscillations that match all properties seen in whole intestinal tissue slow waves. With different recording modes, whole cell currents, voltage and current oscillations were recorded from the same cell, showing that ICC are electrophysiologically unique and that the active inward current driving the slow wave-like oscillations are not voltage dependent. The isolated single ICC were demonstrated to have a specific tyrosine receptor marker protein for ICC, *Kit*, by selective RT-PCR amplification. The slow wave-like oscillations had a reversal potential consistent with a non-specific cation conductance. Although previous research had been done on single smooth muscle cells, there is currently no consensus on the cellular ionic currents present. In this thesis, analysis of different recordings demonstrated that there are at least

four main groups of SMCs with different whole cell current profiles. Different cellular ionic currents were found specifically in different groups, and can be confirmed by reconstructing single channel recordings. One cellular outward current was chosen for further investigation-a fast activating and inactivating transient outward current. This current was characterized by common protocols and with a novel ramp analysis. Characterization revealed two distinct transient outward currents with different kinetic properties. Finally, spontaneous transient outward currents (STOCs) have been recorded in 25% of smooth muscle cells, reflecting quantal $Ca^{2+}$ release from the intracellular stores to the plasmalemma calcium dependent potassium channels. Therefore, the study of STOCs gives direct information not only on the activities of intracellular $Ca^{2+}$ stores, but also on the kinetics of $Ca^{2+}$ release and reuptake in the microenvironment where STOCs originate. From these results, a simple model for GI motility was developed to account for the cellular interactions between nerve, ICC, and smooth muscle.

**Acknowledgments**

I wish to thank everyone who has helped me over the years. My deepest gratitudes to my parents and family who have supported my puckish endeavors and still strive to understand why I had taken a path less traveled (and took so long!). May I make you proud one day. Countless thanks to the friends who have stuck by me, even though they have graduated and/or moved on. May we all find what we are looking for.

**Abbreviations**

$[Ca^{2+}]_i$ - intracellular $Ca^{2+}$
$[Ca^{2+}]_o$ - extracellular $Ca^{2+}$
4-AP - 4-aminopyridine
AA - arachidonic acid
AM - amplitude modulation
ANS - autonomic nervous system
$Ba^{2+}$ - barium ions
BAPTA - 1,2-bis (2-aminophenoxy)ethane-N,N,N',N'-tetraacetic acid
$BK_{Ca}$ - large conductance $Ca^{2+}$-activated potassium channel
bp - base pairs (of DNA or RNA)
BSA - bovine serum albumin
$Ca^{2+}$ - calcium ion
cAMP - cyclic adenosine-monophosphate
CAN - Canada
CbTx - charibotoxin
CCK - cholecystokinin
$Cd^{2+}$ - cadmium ions
cDNA – cloned DNA sequence
CICR – $Ca^{2+}$-induced $Ca^{2+}$ release
ckit – *kit* cDNA sequence
$Cl^-$ - chloride ions
CNS – central nervous system
CPA – cyclopiazonic acid, specific inhibitor of SERCA pump
cpm – cycles per minute, frequency
$Cs^+$ - cesium ions
DAG – diacylglycerol
DMA – direct memory access, dedicated computer I/O
DMSO - dimethyl sulphoxide
DNA – deoxyribonucleic acid
DTT – dithiothreitol
EC coupling - excitation-contraction coupling
ECS - extracellular solution
EDTA - ethylenediaminetetraacetic acid
EGTA - ethylene glycol-O,O'-bis (2-aminoethyl)-N,N,N',N'-tetraacetic acid
EM - electron microscopy
ENS - enteric nervous system
ER - endoplasmic reticulum
FITC - fluorescein isothiocyanate
FM - frequency modulation
GI – gastrointestinal
GΩ - gigaohm, $10^9$ ohms
HEPES - N-(2-hydroxyethyl)-piperazine-N'-2-ethanesulfonic acid

HP – holding potential
Hz – hertz, frequency of 1 cycle per second
I/V – current/voltage relationship
$I_A$ - A-type current
IbTx – iberiotoxin
$I_{Ca}$ - $Ca^{2+}$ current
ICC – interstitial cells of Cajal
ICS – intracellular solution
$I_{dr}$ – delay rectifier-like current
IICR – $IP_3$-induced $Ca^{2+}$ release
$I_{K,Ca}$ – $Ca^{2+}$-activated potassium current
$IP_3$ – inositol 1,4,5-triphosphate
$IP_3R$ – $IP_3$ receptor
$I_{stoc}$ – spontaneous transient outward currents
$I_{to}$ – transient outward current
$I_{to,f}$ - fast transient outward current
$I_{to,s}$ – slow transient outward current
IV – current-voltage relationship
k - slope factor, relating to voltage activation or inactivation curves
$K_A$ - A-type potassium current
$K_{dr}$ – delayed rectifier potassium channel
Kit receptor – specific tyrosine kinase receptor for steel factor (also known as stem cell factor)
kV – kilovolt, $10^3$ volt
LCCB – L-type $Ca^{2+}$ channel blockers
M – molar concentration
mg – milligram, $10^{-3}$ gram
ml – millilitre, $10^{-3}$ litre
mM – millimolar concentration, $10^{-3}$ molar
$Mn^{2+}$ - manganese ion
MP – membrane potential
MRC – Medical Research Council (of Canada)
mRNA – messenger ribonucleic acid
mV – millivolt, $10^{-3}$ volt
MΩ - megaohm, $10^6$ ohms
nA – nanoamp, $10^{-9}$ amp
nM – nanomolar concentration, $10^{-9}$ molar
NO – nitric oxide
nS – nanoSeimens conductance, $10^{-9}$ Seimens
ON – Ontario
pA – picoamp, $10^{-12}$ amp
PCR – polymerase chain reaction technique, molecular biology DNA method
pF – picoFarad capacitance, $10^{-12}$ Farad
Ph.D. – Philosophiae Doctor

Pk – peak current
PKC – protein kinase C
$PLA_2$ – phospholipase $A_2$
PLC – phospholipase C
PMAC - Pharmaceutical Manufacters' Association of Canada
pS – picoSeimens conductance, $10^{-12}$ Seimens
r – correlation coefficient, associated with linear regression
rER – rough endoplasmic reticulum
RMP – resting membrane potential
RT-PCR - reverse transcriptase-polymerase chain reaction technique
RyR – ryanodine receptor
SER – sarcoplasmic/endoplasmic reticulum
sER – smooth endoplasmic reticulum
SERCA - sarcoplasmic/endoplasmic recticulum $Ca^{2+}$ ATPase
SMC – smooth muscle cell
SR – sarcoplasmic reticulum
SS – steady state current
STOC – spontaneous transient outward currents, outward current oscillations by $K_{Ca}$
tau – rate constant of exponential process
TEA – tetraethylammonium
µF – microFarad capacitance, $10^{-6}$ Farad
µM – micromolar concentration, $10^{-6}$ molar
µs – microsecond, $10^{-6}$ second
$V_h$ - half activation voltage
$V_s$ – slope factor
w/v – weight per volume concentration

## Table of Contents

## Table of Figures

# Chapter 1: Introduction

The gastrointestinal (GI) system needs to perform many different physiological functions in order to fulfill its primary goal of nutrient absorption and assimilation. Embedded within the GI system are the complex subsystems involved with absorption, secretion, immunology, regulation, organization, and movement (or motility). This thesis is concerned with non-neuronal aspects of GI motility, such as smooth muscle and interstitial cells of Cajal (ICC). Electrical phenomena in the gut have been observed mostly in intact tissue (Barajas-López *et al.* 1989; Serio *et al.* 1990). Using the versatile patch clamp techniques, electrophysiological activity can be examined at the cellular level, and down to the individual single channel protein level. To arrive at the point at which patch clamp could be done, several important milestones had to be accomplished. A brief background and technical considerations will be given before presenting the project objectives.

## 1.1 Background

### *1.1.1 Anatomy/Physiology of the Gastrointestinal System*

In vertebrates, the gastrointestinal tract has developed into a highly specialized series of tubular organs that process food, extract nutrients, and eliminates the residue. The arrangement is very similar to an assembly line where a product is worked upon progressively and sequentially. Just like the assembly line, there must be a "conveyor

belt" system to move the product (ingesta) to its next progressive stage. In the gut, the same "conveyor belt" type propulsion has additional duties of providing mixing and/or compartmentalization movements. Although there are distinct differences between different organs of the gastrointestinal tract, the basic structures that make up the GI tract remain similar.

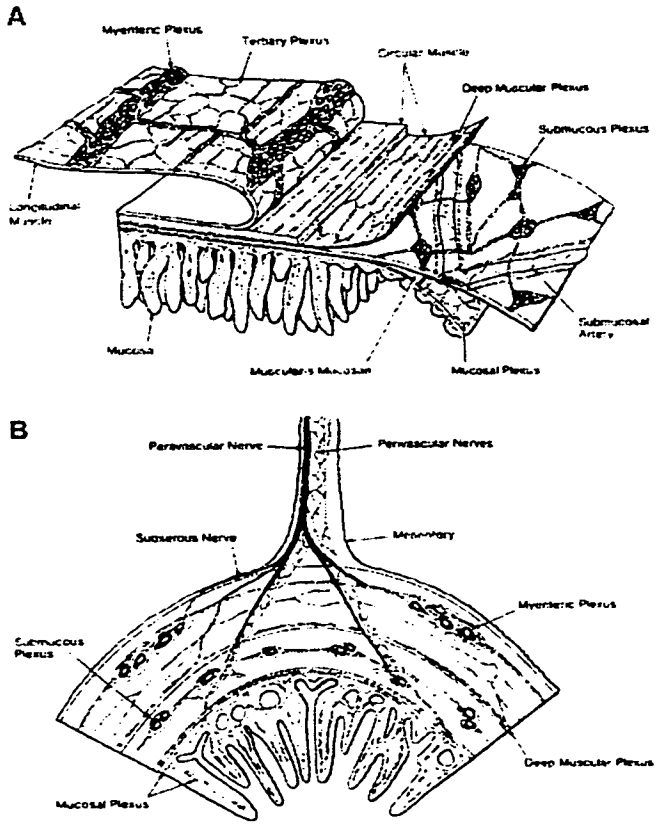


Figure 1-1 Diagram of the major layers of the guinea pig small intestine

A. as whole mounts B. as tranverse section. In the mouse small intestine, the two main ICC networks are found at the myenteric and deep muscular plexus regions. (Reproduced from Furness & Costa, 1980)

The GI tract is composed of distinct layers that wrap around the hollow lumen interior to form the walls of the tract. With sharp dissection, the individual layers can be separated as shown in figure 1 (Furness & Costa, 1980). Starting from the lumen interior, the mucosal layer wraps around the lumen and is followed by the submucosa, submucosal plexus region, circular muscle, myenteric plexus region, longitudinal muscle layer, and finally the serosa. Two major ganglionic plexuses are present in the GI tract. The myenteric plexus forms a continuous enteric nerve plexus that extends from the upper esophagus to the internal anal sphincter. In contrast, the submucosal plexus is prominent only in the small and large intestines. Within the circular muscle of human and mouse colon (Faussone Pellegrini & Cortesini, 1984; Faussone Pellegrini, 1985), there is a dense nerve plexus (deep muscular plexus in the small intestine, and submuscular plexus in the colon) that divides the circular muscle layer into inner and outer aspects. Although the enteric nervous system has been well established in regulating motility, other specialized tissues have been shown to be important also – the smooth muscle proper and the networks of interstitial cells of Cajal (ICC).

### *1.1.2 Smooth Muscle (Muscularis Externae)*

The external muscle layers of the gut are composed of a thin outer longitudinal layer (the fibres run parallel to the long axis of the gut) and a thick circular muscle layer (arranged circumferentially around the gut) (Gabella & Blundell, 1981). An unique feature of smooth muscle cells is that they have a high surface to volume ratio (~1.5 $\mu m^2/\mu m^3$), caused primarily by the presence of caveolae. The caveolae are often

intimately associated with endoplasmic reticulum (ER) at its base, possibly the functional equivalent of transverse (T) tubules in skeletal muscle. Smooth muscle cell membranes have electron dense structures called dense bands to which thin actin filaments are attached. Another important characteristic of smooth muscle is the low amounts of thick filaments and its disorganized arrangement within the cytoplasm (as compared with skeletal and cardiac muscle). Normally, close to 80% of the interior of a smooth muscle cell is occupied by dense bodies and contractile filaments with the remainder consisting of various organelles, including the nucleus, mitochondria, Golgi apparatus, lysosomes, smooth and rough endoplasmic reticulum. The smooth muscle ER has been shown to be involved with cyclic $Ca^{2+}$ storage and release (Katase & Tomita, 1971; Raeymaekers *et al.* 1977; Bitar *et al.* 1986). Smooth muscle cells make specialized cell to cell contacts in the form of intermediate junctions (dense band contacts), gap junctions, and/or close appositional contacts. Gap junction contacts appear to be abundant in circular muscle but are rare or absent in longitudinal muscle and taenia coli (Gabella, 1974; Fry *et al.* 1977; Mikkelsen *et al.* 1997).

### *1.1.3 Longitudinal Smooth Muscle*

Depending on the region and the species of gut examined, the longitudinal smooth muscle layer can have few nerve fibers within its thickness, or simply have a component of the myenteric plexus that lies against the inner surface of the longitudinal muscle (rabbit and guinea pig colon) (Furness & Costa, 1980; Costa & Brookes, 1994). In addition, the electrical coupling is poor (relative to circular muscle), mostly due to the

lack of low resistance pathways such as gap junctions. Therefore, the activation of longitudinal muscle will be more difficult than the circular muscle since nerves do not cover the longitudinal muscle as extensively as circular muscle. Therefore, excitatory events cannot propagate as effectively in longitudinal muscle as compared to circular muscle.

Makhlouf has proposed several major differences in signal transduction between the two smooth muscle layers (Makhlouf & Murthy, 1998). Briefly, excitation in longitudinal smooth muscle is more dependent on membrane depolarization leading to extracellular entry of activating $Ca^{2+}$. The activation of the contractile apparatus appears to be more dependent on CICR ($Ca^{2+}$ induced $Ca^{2+}$ release) and DAG activation of PKC. For the longitudinal muscle layer to operate as seen *in vivo*, it would be expected to have distinctly different electrical and pharmacological properties.

### *1.1.4 Circular Muscle*

The circular muscle layer(s) are different in many ways in comparison to longitudinal muscle. Overall, the circular layer is thicker and more densely innervated than longitudinal muscle. Although circular muscle appears well coupled via various contacts including gap junctions, the circular muscle layers are anatomically separated by connective tissue septa that run circumferentially, forming "rings" of circular muscle (Alvarez, 1948; Ward & Sanders, 1990; Rumessen & Thuneberg, 1991; Rumessen *et al.* 1993; Liu *et al.* 1997). Circular muscle bundles are arranged in stacking rings, or lamellae, especially over the small and large intestine. Between the inner and outer

circular muscle layers is a dense plexus of nerve fibers and various interstitial cells-the deep muscular plexus in the small intestine. This organization does not continue into the colon and surprisingly, Cajal (Cajal, 1911) himself noticed the deep muscular plexus and distinguished it from the submucosal plexus. Even with the physical separation from the annular arrangement of circular muscle, the circular muscle lamellae still represent a significant current sink. This suggests that purely electrical excitation through depolarizing currents would be difficult unless it can overcome the current sink. In terms of signal transduction, Makhlouf has proposed that circular muscle, in addition to phospholipase and CICR signaling, uses predominantly $IP_3$-dependent $Ca^{2+}$ signaling (Makhlouf & Murthy, 1998). There is currently no further data relating to the possibility of further differences within the smooth muscle layers. Collectively, the electrical and pharmacological properties are expected to be different between circular and longitudinal smooth muscle.

### *1.1.5 Functional Implications*

The degree of intercellular coupling is important in predicting its physiological function (Huizinga & Chow, 1988). Longitudinal muscle has poor intercellular coupling and probably performs more like a multi-unit organ where more regulatory systems are needed (i.e. nerves, etc.) to coordinate its function. Alternatively, circular smooth muscle has good intercellular coupling and would be expected to behave like a single unit organ, such as the heart where very few nerve fibers are found. Paradoxically, the longitudinal muscle layer is sparsely innervated (multi-unit organizations tend to have individual

innervation to each unit to effect fine control) while the circular muscle layer is well innervated (single unit organizations tend to be autonomous and do not require much innervation). It appears the key to this paradox may be what lies in between the smooth muscle layers and its innervation.

### *1.1.6 Interstitial Cells of Cajal (ICC)*

In 1893, Cajal was examining the rabbit small intestine when he came across a network of "interstitial neurons" overlying the Auerbach's plexus (Cajal, 1893). He later characterized these interstitial cells as "primitive accessory components that perhaps modify smooth muscle contraction, themselves subject to regulation from principal neurons" (Cajal, 1911). It was later found that many different cells in the interstitium (such as glial, Schwann, fibroblast-like cells, etc.) share similar appearances to Cajal's ambiguous descriptions. Thuneberg refined the definition of interstitial cells of Cajal to be **neither** neurons nor connective tissue cells (Thuneberg *et al.* 1983). The interstitial cells of Cajal demonstrates the following properties:

1. the presence of numerous mitochondria, which would suggest a very metabolically active cell
2. large bundles of intermediate filaments especially in the processes, and no detectable thick filaments
3. abundant surface caveolae and prominent smooth endoplasmic reticulum in special sub base arrangements, suggesting extensive intracellular $Ca^{2+}$ signaling/cycling
4. presence of a large ovoid nucleus with predominant heterochromatin and few rough

endoplasmic reticulum, features that distinguish them from fibroblasts. Also, there are no accumulations of synaptic vesicles nor of neurofilaments, which confirms that they are not neurons.

5. their proximity to other cells such that they form close appositional or gap junctional contacts with smooth muscle cells and other ICC, and synapse-like close appositional contacts between ICCs and tertiary nerve bundles.

Two groups of interstitial cells are of particular importance - those between the longitudinal and circular muscle layers (myenteric plexus region) and at the inner surface of the circular muscle. These ICC are intercalated between nerve fibers and smooth muscle cells, and make specific contacts with other ICC. Thus, as Cajal originally described, these ICC form a network within the neural plexuses and are the most densely innervated cell type within the gut. Collectively, the ultrastructural and histological descriptions of ICCs suggest they play a role in pacemaking (slow wave generation) and/or neurotransmission (Thuneberg *et al.* 1982; Thuneberg *et al.* 1983).

### *1.1.7 Regulation of GI Motility*

The regulation of the gut is a complex mixture of multiple control systems that show considerable regional differences. Generally, there are three main regulatory influences in the gut:

1. Neuronal - consisting of **Extrinsic** (CNS and post- & pre-ganglionic) and **Intrinsic** pathways (Enteric nervous system)
2. Hormonal/Humoral - from hormones like CCK to paracrine factors such as histamine

3. Intrinsic/Myogenic - includes properties from smooth muscle to ICC and/or other intrinsic intestinal cells such as neuroendocrine cells, immune cells, mast cells, etc.

In terms of motility, the end targets are the smooth muscle cells. In the gut, all the regulatory influences tend to be non-localized. Innervation into the smooth muscle layers does not have specific connections, such as neuromuscular junctions found in skeletal muscle. Nerve fibers project into the smooth muscle layers and release their neurotransmitters non-directionally from axonal varicosities. Hormonal/humoral influences depend on the vasculature and/or diffusion through the interstitium to its target. Intrinsic/myogenic influences rely mostly on the syncytial properties of smooth muscle. Thus, all regulatory factors are integrated at the most basic level of smooth muscle before the final resulting excitation to motility occurs.

Along with this integration of regulatory influences, there are two major electrical intrinsic activities all-pervading in the gut:

1. Action potentials - appears in two major forms, fast (spikes) or slow "myenteric" potentials. They can have a variety of different values of frequency, duration, and amplitude. Its distinguishing characteristics are its dependence on L-type $Ca^{2+}$ channel activity (L-type $Ca^{2+}$ channel blockers, LCCBs, abolish action potentials) and its occurrence depends on a voltage threshold.
2. Slow waves - a typical slow wave consists of the following parts: a rapid upstroke (depolarization), followed by a partial repolarization, a sustained plateau, and finally a complete repolarization to the resting membrane potential. This type of

spontaneous voltage oscillations is not susceptible to LCCBs nor have a dependence on a voltage threshold. The amplitude, duration and frequency of slow waves vary with location.

### *1.1.8 Origins of Intrinsic Electrical Activity in the Gut*

In cross-sectional preparations of the dog colon, slow waves can be seen with the largest amplitude at the submucosal border and propagates throughout the circular muscle (Smith *et al.* 1987; Sanders *et al.* 1990; Liu & Huizinga, 1994). Slow waves are rarely seen within the longitudinal muscle. If the circular muscle layer was separated, slow waves can only be seen in the circular muscle segment containing the submucosal border. Experiments like these clearly showed the submucosal border is the point of origin of slow waves in the colon. If the domineering slow waves are removed, slow "myenteric" action potentials can be seen to propagate from the myenteric plexus region (Smith *et al.* 1987; Jimenez *et al.* 1996). With the proper stimulus, such as 0.5 mM $Ba^{2+}$, both longitudinal and circular muscle can be induced to produce spiking activity (Liu & Huizinga, 1994). Therefore, smooth muscle itself is capable of generating action potentials with the right stimulus.

A Ph.D. student (Durdle *et al.* 1983) caught my supervisor's attention when he demonstrated that slow wave activity was localized within the thin strip of the submucosal border. This observation was later confirmed by (Smith *et al.* 1987; Serio *et al.* 1990) and was further shown to originate from the ICC network within the submucosal plexus (Berezin *et al.* 1988). Other studies with chemical ablation of ICC

(Osinski & Bass, 1995) and a mouse strain with mutations in a tyrosine kinase receptor, *kit* (Huizinga *et al.* 1995), both showed the absence of slow waves with the absence of ICC.

## 1.2 Working Hypothesis and Research Objectives

In the small intestine of the mouse, the pacemaker ICC network is located within the myenteric plexus region. Although there have been speculations about the specific roles of ICC (Huizinga, 1997; Sanders, 1996) a long term goal/objective has been the direct demonstration of slow wave generation from ICC themselves. Because of their extensive connections and contacts with other cell and possible contamination with humoral factors, this demonstration can only be done in isolated cells. Another issue of contention was the true nature of the slow wave. The slow wave recorded from tissue represents the summation of events from multiple sources such that the true "heart" of the slow wave has not been seen. This "pacemaker" component was never precisely known and was speculated to be a periodic activation of a non-specific ionic current (Barajas-López *et al.* 1989). Therefore the isolation and electrophysiological study of single ICC is important in resolving these issues.

## 1.3 Technical Considerations

Since there was no previous work done in this lab relating to my research, several major hurdles had to be overcome.

1. Establish a successful single cell isolation procedure that not only yields viable cells,

but also viable ICC that can be examined by patch clamp.

2. Establish a tissue culture system by which cells can be examined over a longer period of time. This was needed since there was no way of identifying/selecting for ICC other than morphology or electrophysiology. A short term culture system was needed to allow the isolated cells to recover to a state such that they can be recognized by their morphology. Selecting ICC by their unique electrophysiology was not possible yet since the identity of the cell could only be arrived at **after** successfully patching the cell. Considering that it was expected ICC would be low in number in comparison to smooth muscle cells, the probability of actually recording from an ICC would be low.
3. Establish criteria by which ICC can be identified in culture. Since ICC from adult mice were isolated before, it was hoped that they retained some aspects of their morphology in culture. Because other interstitial cells and smooth muscle cells in culture can assume similar morphologies to ICC, strict criteria for recognizing ICC from light microscopy must be established.
4. Establish a reliable electrophysiological recording system. Patch clamp recording represents the culmination of electrophysiological techniques, allowing electrical recording resolution down to the single channel level. An extended amount of time was needed to become familiarized with its intricacies and limitations. One of the most challenging technical problems was working with mouse cells from primary culture. Because of their small size (10-15 μm in diameter) and contractile nature, many problems had to be overcome before achieving a stable tight seal.

5. Establish protocols to record and test isolated cells. It was confirmed later that the pacemaker current was **not** voltage activated and therefore common voltage clamp protocols cannot be used. Another major problem was that ICC did not survive long under voltage clamp, and tended to become electrically quiescent with prolonged voltage clamp. Subsequent investigations were later performed mostly with current clamp.

Although a lot of effort was devoted to the study of ICC, the electrophysiological study of smooth muscle is also important. There is currently no consensus on the ionic currents present in GI smooth muscle and how these currents can account for the wide variety of action potentials and "resting" membrane potential changes believed to be generated by smooth muscle. The working hypothesis was that ICC and smooth muscle cells represent potential pacemakers for two different types of intrinsic activity seen throughout the gut - the slow wave and action potentials respectively. The method I chose was whole cell patch clamp recording to examine both ICC and smooth muscle cells as single isolated cells.

# Chapter 2: The generation of slow waves is an intrinsic property of interstitial cells of Cajal

Jonathan C.F. Lee, Lars Thuneberg*, Irene Berezin, and Jan D. Huizinga

Intestinal Disease Research Program, McMaster University, Hamilton, Ontario, Canada

1200 Main Street West, L8N 3Z5

* Visiting professor from the Panum Institute, University of Copenhagen, Copenhagen, Denmark.

Running title: Properties of dissociated ICC in culture

Correspondence address

Dr. Jan D. Huizinga
McMaster University
HSC-3N5C
1200 Main Street West
Hamilton, ON L8N 3Z5

Phone: (905) 525-9140 x22590
Fax: (905) 522-3454
E-mail: huizinga@mcmaster.ca

## 2.a Abstract

To reveal intrinsic properties of interstitial cells of Cajal (ICC), morphological and electrophysiological characteristics of isolated ICC from the adult mouse small intestine were investigated. All typical ultrastructural features of *in situ* ICC were evident in isolated ICC throughout the isolation procedure and short-term culture. Using the nystatin perforated patch clamp technique, ICC revealed spontaneous voltage oscillations that were not abolished by hyperpolarization or by L-type calcium channel blockers. This rhythmic activity occurred, at room temperature, at a frequency of 13.9 ± 11.2 cpm, with an amplitude of 13.4 ± 11.2 mV at membrane potentials from –20 to –70 mV. Smooth muscle cells from the same culture generated action potentials and only at membrane potentials above -35 mV. The action potentials were abolished by hyperpolarization as well as by L-type calcium channel blockers. In whole cell voltage clamp recordings, a large non-inactivating outward current from ICC was observed to be activated (5% threshold) at -49.6 mV with a half activation voltage ($V_h$) of -18.7 mV and slope factor ($V_s$) of 9.9 mV (n=6). In contrast, in smooth muscle cells, transient outward currents were prominent. In conclusion, generation of L-type calcium channel blocker insensitive slow waves in membrane potential is an unique intrinsic property of interstitial cells of Cajal.

Keywords: pacemaker, smooth muscle, interstitial cells of Cajal

Abbreviation: ICC: interstitial cell(s) of Cajal

## 2.1 Introduction

Since the hypothesis was formulated that interstitial cells of Cajal might be involved in intestinal pacemaker activity (13;40) the cellular basis for the generation of electrical activity in the intestine has been in question. Rhythmic electrical activity underlies peristaltic and segmental contractions of the small intestine (1;6;8;21;36). This electrical activity consists of slow waves in membrane potential with superimposed action potentials. The slow wave gives the phasic contractile activity its characteristic frequency (36). The slow wave synchronizes circular muscle contractions along the longitudinal axis of the organ (7;26) and directs the propagation of propulsive contractions in the aboral direction (8;9;33). In the mouse small intestine, slow wave generation has been linked to the presence of a layer of ICC within the myenteric plexus region (20;44). ICC are mesenchymal cells with as one of their distinguishing characteristics the presence of the *Kit* tyrosine kinase membrane receptor (23;44).

Action potentials have been shown to occur in isolated smooth muscle cells (2;3) and can be distinguished from slow wave activity. The action potentials have a fast rate of rise (~500 mV/s) and short duration (~1-50 ms). In tissue, they occur either superimposed on top of the slow wave plateau or they arise directly from depolarized resting membrane potentials such as in the longitudinal muscle of the colon (25). Slow waves have a much slower rate of rise (~100 mV/s) and a relatively long duration (~1-2 s). Pharmacologically, slow waves can be distinguished from action potentials by their insensitivity to L-type calcium channel blockers and voltage insensitivity (19;45). Slow wave activity is also sensitive to agents which interfere with normal intracellular calcium

cycling, such as cyclopiazonic acid (CPA, a specific SERCA pump inhibitor) (27). Micromolar concentrations of CPA potently inhibit the SR $Ca^{2+}$-ATPase pump. When stimulated, action potentials can have a longer duration and can have a slow wave-like appearance (17;31;32) but the activity remain susceptible to L-type calcium channel blockers.

In order to reveal the exact role of ICC in pacemaker function, one needs to know the properties of ICC themselves. This is difficult to achieve in intact tissue because ICC are electrically coupled to smooth muscle cells; hence, electrical activity observed in tissue is likely to be a contribution of many cells. Furthermore, ICC are densely innervated, which implies that activity observed in tissue may be influenced by neural activity. In order to discern the intrinsic properties of ICC, they must be isolated and studied *in vitro*. In a recent communication (37), isolated ICC of the mouse small intestine were shown to exhibit a rhythmic inward current, providing direct evidence that ICC generates pacemaker activity. ICC were identified by showing that they contained *kit* - mRNA. Several important questions are now to be answered. Are special isolation procedures needed to isolate ICC? Do ICC change during short-term culture? What are the characteristics of the "slow wave-like" activity associated with the observed current oscillations? Is the slow wave-like activity sensitive to L-type calcium channel blockers and/or voltage? How does spontaneous activity of isolated ICC compare to that of smooth muscle cells from the same culture? Since it is not practical to characterize each ICC by the presence of kit-mRNA, can they be identified by electrophysiological characteristics? It was the objective of this paper to answer these questions.

## 2.2 Methods

### *2.2.1 Dissociation of the Mouse Small Intestine*

ICC are found at two locations, the myenteric plexus and the deep muscular plexus. The ICC associated with the myenteric plexus are involved in the generation of slow waves in the small intestine (20;44) and cannot be directly dissected out in the mouse. Hence it is important to realize that the external muscle layers must be completely dispersed in order to reveal the myenteric layer which is buried within the muscle layers. In addition, there is substantial connective tissue, in the form of reticular, elastic and collagen fibers, between the main muscle layers (22).

### *2.2.2 Dissection of external musculature from small intestine*

Adult female mice (25-30 g) were sacrificed and a small intestine segment averaging 10 cm was removed proximal to the ileocaecal junction. The mesentery was carefully removed and the small intestine segment was placed in pre-equilibrated M199 media. Subsequently, the segment was opened flat by cutting along the mesenteric line. The segment was pinned flat with the mucosa facing the dissecting dish and the muscularis externae was carefully removed by sharp dissection. Cross-sectional examination of the strip of muscularis externae by electron microscopy revealed that the muscularis externae was separated along the deep muscular plexus region. The deep muscular nerve plexus was retained on the submucosal layer and was absent from the

stripped muscle tissue. The dissected muscularis externae was carefully cut into small pieces (~1-2 mm in length) in preparation for enzymatic dissociation.

### *2.2.3 Enzymatic Dissociation*

The muscularis externae was washed briefly in solution A before incubating at 37°C in solution A + 1mg/ml trypsin for 15 min first, then for 30 min with fresh solution or enzyme. The supernatant was carefully removed and replaced with solution B + 3mg/ml collagenase + 1mg/ml BSA for 15 min, and then for 20 min more with fresh enzyme. The cells were then mechanically dispersed by shaking. The cell suspension was layered on a 20% (w/v) Ficoll cushion and spun at 15 g for 15 min. The cell band located at the interface was transferred to a new container and resuspended with M199 media to the desired density. This cell suspension was plated into Falcon petri dishes with collagen coated coverslips glued to the bottoms. The cells were maintained in 5% $CO_2$/37°C until ready for use. Spontaneous voltage oscillations occurred in totally isolated ICC as well as in ICC connected to smooth muscle cells.

### *2.2.4 Important factors in the dissociation of ICC from the adult mouse small intestine*

Key factors found to be important in obtaining single ICC from the mouse small intestine were the duration of the dissociation process, avoidance of mechanical stress, optimal enzyme combinations and avoidance of overexposure to 0 $Ca^{2+}$ conditions.

### *2.2.5 Duration of dissociation*

In attempts to prevent high concentrations of enzymes, and thus minimize damage, slow digestion procedures were tried. However, it was observed that mouse ICC cannot tolerate long digestion times. This requirement prevented procedures involving slow digestion at low temperatures and prolonged digestions in weak enzyme solutions. The procedure was then modified to proceed as quickly as possible, from stripping the muscularis externae to final plating of the cells.

### *2.2.6 Mechanical stress.*

When preparations were over-stretched during cleaning and removing of the mucosa, the success for obtaining viable ICC was always low. The isolation procedure therefore calls for minimal mechanical force during the muscle preparation procedure. Experiments using trituration, even through large bore pipettes, greatly decreased the chances of success of the subsequent culture. Cells were dispersed using gentle shaking.

### *2.2.7 Enzyme combinations*

The various enzymes that were tried either alone or as enzyme combinations included collagenase, papain, elastase, hyaluronidase, pronase, trypsin, and DNAse. Two enzymes emerged as essential in dissociating the intact tissue: a strong proteolytic enzyme and collagenase. Generally, the two proteolytic enzymes that showed good activity as well as minimal damage to cells were papain with DTT and trypsin. Trypsin was later chosen because it does not require the addition of DTT. Single cells obtained

from the trypsin treatment were released easily from the extracellular matrix and recovered from the enzymatic isolation faster. Collagenase was found to be necessary in releasing the cells. No other extracellular matrix breaking enzyme (elastase, hyaluronidase, pronase) was as effective as collagenase in releasing cells from mouse small intestinal tissue. It was noted that although the enzyme digestion proceeded faster with both trypsin and collagenase together, the cells did not recover as well as cells derived from the current protocol. It was found that for prolonged incubations, the addition of a stabilizing proteinaceous substance, such as BSA, was needed to promote viability in dissociated cells. Unfortunately, the addition of BSA blunted or stopped proteolytic activity. Also, the trypsin lowered the collagenase activity, possibly because trypsin was digesting the collagenase enzyme. Both problems were avoided by separating the essential trypsin and collagenase digestion into two distinct steps.

An important observation was that trypsin and collagenase worked optimally under slightly different conditions. Trypsin worked best in 0 $Ca^{2+}$, pH neutral conditions , while collagenase worked better in the presence of $Ca^{2+}$ and slightly more acidic to pH neutral conditions (5). Better trypsin activity was achieved by providing a divalent ion to stabilize the trypsin protein; see also (35). Since the obvious divalent ion, calcium, was excluded to maintain 0 $Ca^{2+}$ conditions, the next effective divalent ion, $Mn^{2+}$, was chosen as the major divalent ion to replace $Ca^{2+}$ for membrane and trypsin stabilization. The trypsin containing solution (solution A) was deliberately adjusted to a physiologically neutral pH (~7.4). The collagenase enzyme was found to work best in higher $Ca^{2+}$. In order to balance matrix dissociation (which requires $Ca^{2+}$ restriction) with

good collagenase activity (which requires $Ca^{2+}$), the collagenase containing solution (solution B) has a compromise in $Ca^{2+}$ concentration (0.1 mM). BSA was added to the collagenase solution since it did not affect collagenase activity and helped in stabilizing dissociated cells.

### *2.2.8 Minimizing 0 $Ca^{2+}$ exposure*

For good dissociation of tissue, it was found that subjecting the tissue to 0 $Ca^{2+}$ conditions was unavoidable. Allowing even nominal $Ca^{2+}$ (~ 1-10 μM) did not result in good dispersion. Another strategy for successful cell harvest was developed on the finding that $Ca^{2+}$ levels overshoot once $Ca^{2+}$ restricted tissue is re-exposed to normal $Ca^{2+}$ levels (11). To prevent this possible $Ca^{2+}$ toxicity, the addition of $Mn^{2+}$, a $Ca^{2+}$ channel blocker (2 mM in solution A), was used to slow possible $Ca^{2+}$ release from the cell during $Ca^{2+}$ restriction and large $Ca^{2+}$ overshoot after reintroduction into normal $Ca^{2+}$ solutions. In addition, dissociated cells were exposed to a gradual transition of low $Ca^{2+}$ levels (0.1 mM $Ca^{2+}$ in solution B) before placing the cells in normal $Ca^{2+}$ levels (2.5 mM $Ca^{2+}$ in M199 media).

### *2.2.9 Light Microscopy*

Observation through a phase contrast microscope was done using a Nikon inverted microscope (Diaphot-TMD) with either 200X or 400X power. The images were captured either with a conventional optical camera, or with a Hitachi CAD solid state color video camera.

### *2.2.10 Electron Microscopy*

EM study of mouse small intestine culture was performed on the cultured cells grown on glass cover slips in small Falcon petri dishes (3 - 5 days in culture). The cells were fixed *in situ* with 2% glutaraldehyde in 0.05 M sodium cacodylate buffer (pH 7.4) containing 1.2 mM $CaCl_2$ for 40 min at room temperature. Following fixation, the samples were washed overnight in 0.1 M cacodylate buffer (pH 7.4), containing 1.2 mM $CaCl_2$, post-fixed with 1% OsO4 in 0.05 M sodium cacodylate buffer (pH 7.4) for 40 min at room temperature, stained with uranyl acetate for 30 min at room temperature, dehydrated in graded ethanol and embedded in Epon 812 using the "inverted capsule embedding technique" (16). All steps of post-fixation, dehydration and embedding were performed in the same petri dishes used for glutaraldehyde fixation. The separation of prepared cells from glass cover slips was performed after the blocks were hardened. To avoid damage to the cells, the hardened blocks were removed from glass cover slips with a sharp pull without applying dry ice or liquid nitrogen. Additionally some freshly isolated cells of mouse muscularis externa, were fixed 1 hour after enzymatic dissociation with the same fixative for 40 min, embedded in 2% small agar blocks, post-fixed with 1% $OsO_4$ in 0.05 M sodium cacodylate buffer (pH 7.4) for 40 min at room temperature, stained with uranyl acetate for 30 min at room temperature, dehydrated in graded ethanol and propylene oxide, and embedded in Spurr. The ultrastructure of ICC in culture and the ultrastructure of freshly dissociated ICC was compared with the ultrastructure of myenteric plexus ICC *in situ* (38), and the ultrastructure of ICC from dissected

muscularis externa strips used for enzymatic dissociation. The tissue strips were fixed, processed and embedded in Spurr in an identical manner. Thin sections were cut on a Reighert-Jung Ultracut E microtome, stained with lead citrate, and examined under a JEOL-1200 EX Biosystem transmission microscope at 80 kV.

### *2.2.11 Electrophysiology*

Cells were not used beyond 5 days post-isolation because it became nearly impossible to form a tight seal with a glass pipette without enzyme pre-treatment. The cells were continuously bathed with extracellular solution (ECS) at room temperature. Electrical activity in ICC was recorded using the nystatin perforated patch technique. Briefly, 2 μL of 3 mg/ml (w/v DMSO) nystatin stock was added to 1 ml intracellular solution (ICS) to achieve a final concentration of 2 μg/ml. Pipettes were made using a Sutter micropipette puller to typical access resistances of 3-5 MΩ. After filling the pipette tip with normal ICS by suction, the pipette was backfilled with nystatin containing ICS and inserted into the headstage of the patch amplifier (Axopatch 1B, Axon Instruments, Calif.). The pipette was quickly lowered onto the cell surface and suction was applied. Upon formation of a tight seal (~2-5 GΩ), the patch amplifier was switched over to current clamp. Holding potentials were chosen from observations of the membrane potential in current clamp. Results were acquired by Axotape (v1.2, Axon Instruments, Calif.) at 50 Hz using the TM-1 DMA interface.

### *2.2.12 Evaluation of Voltage Clamp*

Because of the branching nature of ICC and the smooth muscle cell contacts made by those branches, possible space clamp problems must be addressed. In voltage clamp recordings from ICC, passive currents generated by ohmic response to the voltage protocols were recorded as well as active currents from the cell membrane. It was assumed that the patch clamp amplifier delivered the voltage pulse to the pipette almost instantaneously (<10 μs). The start-to-steady state ohmic passive current response time was consistently measured to be <50 μs, adequate for whole cell voltage clamp. The active currents evoked by the voltage protocols appeared normal for whole cell currents. Series resistance compensation circuitry was not used because it created instability in the voltage clamp.

### *2.2.13 Solutions, with concentrations in mM*

ECS (Extracellular solution): NaCl 125.0, KCl 5.0, $MgCl_2$ 1.2, $NaH_2PO_4$ 1.2, Glucose 11.0, $NaHCO_3$ 4.0, $CaCl_2$ 2.0, HEPES 10.0, pH 7.35

ICS (Intracellular solution): K-Methanesulfonate 129.0, NaCl 5.0, MgAcetate 2.0, $CaCl_2$ 1.0, EGTA 11.0, HEPES 10.0, pH=7.25

Solution A: NaCl 134.0, KCl 3.0, Taurine 5.0, EDTA 5.0, $MnCl_2$ 2.0, HEPES 10.0, pH 7.40

Solution B: NaCl 133.0, KCl 3.0, Taurine 5.0, $CaCl_2$ 0.1, $MgCl_2$ 2.0, Glucose 10.0, HEPES 10.0, pH 7.35

M199 media: 1X M199 media, $NaHCO_3$ 26.0 mM, Glutamine 2.0, Penicillin 0.25 mg/ml, FBS 10%

Drugs: Verapamil and nifedipine were dissolved in 70% EtOH as $10^{-2}$ M stock solutions. CPA was dissolved in DMSO as $5X10^{-2}$ M stock solution

Chemicals and drugs were purchased from Sigma-Aldrich Canada Ltd.

Media was obtained from Gibco-Life Sciences Canada.

## 2.3 Results:

### *2.3.1 Identification of ICC using light microscopy:*

ICC and smooth muscle cells derived from the isolation procedure appeared as contracted spindles. After plating in M199 media, the cells became rounded into balls. ICC attained their typical structure after ~2-5 days in cell culture. Identification of ICC by phase contrast microscopy was based in part on their significantly darker appearance compared to other cells (Figure 1). In addition, the cell body was generally triangular or stellar in shape and not flattened like smooth muscle cells. Under high magnification (x400) a large nucleus with very little cytoplasm could be discriminated. From the cell body, there were generally 3-5 primary processes that branched into secondary and tertiary processes. These processes were distinct in that they were of medium thickness (~0.1 to 0.2 μm); not as thick as branching smooth muscle processes (0.4-0.8 μm) and not as thin as neuronal processes (<0.1 μm). The branching pattern was distinctively different from both branching smooth muscle and neurons. The ICC branches formed a diffuse network tree with two or three secondary branches from a primary branch and often made

contact with one or more smooth muscle cells. A distinguishing physical structure particular to ICC was the occurrence of large triangular bifurcations at junction points. These triangular bifurcations were sometimes quite large, up to almost one-fifth the size of a cell body. The ICC were frequently found in close proximity to smooth muscle cells with processes terminating onto smooth muscle cells. The connections to smooth muscle cells averaged 1-2 connections per smooth muscle cell. However, ICC were also observed as completely isolated cells.

### *2.3.2 Isolated ICC were capable of spontaneous contractions*

At temperatures between ~30 - 39° C, ICC demonstrated spontaneous rhythmic contractions with a frequency from 5 to 30 contractions per min as demonstrated previously (37), often with the processes contracting independently of the cell body. Sometimes second order branches were contracting apparently independent of the rest of the cell. Contractions were most often seen in those ICC that contacted smooth muscle. Contraction patterns ranged from seemingly disorganized contractions to synchronized contractions with adjacent smooth muscle cells.

### *2.3.3 Electron microscopy*

The dissected muscularis externa strips were composed of the longitudinal and inner circular muscle layer and the myenteric plexus. The mucosa, submucosa and innermost circular muscle layer including the deep muscular plexus were removed. Compared with ICC from intact tissue (Figure 2a), ICC from dissected tissues were

characterized by the high electron density of their nuclei and cytoplasm, there were no structural signs of prominent cell injury (Figure 2b). The ICC had all the major characteristics of intact tissue ICC: branched cell profiles, cytoplasm containing abundant ribosomes, mitochondria, thin and intermediate filaments, cisternae of endoplasmic reticulum, and numerous plasma membrane caveolae (Figure 2b). ICC formed close contacts with neighboring smooth muscle cells, and were surrounded by an extracellular matrix of collagen fibrils and elastic fibers (Figure 2b).

One hour after isolation, ICC and smooth muscle cells were round and free from extracellular matrix (Figure 3a). At this point, the freshly dissociated ICC had many ultrastructural features similar to ICC from dissected strips (Figures 3b,4a). Their cytoplasm was composed of thin and intermediate filaments, contained numerous mitochondria and free ribosomes (Figure 3a, inset), They had high electron dense nuclei and cytoplasm. Most of the plasma membrane caveolae were internalized, the possible result of cell contraction. The presence of caveolae in the dissociated ICC excluded the possibility that these rounded cells were glial cells, macrophages or fibroblasts. Freshly dispersed ICC lost cellular processes because of strong retraction into a ball shape (Figure 3).

Electron microscope analysis of isolated ICC after a few day in culture (1-4 days) showed structural modification (Figures 3b, 4a,b). Two concurrent changes took place: i. regression of the filament system and ii. proliferation of free ribosomes in the cytoplasm and dispersion of nuclear chromatin. After 1 day in culture ICC were still round, but no membrane-bounded spaces were seen in the cytoplasm (Figure 3b). Nuclei turned

euchromatic, and numerous ribosomes appeared free in the cytoplasm indicating an increase of synthetic activity. After 2-4 days in culture, ICC had started extended processes and contacts with smooth muscle cells, similarly seen by light microscopy (Figures 4a,b). Similar to day one, ICC after 2-4 days in culture displayed some characteristics of a synthetic phenotype. The ICC cytoplasm was dominated by a large number of free ribosomes, frequent slightly distended cisternae of rER and sER, numerous mitochondria and few lysosomes . The nuclei were completely euchromatic. Lipid droplets were seen in some ICC processes. After 1 day in culture and in later days, no prominent bundles of regularly organized intermediate filaments were seen in the perinuclear cytoplasm and in large processes of ICC (Figures 3b,4b). The intermediate filaments were evident only in terminal ICC processes. In contrast with ICC, the cytoplasm of most of smooth muscle cells after 4 days in culture was still dominated by numerous filaments (Figures 4a,b). After 1-4 days in culture ICC could be distinguished from other cells by the presence of surface caveolae, and occasional gap junctions between ICC and smooth muscle cells.

### *2.3.4 Electrophysiology*

ICC were patched at the cell body with the nystatin perforated patch technique. Cells were chosen when they conformed to ICC criteria (see above) *and* showed spontaneous contractile activity when examined at 37°C. The patch clamp experiments were carried out at room temperature since pipette contact to an ICC or smooth muscle cells would induce a strong contraction at 37°C. Some intestinal tissue becomes

electrically quiescent at room temperature (10). At room temperature, the mouse small intestine musculature generated slow wave activity (n=6), as measured in tissue with intracellular microelectrodes, with a frequency reduced from 35.1 ± 1.1 cpm to 16.2 ± 1.5 and membrane potential depolarized from -58.1 ± 1.5 to -47.6 ± 1.8 (figure 5).

### *2.3.5 Isolated ICC demonstrated spontaneous electrical activity.*

Single ICC demonstrated spontaneous oscillations in membrane potential at a frequency of 13.9 ± 11.2 cpm, with an amplitude of 13.4 ± 11.2 mV, duration 1.2 ± 0.6 s, and resting membrane potential -37.1 ± 7.9 mV at room temperature (n=9) (figure 6). The spontaneous voltage oscillations observed in all ICC were *resistant* to L-type $Ca^{2+}$ channel blockers, verapamil and D600 (up to 10 μM), nifedipine (up to 5 μM), and diltiazem (up to 5 μM) (figure 6). Unlike action potentials in smooth muscle, the voltage oscillations from ICC could not be evoked by either depolarizing current injection pulses or by anodal break (see below).

### *2.3.6 Spontaneous electrical activity in smooth muscle cells*

Spontaneous voltage oscillations were also recorded from smooth muscle cells from the same cultures (figure 7). These oscillations had the properties of smooth muscle action potentials at a frequency of 103.5 ± 30.4 cpm, an amplitude of 20.2 ± 3.6 mV, a maximum rate of rise of 364.8 ± 119.1 mV/s, and a duration of 0.38 ± 0.08 s. The action potentials were abolished by L-type calcium channel blockers, such as diltiazem (1 μM,

n=3) (figure 7). Examination of individual spiking activity revealed prepotential depolarization before the upstroke.

### *2.3.7 The effect of forskolin on spontaneous oscillations in ICC*

In some ICC, spontaneous voltage oscillations occurred of variable amplitude and irregular frequency. In tissue, as recorded with intracellular microelectrodes, forskolin hyperpolarizes the cell membrane, reduces membrane noise and increases the slow wave amplitude (Malysz and Huizinga, unpublished). For this reason, forskolin was added to ICC with irregular activity. The addition of forskolin (1 μM) or 8-Br-cAMP (1 μM) produced a hyperpolarization of the cell membrane and a marked reduction in membrane noise (figure 8). Forskolin (1 μM) produced hyperpolarizations of -18.3 ± 7.4 mV, the membrane potential changed from -30.8 ± 4.9 mV to -55.5 ± 16.2 mV. The maximum rate of rise of the voltage oscillations increased from 98.3 ± 75.6 mV/s to 200.7 ± 175.0 mV/s along with an amplitude increase from 12.9 ± 4.1 mV to 19.7 ± 7.6 mV (n=4). The frequency of the oscillations (> 5 mV) was 8.5 ± 5.6 cpm.

### *2.3.8 The effects of CPA*

In whole tissue (27;28) cyclopiazonic acid (CPA), a specific inhibitor of the sarcoplasmic reticulum $Ca^{2+}$-ATPase pump, caused a very characteristic abolishment of slow wave activity in a reversible manner. The inhibition can be preceded by a pattern where some slow waves are increased in duration (27). The effects of CPA were similar in isolated ICC (n=3) (figure 9). The membrane potential depolarized slightly (+ 5mV).

The spontaneous oscillations returned upon washout of CPA albeit with altered frequency and amplitude, similar to washout effects in tissue.

### *2.3.9 Voltage insensitivity of spontaneous activity present in ICC*

In the presence of 1μM forskolin to promote regular stable oscillations and typical resting membrane potentials of -50 to -60 mV, depolarizing or hyperpolarizing current was injected into isolated ICC. Under such conditions, voltage oscillations occurred between -70 and –30 mV without significant changes in frequency. In contrast, spontaneous action potentials in smooth muscle cells were voltage sensitive. With action potentials present at –40 mV, they were abolished by hyperpolarizing current injection to -60 mV (figure 10). The inhibition by hyperpolarization was readily reversible, once the hyperpolarizing current was switched off, the spontaneous action potentials reappeared (n=3). Studied in another way, for smooth muscle cells, action potentials were activated at a sharp voltage threshold as illustrated in figure 11. In smooth muscle cells with spontaneous action potential activity, hyperpolarizing current was injected to bring the membrane potential to ~ -60 mV and the cell into quiescence. Applying depolarizing (20 mV) square current pulses at 1 Hz did not evoke action potential activity at this point. The changes in membrane potential reflect purely passive responses to the square current pulses. The hyperpolarizing current injection was slowly reduced until action potential activity could be seen *only* at the tops of the depolarizing square current pulses. Note that action potentials were only evoked when the tops of the square current pulses had reached the voltage threshold for action potential activation (~ -37 mV). Therefore, action

potentials can be made to appear as bursts that are limited exclusively by the duration of the depolarizing pulses. Also, while there was action potential activity occurring at the tops of the square pulses, the resting membrane potential was still in the inexcitable voltage range (~ -55 mV).

### *2.3.10 Profiles of whole cell currents in ICC and smooth muscle cells*

Whole cell patch clamp was done with as only objective to investigate if whole cell current profiles could distinguish ICC from smooth muscle cells. We have shown previously that ICC produce spontaneous inward currents that are not activated by voltage related to the spontaneous depolarizations (37). We now show that voltage steps from -70 mV to +30 mV for 500 ms evoked whole cell currents as shown in figure 12. The whole cell currents from ICC were predominantly outward (n=7). The outward currents had a fast activation before proceeding to a steady state. The large tails confirmed the dominance of the outward currents to the total whole cell currents. The whole cell currents were not blocked by nifedipine (5 μM) nor by TEA (5 mM). The currents showed slight inactivation, especially at depolarized ranges (>+20 mV). Current-voltage (I/V) curves showed a sharp voltage activation takeoff at -40 mV. The slight voltage dependent inactivation was confirmed by comparing the currents at a prepulse of -30 mV to a prepulse of -100 mV (n=3). Currents elicited with the -30 mV prepulse were smaller in amplitude only in more depolarized ranges, as shown in the IV relationship.

For smooth muscle cells, the currents elicited by prepulses of -100 mV and -30 mV were distinctly different (figure 13). One of the prominent features of smooth muscle

cells was the presence of transient outward currents that undergo voltage dependent inactivation. Currents elicited with the -30 mV prepulse were missing the transient outward currents. Another prominent feature of smooth muscle cells was the presence of spontaneous transient outward currents (STOCs) in response to depolarizing voltages. The IV relationship shows the decrease in currents with the -30 mV prepulse in comparison with the -100 mV prepulse from the prepulse inhibition of the transient outward currents. The outward currents from smooth muscle cells were sensitive to block from both TEA and L-type $Ca^{2+}$ channel blockers (not shown).

### *2.3.11 Voltage activation of outward currents in ICC and smooth muscle cells*

Normalizing the tail currents occurring after the end of the voltage steps from the voltage protocol, revealed the relative conductances present over the voltage steps for the ICC outward currents. The activation of the outward current followed a Boltzman distribution and was fitted by the least squares method (figure 14). The half activation voltage ($V_h$) was estimated to be at -18.7 mV with a slope factor ($V_s$) of 9.9 mV. Since the Boltzman relationship was asymptotic at both ends, the threshold and steady state voltages were arbitrary determined to be at 5% and 95% of activated relative currents/conductances respectively. The threshold for activation (5%) was calculated to be -49.6 mV and the voltage at which the outward conductance goes to the chord conductance was at +14.2 mV (n=6).

For smooth muscle cells, the tail currents deactivated too quickly to be accurately measured. Instead, peak outward currents from each voltage step were normalized to be a

conductance. The plot of normalized conductances over the voltage range yielded the voltage activation curve with $V_h$ of +2.3 mV and $V_s$ of 16.4 mV. The threshold for activation (5%) was -49.0 mV and the chord conductance voltage was 50.6 mV. Thus, the peak outward currents for smooth muscle cells activates and goes to chord conductance at a different range than the outward currents for ICC.

## 2.4 Discussion:

### *2.4.1 Main findings*

An isolation procedure that avoided stretch could isolate ICC that maintained all ultrastructural characteristics, from freshly isolated, when cells were rounded, into short term culture. In addition, ICC obtained characteristics of a synthetic phenotype. Comparing ICC with smooth muscle cells, spontaneous electrical activity as well as whole cell current profiles were distinctly different. The slow wave-like activity that was observed in a single isolated ICC only had many characteristics of slow waves as observed in tissue.

### *2.4.2 Isolation and identification of ICC*

A cell dissociation protocol for obtaining long term viable single cells was developed after several key observations were made. These included optimizations for enzymatic digestion, proper exposure to 0 $Ca^{2+}$ conditions, and the importance of preventing $Ca^{2+}$ overload after return from 0 $Ca^{2+}$ conditions. The dissociated cells were allowed to recover in short term culture, in which ICC regained their *in situ* morphology.

Under phase contrast microscopy, ICC were found to have distinctive characteristics. Developing ICC were considerably more phase dark than other cells in culture, had triangular or stellar cell bodies with a large nucleus, extending 3-5 cell processes of 0.1 to 0.2 μm thickness. From these primary branches, two or three secondary branches grew further and made contact with one or more smooth muscle cells with distinctive triangular bifurcations at each division of the branches. At physiological temperatures (~35-37°C), isolated ICC were spontaneously contractile, often with regular rhythmicity. After establishing itself in culture, ICC were found in isolation, in contact with other ICC or with smooth muscle cells.

The smooth muscle cells could also form processes. Under the light microscope, it was possible to discriminate between branching smooth muscle cells and ICC. The smooth muscle cell body was never triangular or stellar in shape, adopting either a spindle or flattened shape. The branches from smooth muscle cells were thicker than those of ICC, did not extend extensively and did not bifurcate.

The interstitial cells of Cajal were difficult to isolate from whole tissue. *In situ*, these cells are intimately associated with several cell types such as smooth muscle cells and nerve fasciculi. Furthermore, ICC are embedded in a dense matrix of connective tissue, in particular collagen fibres in the adult intestine (12). In addition, mechanical stress, especially stretching stress on the tissue while dissecting, is detrimental (39). This is not surprising considering the extensive branching pattern of the ICC and the delicacy of the branches seen in whole tissue. The isolation procedure produced isolated ICC, which were rounded up. These rounded up ICC needed 2-3 days in short term culture in

order to be identifiable with light microscopy. The rounding up of dissociated cells is not uncommon; most dissociation techniques including trypsinization, alter the appearance of isolated cells (14).

Isolated ICC in short term culture were observed to contact each other as well as smooth muscle cells. This suggests that there may be a target-specific interaction that promotes the development of "mature" ICC. The presence of the Kit receptor on ICC, shown by other studies (20;23;43), suggests that specific differentiation signals are needed for the proper development of "mature" ICC. In short term culture of adult ICC however, the addition of Steel factor (a.k.a. stem cell factor) to the culture medium, did not affect ICC (Farraway and Huizinga, unpublished).

ICC changed from round cells just after isolation, to branching cells that contacted each other and smooth muscle cells. Although gap junction contact between ICC from the Auerbach's plexus region and smooth muscle cells is rare *in situ*, they were observed in culture. All prominent ultrastructural features were preserved throughout the isolation procedure and short-term culture. However, ultrastructural changes did occur. In particular the prominent appearance of a large number of free ribosomes, and distended cisternae of rER and sER with euchromatic nuclei. To accommodate for this, contractile filaments were moved to the periphery of the cell body. The prominence and central location of contractile filaments in cell processes was not affected. These ultrastructural changes reflect synthetic activity, which will in large part be reflective of the restoration of the ICC processes.

Because of our strict criteria to identify ICC, there were likely many more ICC in culture than positively identified. When we followed ICC in short term culture using time lapse video recording, we saw ICC change to different morphologies over time (24). It is therefore important to identify ICC by other criteria such as the presence of the Kit receptor. Kit positive cells were identified in a recently published isolation procedure (42) but these cells were not positively identified as ICC. The use of an antibody against an extracellular domain of this receptor on freshly isolated cells is very challenging because of the high chance this receptor is altered by the trypsin treatment. Our attempts to do this resulted in macrophages being "stained" positive for Kit, likely because of non-specific uptake (Farraway and Huizinga, unpublished results). Hence, immunohistochemical staining of freshly isolated cells using Kit antibodies could not be used to unequivocally identify ICC.

### *2.4.3 Electrophysiology of ICC*

Isolated ICC generated voltage oscillations in a dramatic rhythmic fashion, showing a high similarity with tissue slow waves. In the presence of forskolin, the slow waves rose sharply from a resting membrane potential of ~ -60 mV with a shape that was identical to that of tissue slow waves. CPA abolished the voltage oscillations within 10 min. Prior to abolishment, it caused an increase in duration of some voltage oscillations, similar to the effect of CPA on slow waves in tissue (27;30). CPA inhibits calcium cycling in the sarcoplasmic reticulum and the intracellular calcium cycling may be an essential step in the triggering of the rhythmic voltage oscillations (27).

It is controversial whether or not the intestinal pacemaker activity is driven by voltage activated currents similar to the cardiac pacemaker. The alternative is that the slow waves are driven by currents initiated by intracellular metabolic events. The voltage oscillations in the ICC occurred under current clamp and could not be triggered by depolarization. Furthermore, they occurred at a range of voltages, from -20 mV to -70 mV and were influenced by changes in intracellular $Ca^{2+}$ store status. Hence this study is consistent with the hypothesis that ICC can generate metabolically driven voltage oscillations. This is consistent with the observations that slow waves in tissue are relatively insensitive to voltage and are driven by metabolically sensitive events (10;18;27).

The activity seen in isolated ICC was irregular at times. This variability probably arose from instability of the pacemaker system in single cells. Similar observations have been made in isolated heart pacemaker cells (4;15;41) in which the pacemaker action potentials appear different from the whole heart action potentials and increases in stability of pacemaker action potentials can be seen to correlate with increases in the number of cells in a cluster (34). Establishment of cell-to-cell contact and electrical coupling is important for frequency stability (4). Similarly, ICC in tissue are extensively coupled among themselves in a network structure coupled by gap junctions. Therefore, the instability and variability seen in isolated ICC can be explained by the fact that they have little or no cell-to-cell communication by which to enhance their intrinsic pacemaker activity. ICC in tissue are always coupled to each other by gap junctions, whereas their coupling to smooth muscle cells is usually devoid of gap junctions but

consisting of close apposition contacts. The gap junction contacts between ICC might be essential for metabolic coupling to synchronize metabolic products driving the slow wave activity.

### *2.4.4 Electrophysiology of ICC versus smooth muscle cells.*

Electrophysiologically, the ICC were shown to be distinct from smooth muscle cells. Whole cell current profiles from these two cell types, ICC and smooth muscle cells, were found to be completely different. ICC had large outward currents that showed little to no inactivation. Smooth muscle cells on the other hand, had smaller but distinctive outward currents that included transient outward currents. Superimposed on the smooth muscle cell outward currents, spontaneous transient outward currents occurred from periodic activation of $I_{K,Ca}$. The transient outward currents showed strong voltage-dependent inactivation. Current versus voltage plots of peak currents at prepulse -100 mV versus -30 mV showed different voltage takeoffs since the transient outward current activated at a more hyperpolarized range (~-50mV) in contrast to the non-inactivating outward current takeoff (~-20mV). In comparison, ICC currents were larger in amplitude than smooth muscle cell currents, showed a lesser degree of conductance noise, and showed only slight voltage dependent inactivation.

Both ICC and smooth muscle cells were capable of generating spontaneous rhythmic oscillations. Spontaneous membrane potential oscillations from ICC were distinct from the characteristic action potentials generated by smooth muscle cells. The

action potentials showed a relatively fast rate of rise and were sensitive to L-type $Ca^{2+}$ channel blockers and hyperpolarization, noted before in other smooth muscle cells (2;32).

The experiment shown in figure 11 illustrates a model of tissue slow wave activity in isolated smooth muscle cells. As mentioned previously, the resting membrane potential is in the non-excitable voltage range while action potentials occur on the tops of depolarizing pulses. The occurrence of action potentials can be controlled simply by controlling the duration of the depolarizing pulses that surpass the voltage threshold for action potential generation.

In summary, ICC from the small intestine can be isolated, cultured, and identified successfully by morphological criteria and electrophysiological characterization. The spontaneous membrane potential oscillations observed in ICC are insensitive to L-type calcium channel blockers, are not abolished by hyperpolarization to ~ -70 mV, and have a frequency similar to that of slow waves in tissue at room temperature. These data together with those from a recent paper (37) provide the strongest evidence to date that pacemaker activity (i.e. the L-type calcium channel insensitive part of intestinal slow waves) is an intrinsic property of the ICC.

## 2.5 Acknowledgments

JL was supported by a PMAC/MRC scholarship. JDH was supported by a MRC Scientist award. Funding was provided by the MRC of Canada. We gratefully acknowledge the collaboration with Laura Farraway and John Malysz. Image analysis equipment was purchased with the support of Dr. M.O. Christen and Solvay France.

## 2.6 References


1. **Alvarez, W.C. and L.J. Mahoney.** Action current in stomach and intestine. *Am.J.Physiol.* 58: 476-493, 1922.
2. **Benham, C.D., T.B. Bolton, J.S. Denbigh, and R.J. Lang.** Inward rectification in freshly isolated single smooth muscle cells of the rabbit jejunum. *J.Physiol.(Lond)* 383: 461-476, 1987.
3. **Bolton, T.B., R.J. Lang, T. Takewaki, and C.D. Benham.** Patch and whole-cell voltage-clamp studies on single smooth muscle cells. *J.Cardiovasc.Pharmacol.* 8 Suppl 8: S20-S241986.
4. **Bouman, L.N. and H.J. Jongsma.** The sinoatrial node: structure, inhomogeneity and intercellular interaction. In: *Pacemaker Activity and Intercellular Communication*, edited by J.D. Huizinga. CRC Press: Baton Rouge, 1995, p. 37-50.
5. **Boyer, P.D.** *Hydrolysis: peptide bonds.* NY: Academic Press, 1971.
6. **Bulbring, E.** Electrical activity in intestinal smooth muscle. *Physiol.Rev.* 42: 160-178, 1962.
7. **Conklin, J.L. and C. Du.** Pathways of slow-wave propagation in proximal colon of cats. *Am.J.Physiol.* 258: G894-G9031990.
8. **Der-Silaphet, T., J. Malysz, A.L. Arsenault, S. Hagel, and J.D. Huizinga.** Interstitial cells of Cajal direct normal propulsive contractile activity in the small intestine. *Gastroenterology* 114: 724-736, 1998.
9. **Diamant, N.E. and A. Bortoff.** Nature of the intestinal slow-wave frequency gradient. *Am.J.Physiol.* 216: 301-307, 1969.
10. **El-Sharkawy, T.Y. and E.E. Daniel.** Electrical activity of small intestinal smooth muscle and its temperature dependence. *Am.J.Physiol.* 229: 1268-1276, 1975.
11. **Fabiato, A.** Role of the intercalated disks in the chemical skinning of enzymatically separated adult cardiac cells. In: *Electrophysiology of single cardiac cells*, edited by D. Noble and T. Powell. 1987, p. 125-138.
12. **Faussone-Pellegrini, M.S.** Histogenesis, structure and relationships of interstitial cells of Cajal (ICC): from morphology to functional interpretation. [Review]. *Eur.J.Morphol.* 30: 137-148, 1992.
13. **Faussone-Pellegrini, M.S., C. Cortesini, and P. Romagnoli.** Sull'ultrastruttura della tunica muscolare della porzione cardiale dell'esofago e dello stomaco umano con particolare riferimento alle cosiddette cellule interstiziali di Cajal. *Arch.Ital.Anat.Embriol.* 82: 157-177, 1977.
14. **Freshney, R.I.** *Culture of animal cells, manual of basic technique.* NY: Wiley Liss, 1994.
15. **Giles, W.R.** Generation of pacemaker activity in mammalian sinoatrial node. In: *Pacemaker Activity and Intercellular Communication*, edited by J.D. Huizinga. CRC Press: Baton Rouge, 1994, p. 15-36.
16. **Glauert, A.M.** *Fixation, dehydration and embedding of biological specimens.* Amsterdam. New York. Oxford: North-Holland Publishing Company, 1981.
17. **Huizinga, J.D., K. Ambrous, and T.D. Der-Silaphet.** Cooperation between neural and myogenic mechanisms in the control of peristalsis in the small intestine:

comparison between control and *W* mutant mice. *J.Physiol.(Lond)* 506: 843-856, 1998.

18. **Huizinga, J.D., L. Farraway, and A. Den Hertog.** Effect of voltage and cyclic AMP on frequency of slow wave type action potentials in colonic smooth muscle. *J.Physiol.(Lond)* 442: 31-45, 1991a.
19. **Huizinga, J.D., L. Farraway, and A. Den Hertog.** Generation of slow-wave-type action potentials in canine colon smooth muscle involves a non-L-type $Ca^{2+}$ conductance. *J.Physiol.(Lond)* 442: 15-29, 1991b.
20. **Huizinga, J.D., L. Thuneberg, M. Klüppel, J. Malysz, H.B. Mikkelsen, and A. Bernstein.** The *W/kit* gene required for interstitial cells of Cajal and for intestinal pacemaker activity. *Nature* 373: 347-349, 1995.
21. **Huizinga, J.D., L. Thuneberg, J.M. Vanderwinden, and J.J. Rumessen.** Interstitial cells of Cajal as pharmacological targets for gastrointestinal motility disorders. *Trends Pharmacol.Sci.* 18: 393-403, 1997.
22. **Jessen, H. and L. Thuneberg.** Interstitial cells of Cajal and Auerbach's plexus. A scanning electron microscopical study of guinea-pig small intestine. *J.Submicrosc.Cytol.Pathol.* 23: 195-212, 1991.
23. **Klüppel, M., J.D. Huizinga, J. Malysz, and A. Bernstein.** Developmental origin and Kit-dependent develcpment of the interstitial cells of Cajal in the mammalian small intestine. *Developmental Dynamics* 211: 60-71, 1998.
24. **Lee, J.C.F., L. Thuneberg, L. Farraway, and J.D. Huizinga.** Plasticity in ICC isolated from the mouse small intestine. *Dig.Dis.Sci.* 41: 1904, 1996.(Abstract)
25. **Liu, L.W.C. and J.D. Huizinga.** Electrical coupling of circular muscle to longitudinal muscle and interstitial cells of Cajal in canine colon. *J.Physiol.(Lond)* 470: 445-461, 1993.
26. **Liu, L.W.C., R. Ruo, and J.D. Huizinga.** Circular muscle lamellae of canine colon are electrically isolated functional units. *Can.J.Phys.Pharm.* 75: 112-119, 1997.
27. **Liu, L.W.C., L. Thuneberg, and J.D. Huizinga.** Cyclopiazonic acid, inhibiting the endoplasmic reticulum calcium pump, reduces the canine colon pacemaker frequency. *J.Pharmacol.Exp.Ther.* 275: 1058-1068, 1995.
28. **Malysz, J. and J.D. Huizinga.** Regulation of pacemaker activity in the mouse small intestine involves $IP_3$ sensitive calcium release. *Dig.Dis.Sci.* 41: 18881997.
29. **Malysz, J., D. Richardson, L. Farraway, M.O. Christen, and J.D. Huizinga.** Generation of slow wave type action potentials in the mouse small intestine involves a non-L-type calcium channel. *Can.J.Phys.Pharm.* 73: 1502-1511, 1995a.
30. **Malysz, J., D. Richardson, L. Farraway, M.O. Christen, and J.D. Huizinga.** Initiation of slow wave type action potentials in the mouse small intestine involves a non-L-type calcium channel. *Neurogastroenterol.Motil.* 7: 2721995b.(Abstract)
31. **Malysz, J., L. Thuneberg, H.B. Mikkelsen, and J.D. Huizinga.** Action potential generation in the small intestine of *W* mutant mice that lack interstitial cells of Cajal. *Am.J.Physiol.* 271: G387-G3991996.
32. **Post, J.M. and J.R. Hume.** Ionic basis for spontaneous depolarizations in isolated smooth muscle cells of canine colon. *Am.J.Physiol.* 263: C691-C6991992.
33. **Sarna, S.K. and M.F. Otterson.** Small Intestinal Physiology and Pathophysiology. *Gastro.Clin.North Am.* 18: 375-405, 1989.
34. **Schanne, O.F., R. Dumaine, and E. Ruiz Petrich.** Pacemaker activity in explanted cardiac cells. In: *Pacemaker Activity and Intercellular Communication*, edited by J.D. Huizinga. CRC Press: Baton Rouge, 1994, p. 133-155.

35. **Sipos, T. and J.R. Merkel.** An effect of calcium ions on the activity, heat stability, and structure of trypsin. *Biochemistry* 9: 2766-2775, 1970.
36. **Szurszewski, J.H.** Electrophysiological basis of gastrointestinal motility. In: *Physiology of the gastrointestinal tract*, edited by L.R. Johnson. New York: Raven Press, 1987, p. 383-422.
37. **Thomsen, L., T.L. Robinson, J.C.F. Lee, L. Farraway, M.J.G. Hughes, D.W. Andrews, and J.D. Huizinga.** Interstitial cells of Cajal generate a rhythmic pacemaker current. *Nature Medicine* 4: 848-851, 1998.
38. **Thuneberg, L.** Interstitial cells of Cajal: intestinal pacemaker cells? *Adv.Anat.Embryol.Cell Biol.* 71: 1-130, 1982.
39. **Thuneberg, L.** Isolation of neonatal ICC in the mouse small intestine. *Neurogastroenterol.Motil.* 1996.(Abstract)
40. **Thuneberg, L., J.J. Rumessen, and H.B. Mikkelsen.** Interstitial cells of Cajal - an intestinal impulse generation and conduction system? *Scandinavian Journal of Gastroenterology - Supplement* 71: 143-144, 1982.
41. **Thuneberg, L., J.J. Rumessen, H.B. Mikkelsen, S. Peters, and H. Jessen.** Structural aspects of interstitial cells of Cajal as intestinal pacemaker cells. In: *Pacemaker Activity and Intercellular Communication*, edited by J.D. Huizinga. CRC Press: Baton Rouge, 1995, p. 193-222.
42. **Tokutake, N., H. Maeda, Y. Tokutomi, D. Sato, M. Sugita, S. Nishikawa, S.I. Nishikawa, J. Nakao, T. Imamura, and K. Nishi.** Rhythmic $Cl^-$ current and physiological roles of the intestinal c-kit positive cells. *Pflügers Arch.-Eur.J.Physiol.* 431: 169-177, 1995.
43. **Ward, S.M., A.J. Burns, S. Torihashi, S.C. Harney, and K.M. Sanders.** Impaired development of interstitial cells and intestinal electrical rhythmicity in steel mutants. *Am.J.Physiol.* 269: C1577-C15851995.
44. **Ward, S.M., A.J. Burns, S. Torihashi, and K.M. Sanders.** Mutation of the proto-oncogene *c-kit* blocks development of interstitial cells and electrical rhythmicity in murine intestine. *J.Physiol.(Lond)* 480: 91-97, 1994.
45. **Ward, S.M. and K.M. Sanders.** Upstroke component of electrical slow waves in canine colonic smooth muscle due to nifedipine-resistant calcium current. *J.Physiol.(Lond)* 455: 321-337, 1992.

## 2.7 Figure Legends

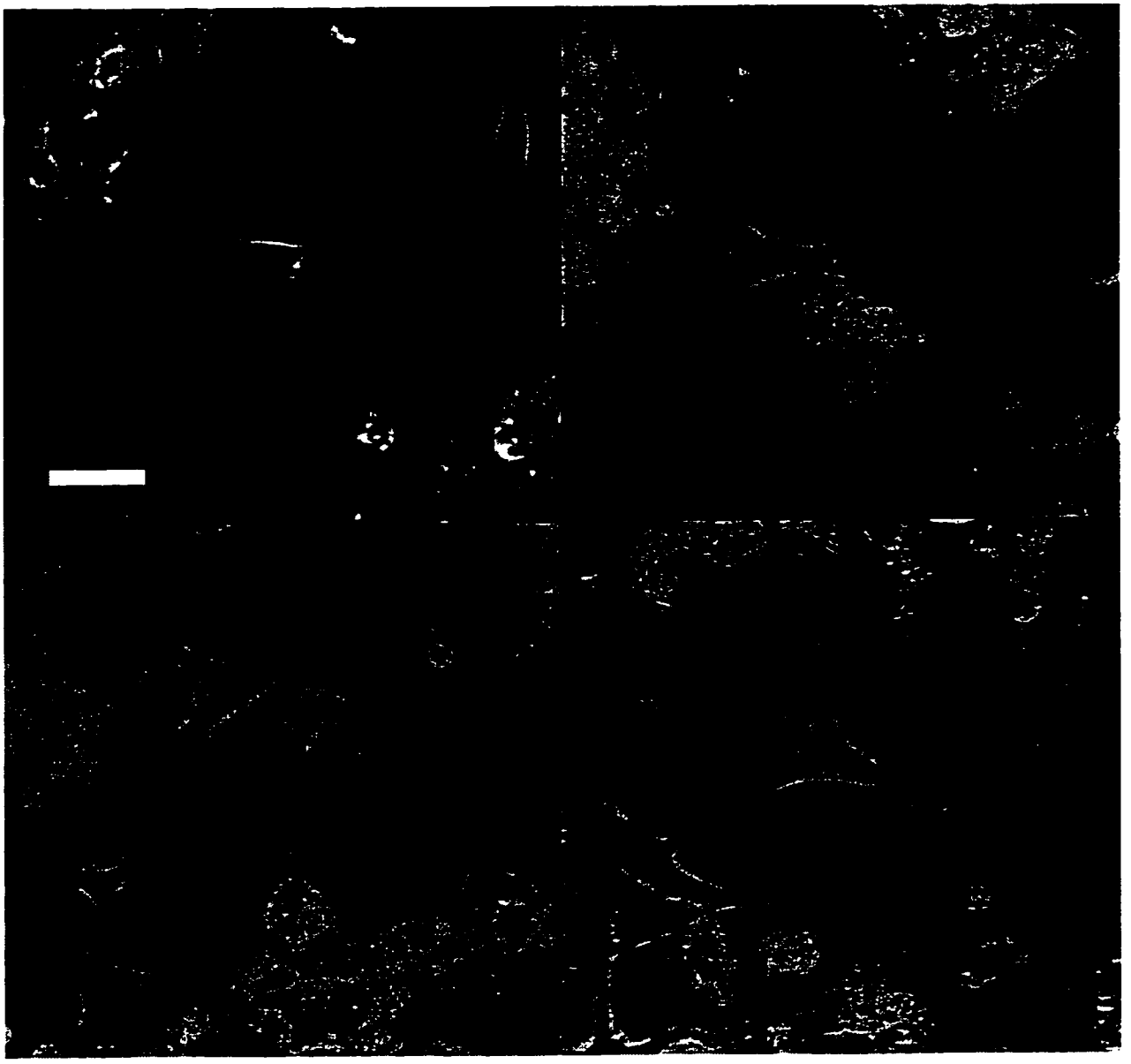

Figure 2-1 Interstitial cells of Cajal in primary culture

Single cells were dissociated from the adult mouse small intestines and grown in short-term culture (5-6 days). ICC typically attained their distinctive morphology after ~2 to 3 days in culture. a. Under the phase contrast microscope, ICC could be distinguished by

being significantly more phase dark than other cell types. The cell body was triangular in shape, and compact. ICC generally extended 3-4 main branches from the cell body. b. ICC in short-term culture were seen with variations in cell body shape from strictly triangular to elongated triangles. This ICC did not have well-developed processes. The processes were short and not many contacts were made with neighboring cells. There was a distinctive triangular thickening at each bifurcation point of a process. The cell body was seen to contain a large nucleus with little surrounding cytoplasm. c. Since the density of dissociated ICC in the cultures was low, it was rare to see ICC in contact with each other. When contacts between two ICC were established, contact was always made with processes and never between cell bodies. d. This ICC had a distinctive branching pattern, extending as a diffuse tree around the cell body and making several contacts with surrounding smooth muscle cells. x400. All magnification bars - 25 μm.

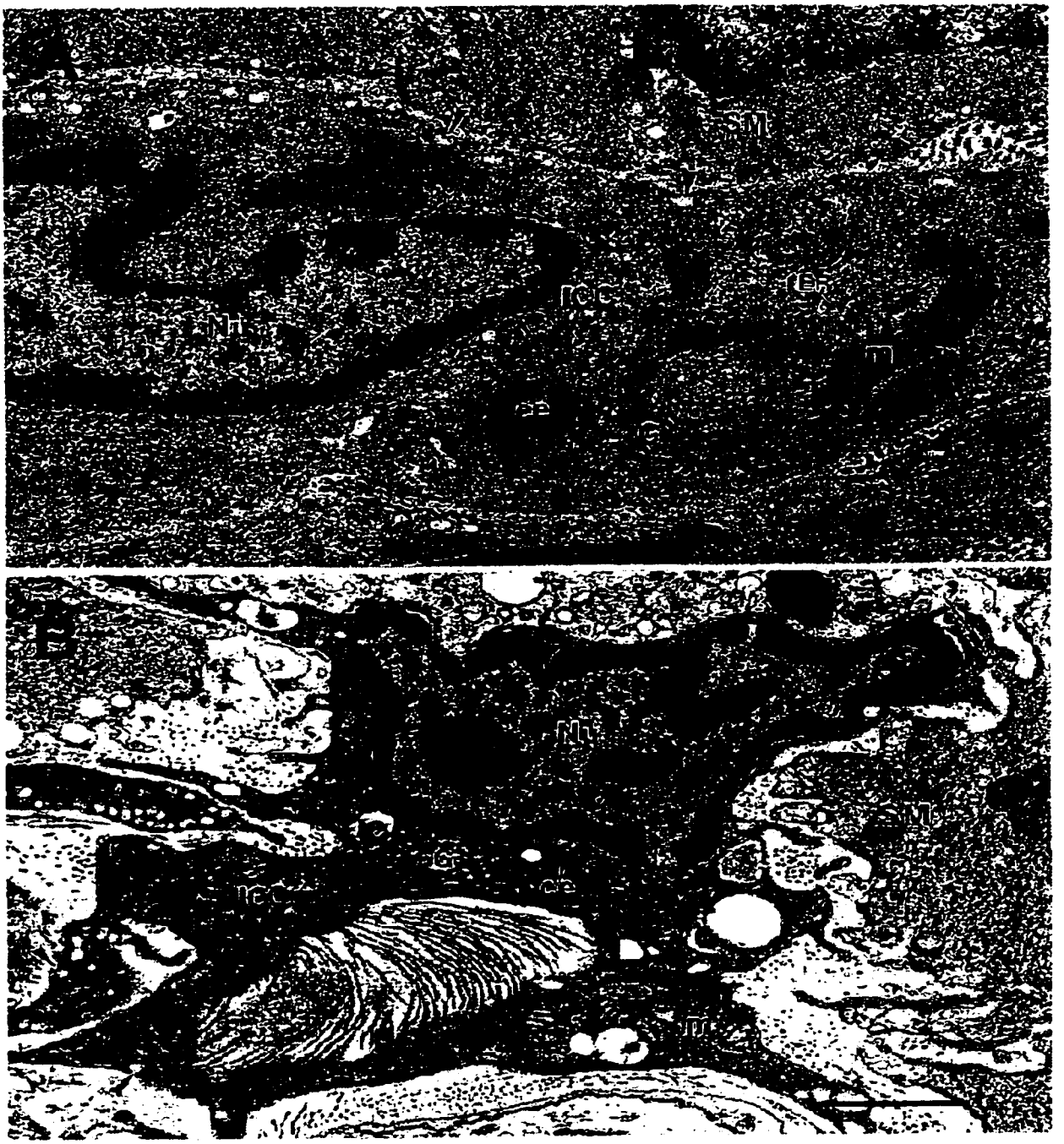

Figure 2-2 Electron micrographs of ICC from the myenteric plexus of adult small intestine.

(a) An ICC fixed *in situ* had all major structural characteristics described previously.

(38): large euchromatic nucleus (Nu), perinuclear well-developed Golgi complexes (G), and centriole (ce). The cytoplasm contained mitochondria (m), many free ribosomes, intermediate filaments (large circle), and thin filaments (small circle). The presence of caveolae (arrowheads) distinguished ICC from fibroblasts and macrophages. x 28,500. Bar - 500 nm. (b) ICC from dissected tissue were characterized by a dark electron dense cytoplasm and nucleus as a possible result of cell contraction. Note typical ICC characteristics: branched profile, perinuclear Golgi complex (G) and centriole (ce), numerous mitochondria (m) and ribosomes. Most of caveolae (arrowheads) were internalized. The tissue ICC was surrounded by collagen fibers (co), and formed a close contact with a smooth muscle cell (SM). x21,150. Bar - 1μm.

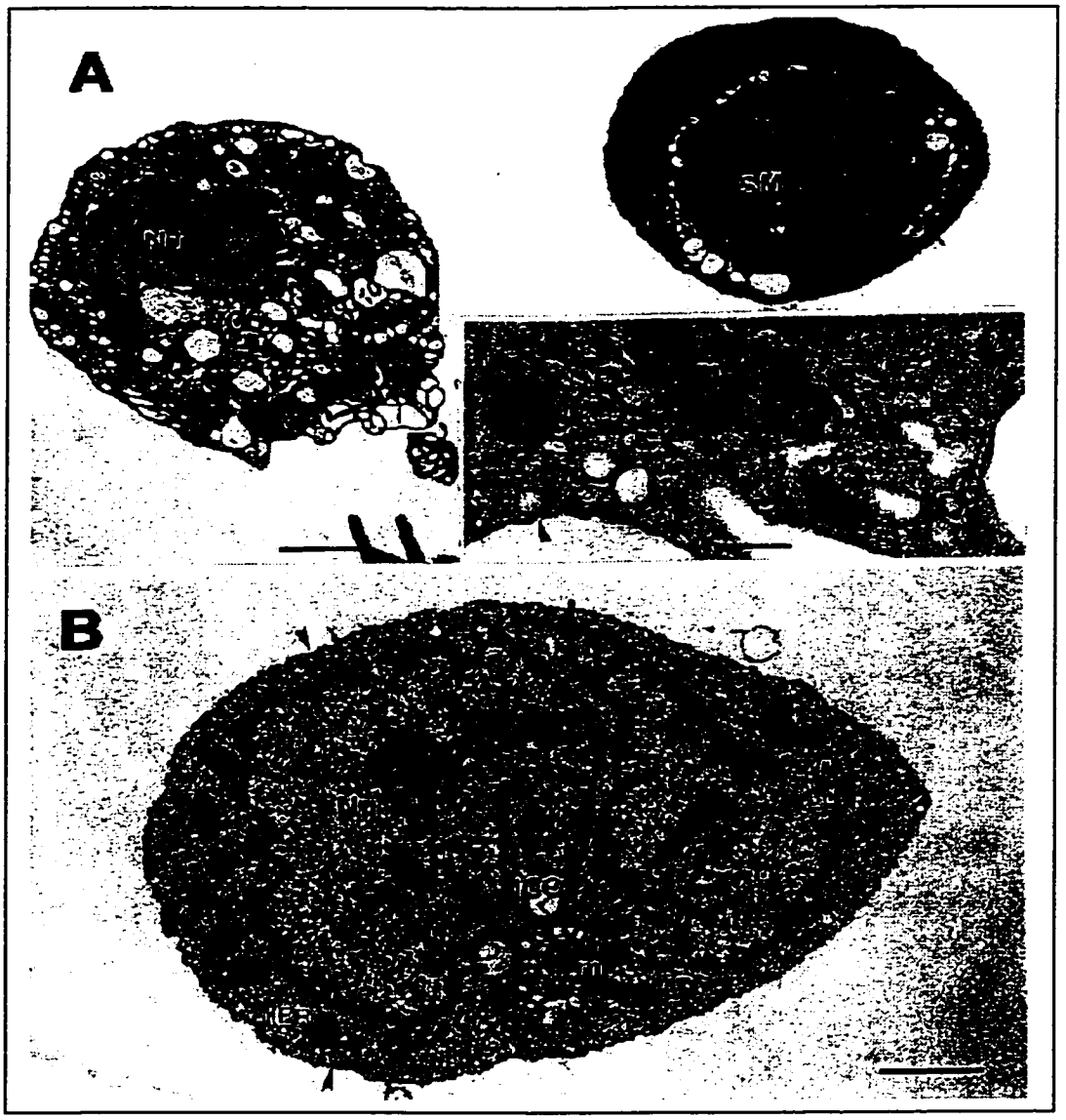


Figure 2-3 Electron micrographs of freshly isolated cells.

a. Low magnification micrograph of two isolated cells: a smooth muscle cell (SM), and an ICC, fixed 1 hr after the dissociation procedure. Both cells were rounded up, free of collagen fibres. Similar to an ICC from dissected tissue, this ICC was characterized by a dark, electron dense cytoplasm and a heterochromatic nucleus (Nu). Its cytoplasm contained many membrane-bounded large empty spaces, probably as the result of

extensive surface internalization due to cell contraction into a ball. x 5,570. Bar - 2μm. Inset. High magnification micrograph of boxed area in Figure 3a. shows the distinctive features of a 1 hr old dissociated ICC: numerous intermediate filaments (large circle), thin filaments (small circle), free ribosomes, Most of plasma membrane caveolae (arrowhead) were internalized. x 60,000. Bar - 200nm. b. This ICC after 1 day in culture was characterized by an oval, smooth profile, large, partially folded euchromatic nucleus (Nu) and cytoplasm filled with mitochondria (m), small cisternae of rER, and an increased number of free ribosomes. G – Golgi complex. Arrowheads - caveolae. x 15,400. Bar - 1μm.

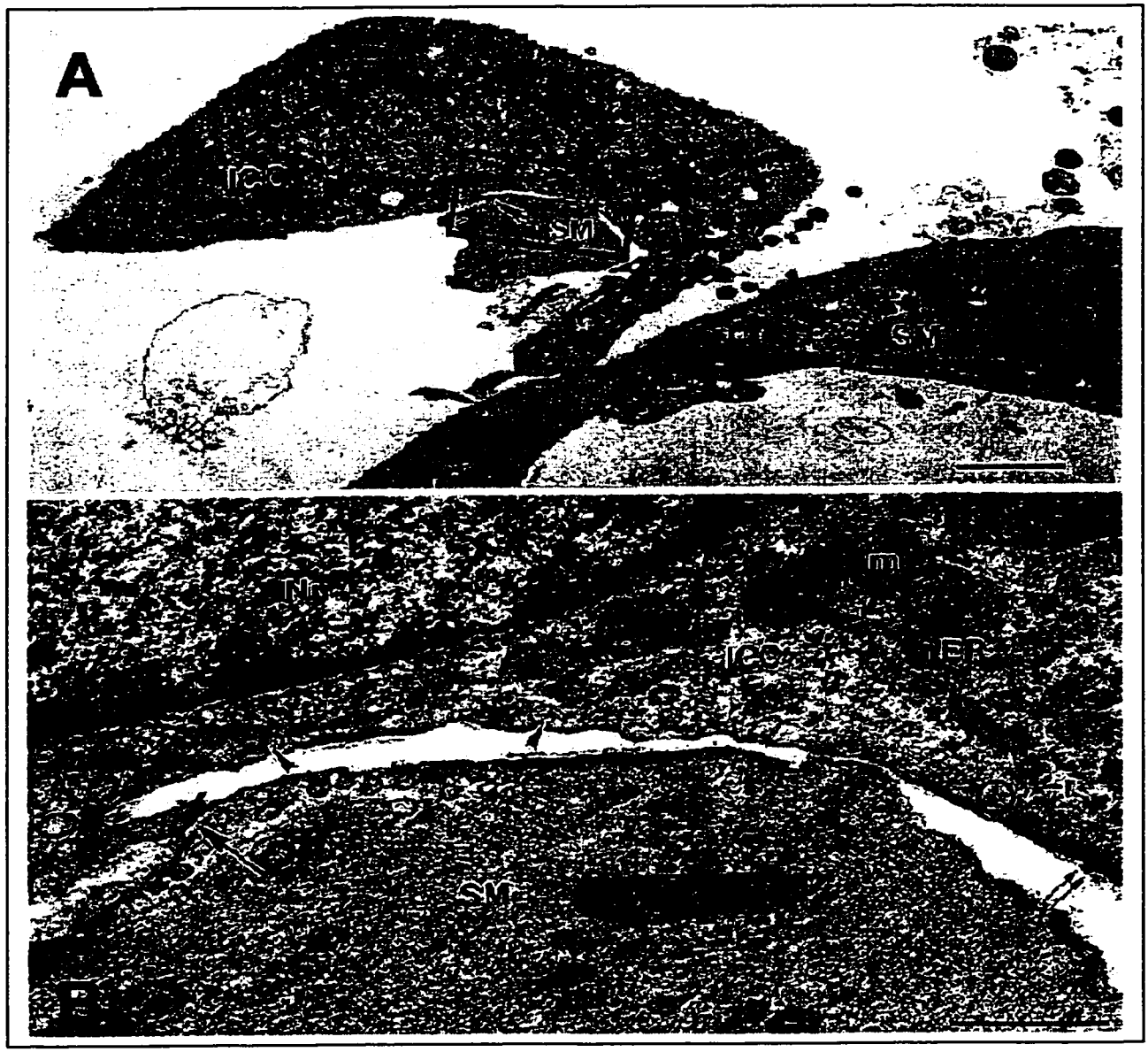


Figure 2-4 Electron micrograph of an ICC from a 4 day culture.

a. Low magnification micrograph of the nucleated part of an ICC that was in gap junction contact (arrow) with a smooth muscle cell (SM). The smooth muscle cells were recognized by a myofilament dominated cytoplasm. An angular shape characterized the nucleated part of the ICC. It contained an euchromatic nucleus (Nu), numerous

mitochondria (m), and ribosomes. x 7,170. Magnification bar - 2μm. b. High magnification micrograph of the boxed area of figure 4a. Free polyribosomes (r), cisternae of rER and sER, and mitochondria (m) were the major components of the ICC cytoplasm. Groups of thin filaments (circle) were predominantly located under the plasma membrane. The ICC was distinguished from fibroblasts, macrophages and glial cells by the presence of caveolae (arrowheads), and by a gap junction contact (arrow) with a neighboring smooth muscle cell (SM). x 48,200. Bar - 500nm.

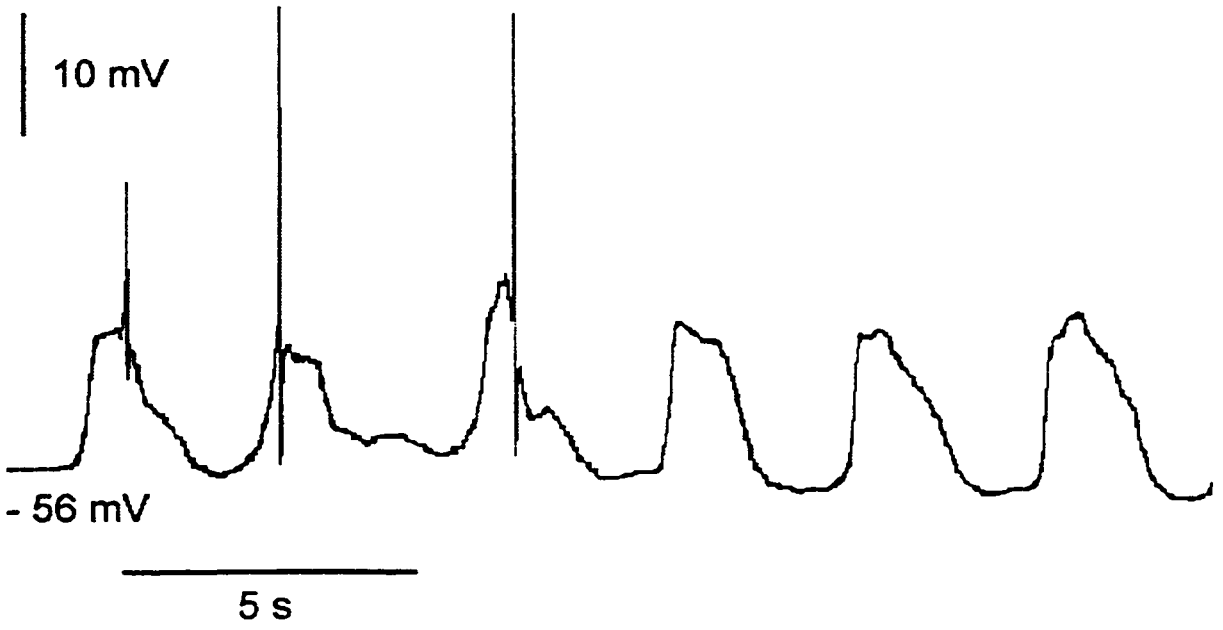


Figure 2-5 Slow wave activity in small intestine tissue at room temperature.

Not all gastro-intestinal preparations retain slow wave activity at room temperature, but the mouse small intestine does at a lower frequency compared to 37°C.

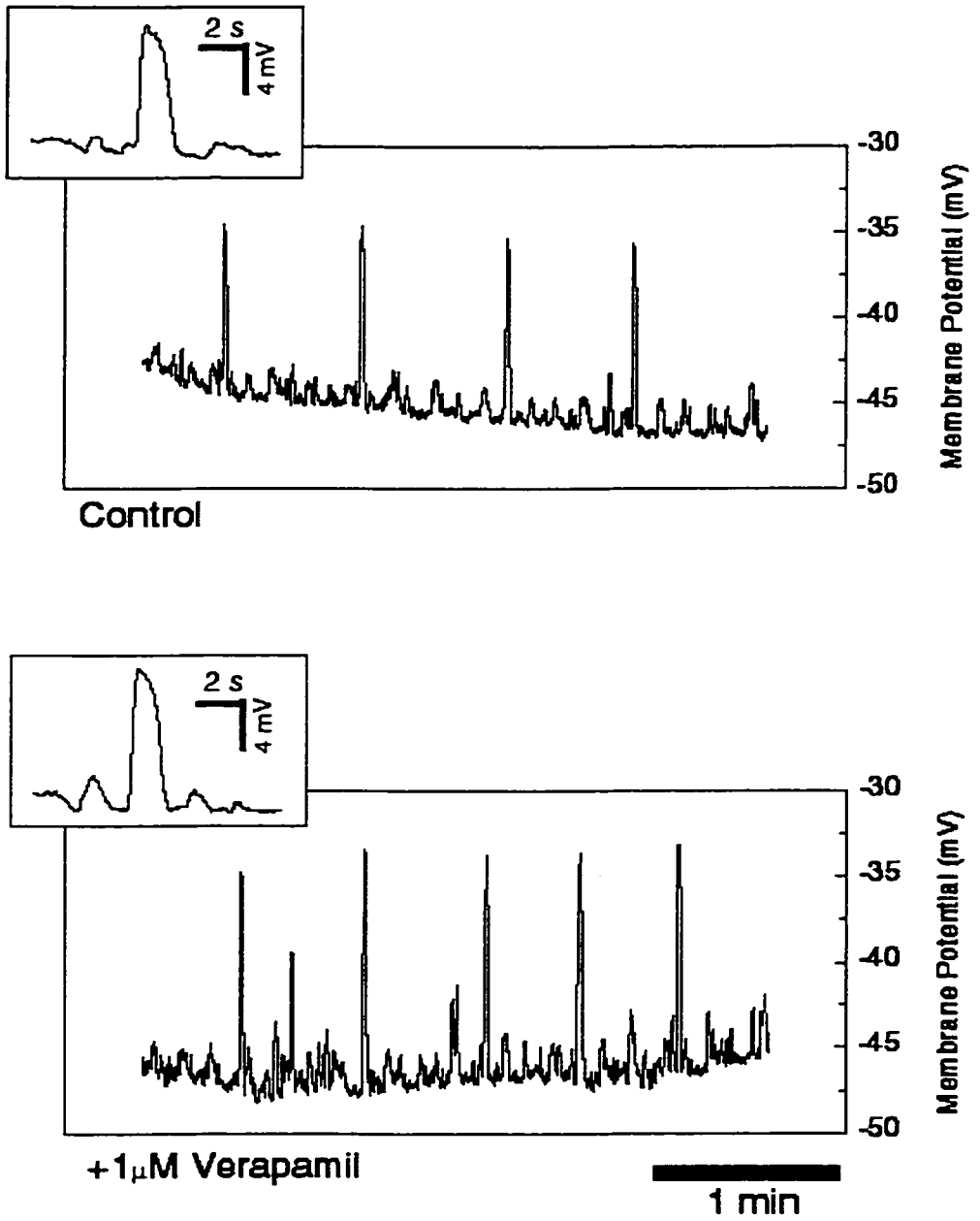


Figure 2-6 Spontaneous voltage oscillations recorded from an isolated ICC.

High amplitude voltage oscillations arose sharply from the resting membrane potential at regular intervals. The inset shows the striking resemblance to tissue slow waves, the upstroke occurred independent of a prepotential component. The voltage oscillations were unaffected by the L-type calcium channel blocker verapamil (1μM).

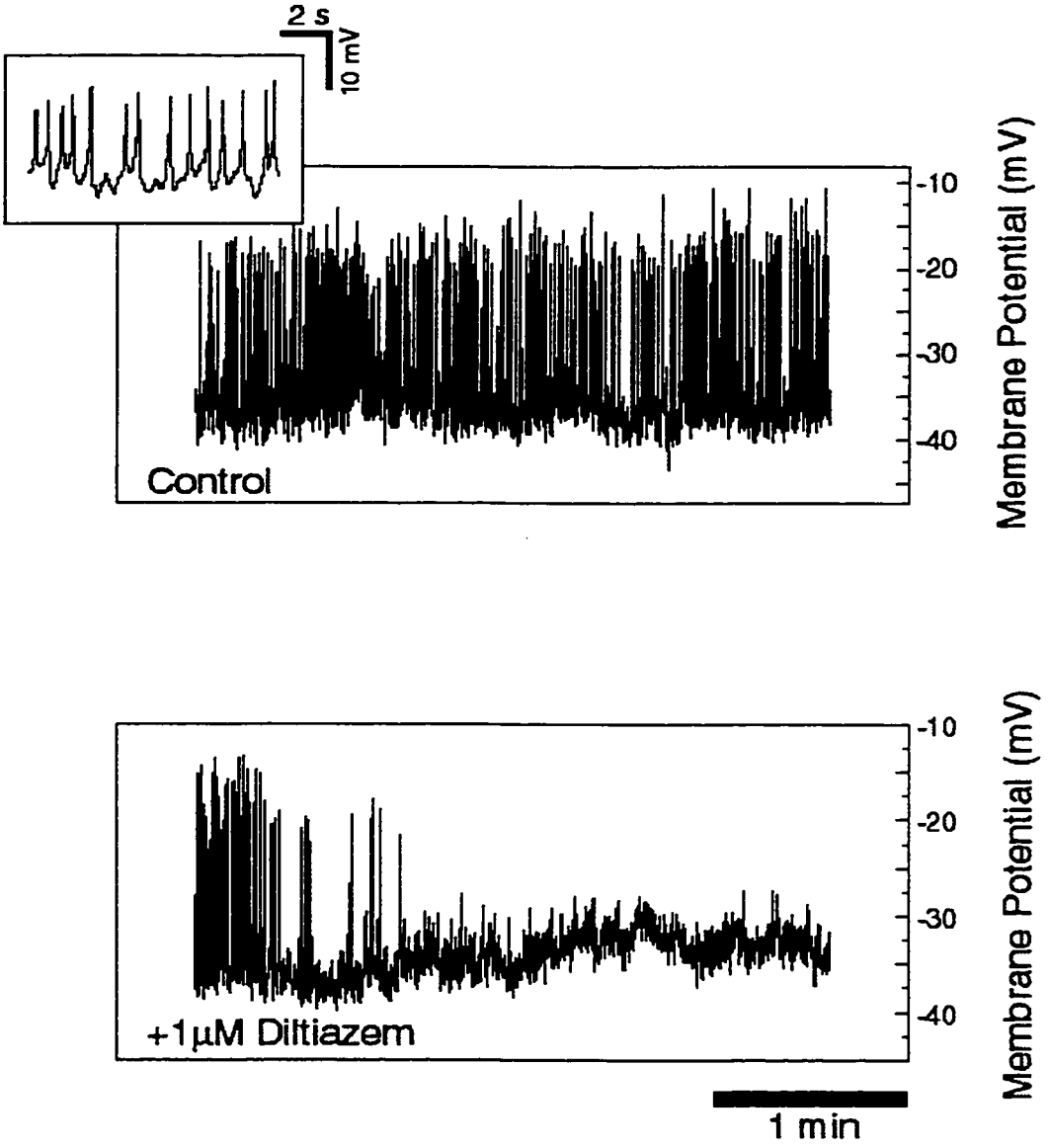


Figure 2-7 Spontaneous generation of action potentials recorded from an isolated smooth muscle cell.

Generation of action potentials occurred at irregular frequencies. The inset shows that a prepotential depolarization is preceding each action potential. All action potential

activity was abolished by the L-type $Ca^{2+}$ channel blocker diltiazem (1μM). Both recordings were from the same cell as part of a continuous recording. Diltiazem was applied at the beginning of the bottom trace.

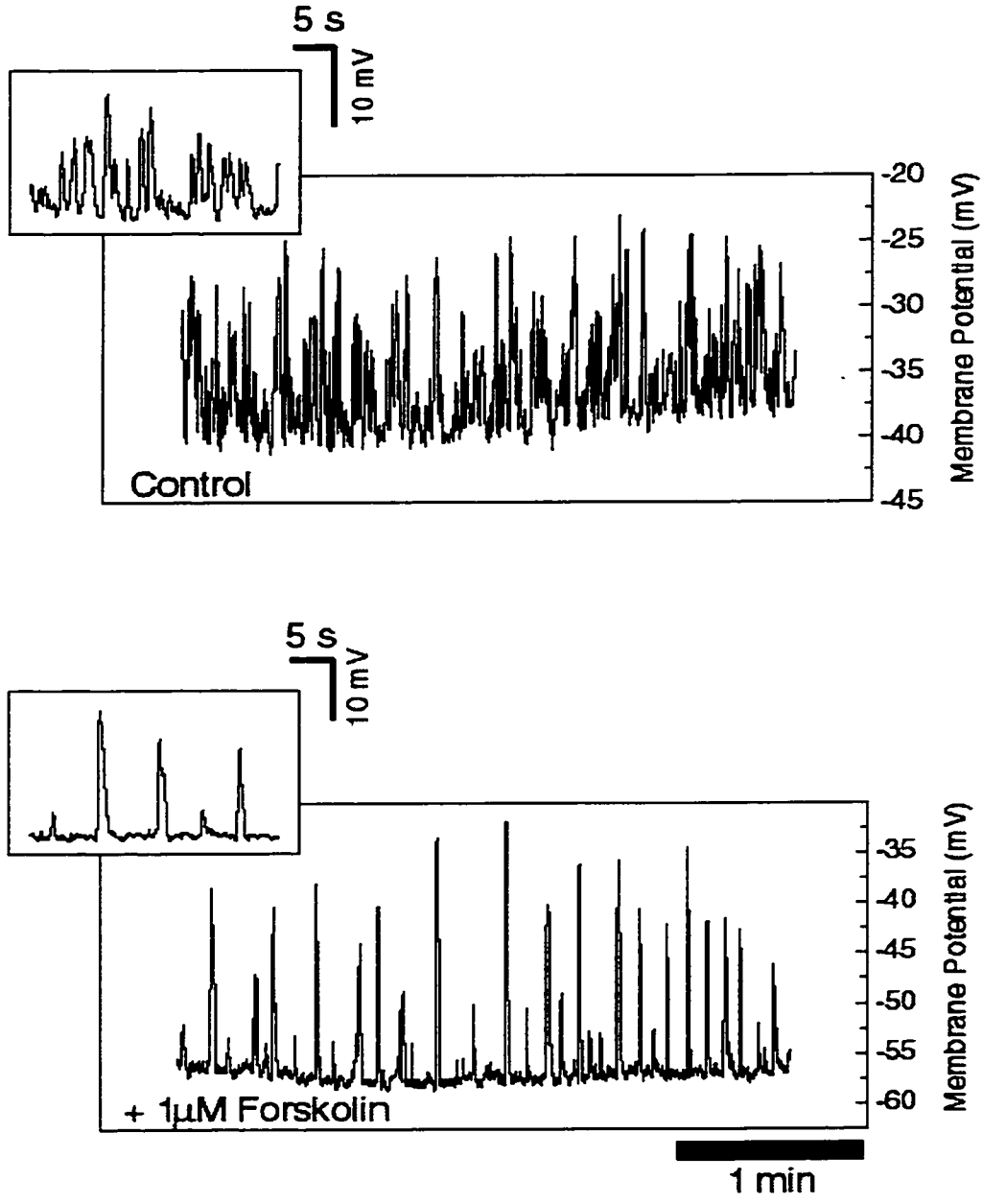


Figure 2-8 The effect of forskolin on voltage oscillations in isolated ICC.

At a membrane potential of - 40 mV, voltage sensitive spiking events or membrane noise was occasionally observed in ICC. The addition of 1μM forskolin

resulted in hyperpolarization of the resting membrane potential. This resulted in strong reduction of membrane noise while increasing the oscillation amplitude. The inset shows the dramatic resemblance of the oscillations to tissue slow waves (29). The addition of 1 μM 8-Br-cAMP gave similar results (not shown).

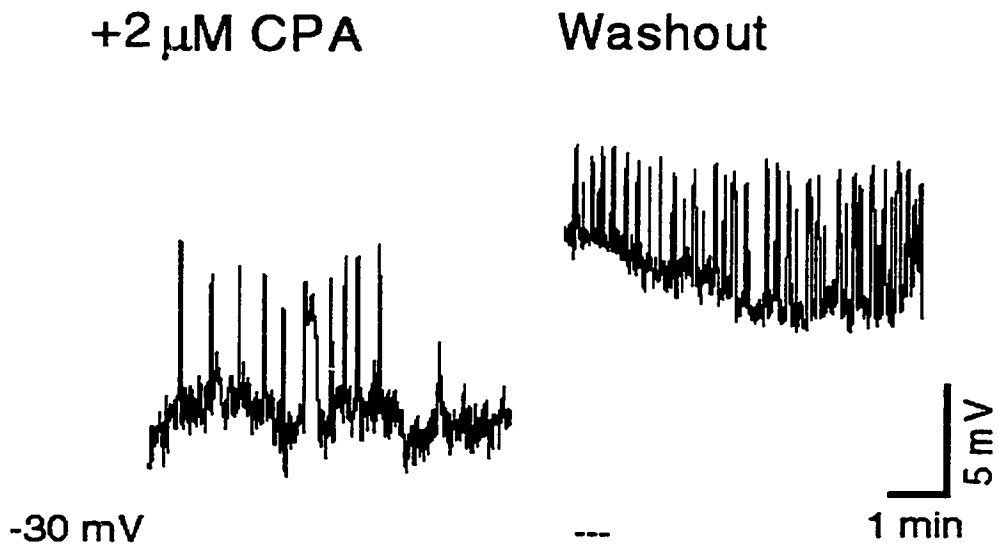


Figure 2-9 CPA increased duration and thereafter abolished spontaneous voltage oscillations in ICC.

In the presence of 5 μM D600, 2 μM CPA was added which caused a characteristic increase in duration before abolishing the voltage oscillations. Upon washout, the effect was fully reversible.

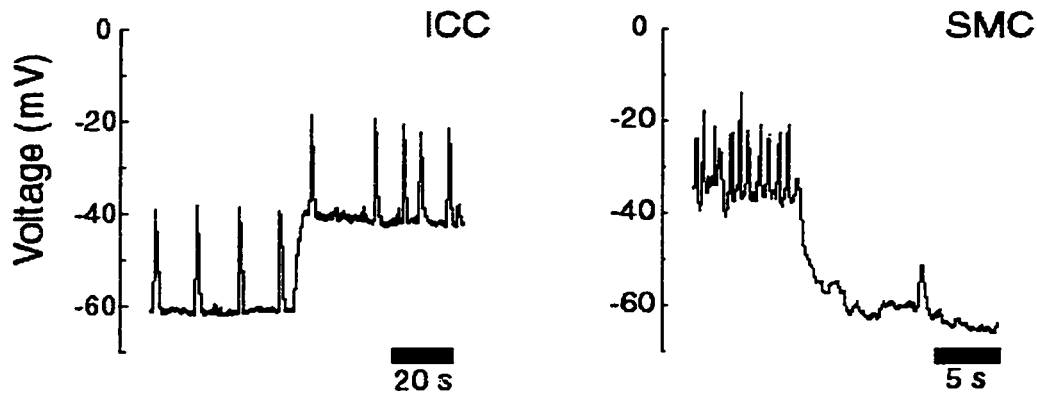


Figure 2-10 Voltage sensitivity of spontaneous activity from an ICC and a smooth muscle cell.

From a resting membrane potential of -60 mV, regular 20 mV oscillations were observed. The membrane potential was then depolarized to -40 mV by current injection. The spontaneous activity was not affected by the depolarization. In contrast, action potential generation in a smooth muscle cell was very voltage sensitive. Action potentials typically occurred at a membrane potential of -37 mV. By current injection, the membrane potential was hyperpolarized to -60 mV. The action potentials were abolished by hyperpolarization below ~ -40 mV.

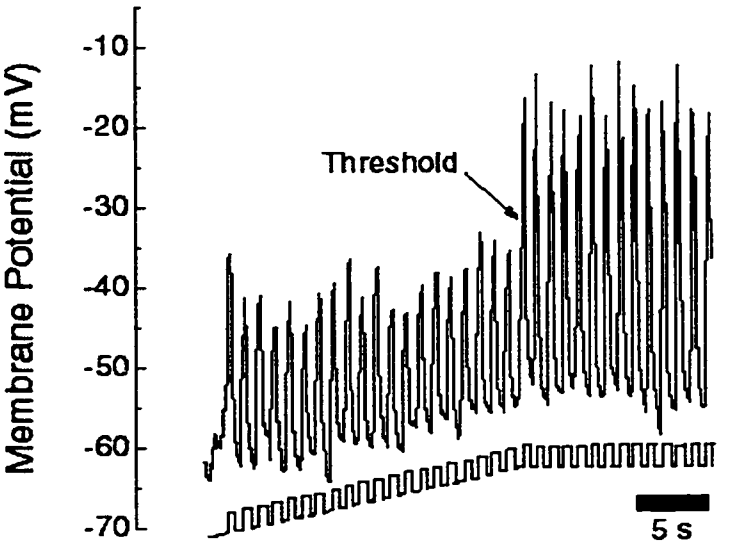


Figure 2-11 Action potentials can be evoked and paced in smooth muscle cells but not in ICC.

The resting membrane potential was hyperpolarized below the voltage threshold to abolish action potential generation. Depolarizing current pulses (1 Hz) were given so that 20 mV depolarizations were superimposed on a slowly depolarizing ramp. Once the peaks of the depolarizing pulses reached threshold (-37 mV), action potentials occurred at the peak of each depolarizing pulse. Since action potentials only occurred at the peak of the depolarizing pulses, their frequency of occurrence was dependent on the duration of the depolarizing pulse and its intrinsic frequency. Using the same current injection protocol on ICC produced no effects (not shown).

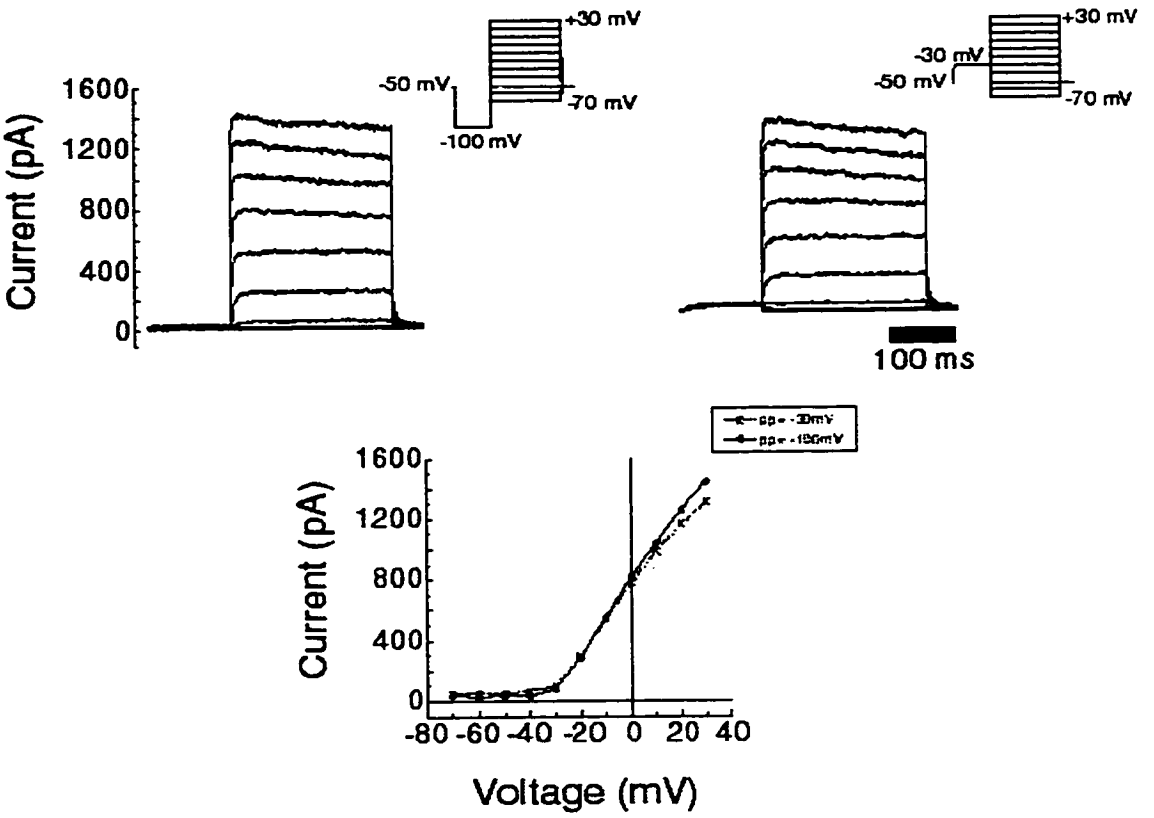


Figure 2-12 Whole cell current profiles from ICC.

Large outward whole cell currents were elicited by the voltage clamp protocols shown (n=7). Prepulses of either -100 or -30 mV were given before the test pulses in the same cells. The large outward currents were only slightly inactivated by the -30 mV prepulse. The current -voltage (IV) relationships of the peak currents of either the -100 or -30 mV prepulse protocols were similar. Note the tail currents resulting from the slow deactivation of ICC outward currents.

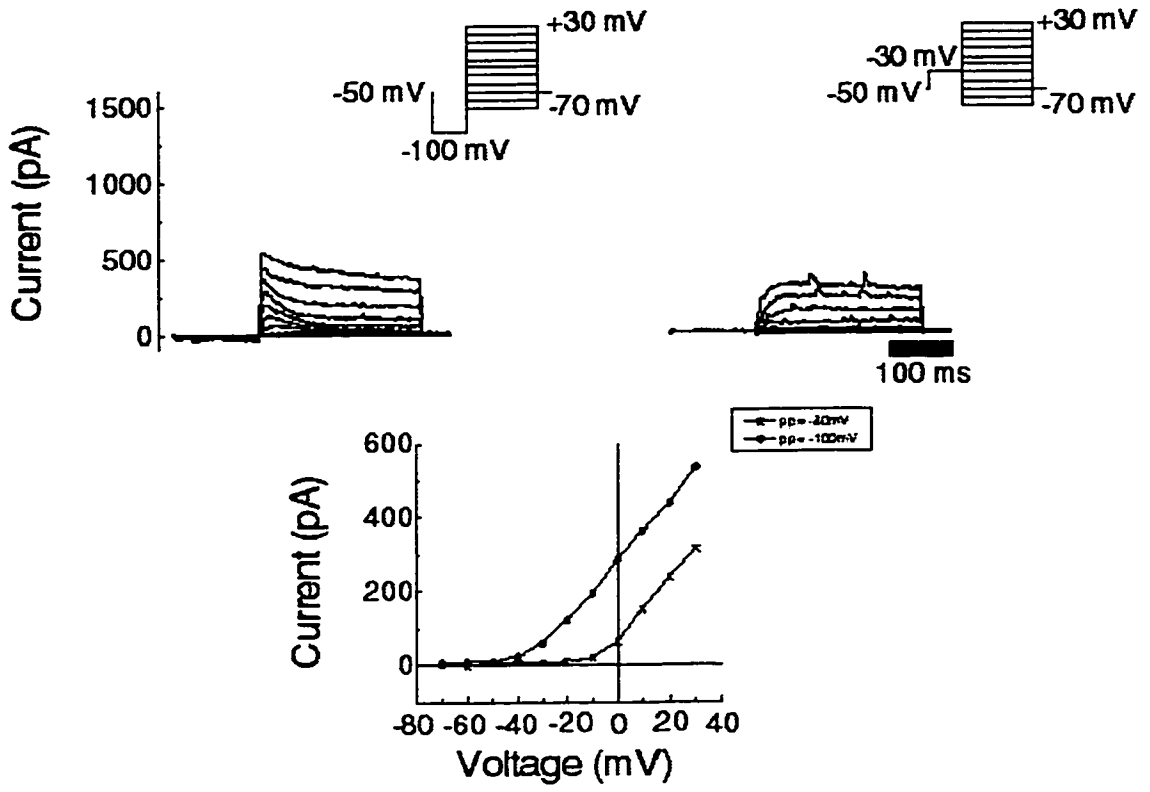


Figure 2-13 Whole cell current profiles from smooth muscle cell.

Whole cell currents were generated using the voltage protocols shown (n=5). The whole cell currents from the smooth muscle cells were much smaller than those from ICC and included distinctive transient outward currents. Applying a -30 mV prepulse inactivated the transient outward currents, leaving only delayed rectifier-like currents. Comparing the whole cell profiles with -30 and - 100 mV prepulses, the current-voltage (IV) relations were different. The different IV with the depolarized prepulse (-30 mV) confirmed the large contribution of voltage dependent inactivation to whole cell currents.

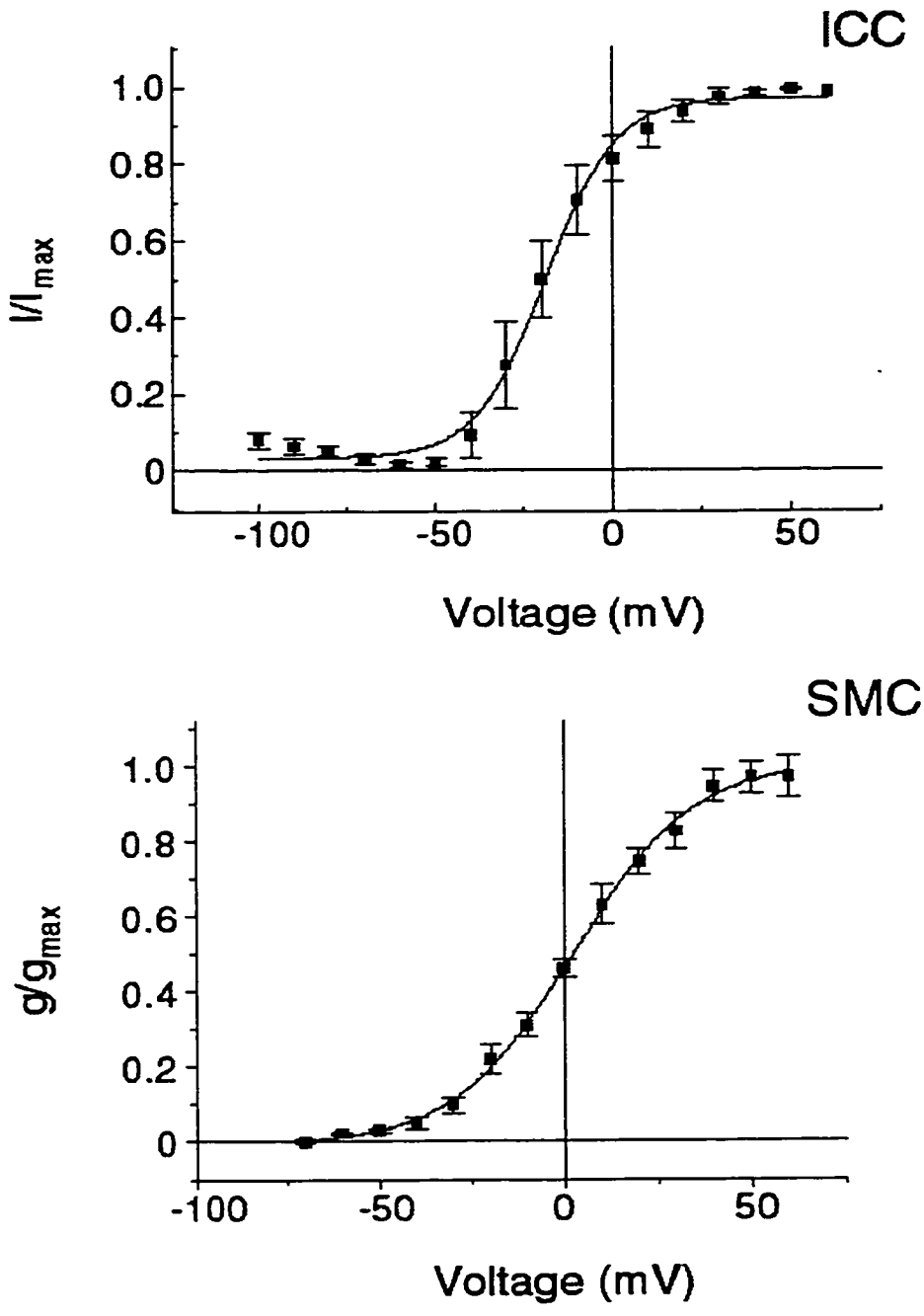


Figure 2-14 Voltage activation of the large outward currents in ICC and smooth muscle cells.

Analysis of normalized tail currents from ICC outward currents yielded the voltage activation plot shown (n=6). The tail currents were taken approximately 15-20 ms after the end of the test pulse to be certain that the RC artifact would not contribute. The curve was fitted by the least squares method. The large outward current in ICC has a half activation voltage ($V_h$) of -18.7 mV with a slope factor ($V_s$) of 9.9 mV. Using 5% and 95% points as the threshold and steady-state points respectively, this large outward current was found to activate at approximately -49.6 mV and reached steady state by 14.2 mV. Similarly, the peak outward currents in smooth muscle cells were normalized as conductances and plotted as a voltage activation plot. The peak outward currents in smooth muscle cells have a $V_h$ of 2.3 mV with a $V_s$ of 16.4 mV. The 5% and 95% thresholds were -49.0 mV and 50.6 mV respectively.

# Chapter 3: Interstitial cells of Cajal generate a rhythmic pacemaker current

Lars Thomsen, Tim L. Robinson, Jonathan C.F. Lee, Laura A. Farraway, Martin J.G. Hughes, David W. Andrews and Jan D. Huizinga

Departments of Biomedical Sciences and Biochemistry, and the Intestinal Disease Research Program, McMaster University, Hamilton, Ontario L8N 3Z5, Canada

Address for correspondence:

Dr. Jan D. Huizinga
McMaster University
HSC-3N5C
1200 Main Street West
Hamilton, ON L8N 3Z5
Phone: (905) 525-9140 x22590
Fax: (905) 522-3454
E-mail: huizinga@mcmaster.ca

## 3.a Abstract

Pacemaker activity in the gastrointestinal musculature is provided by rhythmic slow transient depolarizations (so called 'slow waves') of the muscle cell membrane [1,2]. Recent evidence established that interstitial cells of Cajal (ICC) are in some way essential for this slow wave activity to occur [2-4]. However, the question remained whether ICC are in fact pacemaker cells actually providing a pacemaker current that could initiate slow waves. Here we provide the first direct evidence that a single cell, identified as an interstitial cell of Cajal by light microscopy, electron microscopy and expression of *kit* mRNA, generates spontaneous contractions and a rhythmic inward current that is insensitive to L-type calcium channel blockers. Furthermore, the inward current is associated with membrane potential oscillations, consistent with the periodicity and pharmacology of tissue slow wave activity. The inward current has a reversal potential of +10 mV indicating the involvement of a non-specific cation channel. Spontaneous activity similar to that observed in ICC was never observed in smooth muscle cells. In conclusion, positively identified isolated ICC generate a spontaneous periodic inward current consistent with a pacemaker function.

## 3.1 Introduction

A specific network of interstitial cells of Cajal embedded in Auerbach's plexus of the gastrointestinal tract may act as the source of pacemaker activity for gastro-intestinal motility. This original and remarkable hypothesis was formulated in 1977 by Faussone-Pellegrini [5] and in 1982 by Thuneberg and co-workers [6]. Ever since then, there was the realization that the only way to validate this hypothesis was to show that single isolated interstitial cells of Cajal (ICC) would generate spontaneous rhythmic electrical activity, electrophysiologically consistent with tissue pacemaker activity, the so called "slow wave" [2]. Here we report conclusive proof that ICC can function as pacemaker cells of the gut. The objective of this study was to obtain stable and reliable electrophysiological recordings from high quality primary cultures of ICC, identified both morphologically and by expression of *kit* mRNA. Recording conditions were made optimal for identification of spontaneous inward currents consistent with the current underlying the initiation of the slow wave in intestinal tissue [7].

ICC are mesenchymal cells [8,9] with myoid, smooth muscle like features [3]. They occur as single layer networks in most neural plexuses associated with the gastrointestinal musculature, and as three-dimensional networks within some smooth muscle layers. They are characterised *in situ* by a small, often triangular or stellate shaped cell body, with several long processes overlapping extensively with processes from neighbouring ICC to form a network of cells. ICC form close apposition and/or gap junction contacts with neighbouring smooth muscle cells. In addition, ICC form close contacts with nerve

varicosities. Recently, ICC have been shown to possess the *Kit* tyrosine kinase membrane receptor [10-13].

The gut musculature continuously generates periodic oscillations of the cell membrane potential, so called slow wave activity. Slow waves have a characteristic frequency ranging between 3 and 50 cycles per minute depending on the location within the gastrointestinal tract, and the species studied. In this way, the muscle cell switches back and forth between a state of low and high excitability, where the latter state often causes the initiation of action potentials that lead to rhythmic, propagating contractions. A key characteristic of slow waves is that they occur over a wide voltage range, suggesting the involvement of a current showing little or no voltage activation. Tissue experiments have provided evidence that the upstroke of the slow wave is generated by inward currents that are insensitive to L-type calcium channel blockers [7,14].

Recently, substantial evidence has been produced to suggest that ICC are essential for the generation of the slow wave activity. *W/W$^v$* mice, which lack a functional Kit receptor, fail to develop the network of ICC associated with Auerbach's plexus [10,11]. As a result, the small intestine of *W/W$^v$* mice does not generate slow wave activity [15]. These data corroborated evidence from many other species in which the physical removal of a layer of tissue, which included ICC, resulted in abolishment of slow wave activity [2,4]. The small intestine of *W* mutant mice also lack the capacity to generate slow wave driven, aborally propagating peristaltic contractions, proving the loss of pacemaker activity *in vivo* [16].

Although these data indicated an essential role for ICC, it is still not known whether ICC provide an essential component of slow wave activity (for example a biochemical trigger that would be transferred by gap junctions or close apposition contacts to smooth muscle cells), or actually provide a pacemaker current. Attempts have been made to study isolated ICC. Certain interstitial cells of the dog colon have been isolated, and an L-type calcium channel was identified which differed in kinetics from those of smooth muscle cells [17]. Although these experiments revealed some properties of these interstitial cells, they did not reveal a pacemaker current that must be insensitive to the L-type calcium channel blockers, recently confirmed by these authors [4]. *kit* positive cells were isolated from the mouse small intestine and revealed to have spontaneous chloride currents, but no voltage activated $Ca^{2+}$ currents [18]. However, chloride currents are unlikely to represent pacemaker activity, since tissue data on slow waves have not revealed an essential role for chloride currents [19]. Furthermore, Tokutake et al. tried to identify living isolated ICC by immuno-histochemical coupling to a Kit antibody FITC complex; however, this leads to prominent staining of macrophages in the same culture due to uptake of the antibody-FITC complex (Farraway and Huizinga, unpublished data). Hence in such a study, positive identification of the cells studied is an essential step that was not carried out.

## 3.2 Results

For the present study, an isolation method was developed to optimize the survival of the ICC from the mouse myenteric plexus in short term cell culture [20]. Cells were used

after three to four days in culture. The ICC were characterized morphologically by a triangular or stellate shaped cell body, with three or more branching projections (Figure 1). This appearance was strikingly similar to that of ICC observed *in situ* after methylene blue staining [2,3]. These branching cells were also investigated by electronmicroscopy, which still provides the gold standard for ICC identification [2,3]. Figure 2 illustrates the dominance of intermediate filaments in the processes of the ICC. The cells also contained numerous condensed type mitochondria and plasma membrane caveolae, established structural criteria for identification of ICC [21].

At 37°C, distinct patterns of spontaneous rhythmic contractile activity of ICC were observed. Figure 1 shows an ICC in two different contractile states, and rhythmic contractions of three different cells are shown in video format at http://www.medicine.nature.com/..... (see appendix). Contractile activity was found either along the entire length of the processes, or at localized positions. These movements sometimes spread to the cell body, and caused a complete change in location of the cell body. This contraction pattern was distinctly different from that of smooth muscle, where contractions always involved the whole cell. Such localized contractions in ICC may reflect local release of calcium from intracellular stores. Sarcoplasmic reticulum, associated with the plasma membrane, is very prominent in ICC, and thought to be involved in pacemaker activity [22].

We investigated this distinct cell type with the patch clamp technique, and found a spontaneous rhythmic inward current in 30 of 38 cells (Figure 3,4,5). The average current amplitude was 32 ± 8 pA. The frequency of the spontaneous inward current was always

very regular, with an inter-cycle period of ~ 5 s, or a frequency of 12.1 ± 1.5 cycles per minute at 20°C. Although slow wave activity in tissue of the mouse small intestine can reach up to 50 cycles per minute, we observed that the frequency slows down to ~ 10 –15 cpm at room temperature (n=5). Nifedipine (1 μM up to 10 μM) or verapamil (1μM) did not affect the spontaneous inward current. During the recording of the spontaneous inward current, the amplifier was switched to the current clamp mode, and spontaneous oscillations in the membrane potential were observed at the same frequency as the transient periodic inward current (Figure 5). These data indicate that the isolated ICC can generate a spontaneous rhythmic current and 'slow waves' in the membrane potential. Some ICC were connected to smooth muscle cells, and recorded activity could have been generated by the smooth muscle cells. However, the branches of the ICC often withdrew upon electrode attachment, and spontaneous activity was then recorded from truly isolated ICC. Furthermore, similar rhythmic spontaneous inward currents were never observed in isolated smooth muscle cells.

To definitely prove that the morphologically identified cells that generated the spontaneous rhythmic inward current were ICC, we applied the single cell PCR technique to determine if the identified cells expressed the *kit* mRNA. *In situ* hybridization experiments in *tissue* localized *kit* mRNA to the ICC within the musculature [10]. Kit staining is not associated with neural structures as shown by developmental studies [8,23]. Figure 6 illustrates a series of single cell PCR experiments on cDNA harvested from morphologically identified ICC, intestinal smooth muscle cells, and from a P815 mast cell line used as a positive control [24]. Both mast cells and the morphologically identified

ICC produced bands on the agarose gel indicating the expression of *kit* mRNA. Intestinal smooth muscle cells did not express *kit* mRNA. Absence of the band in smooth muscle also indicates that contamination with the *kit* product is not present in these experiments, and thus false positives due to contamination are not a concern. Expression of the *kit* mRNA was found in 17 morphologically identified ICC.

The reversal potential of the spontaneous repetitive inward current was determined to be +10 mV (figure 7). The equilibrium potential for chloride was –75 mV, making it unlikely that $Cl^-$ contributed to the inward current. The equilibrium potentials for the cations present in the intra- and extra-cellular solutions were: $E_{Na}$=+73 mV, $E_{Cs}$=-100 mV and $E_{Ca}$ » +150 mV. This indicates that the inward current is probably carried by a mixture of cations. The I/V curve (Figure 7) shows a linear relationship between membrane potential and current amplitude, indicating that the current amplitude is only related to the driving force of the ions (equilibrium potential minus membrane potential). Hence, the initiation or activation of the inward current is voltage insensitive. This is the first time that such an inward current has been described in ICC. The study of the ionic basis of the tissue pacemaker activity had predicted the existence of such a current as the basis for the repetitive slow wave. Ion substitution and pharmacological experiments, both in the dog colon [7,14] and the mouse small intestine [19], suggested that the depolarizing phase of the slow wave was initiated by an inward current through a non - L- type calcium channel, or a non-specific cation channel. In addition, the slow waves occurred over a wide range of voltages, with little effect on frequency, indicating that the pacemaker current was not activated by a voltage change [25,26]. These data indicate that

the spontaneous inward current generated by ICC, observed in the present study, has the characteristics of a pacemaker current.

## 3.3 Conclusion

We have demonstrated that single isolated ICC, positively identified by morphology and presence of *kit* mRNA, exhibit a spontaneous rhythmic inward current which has the characteristics of a pacemaker current.

## 3.4 Methods

### *3.4.1 Electrophysiology*

Patch clamp experiments were carried out in standard whole cell configuration, with a pipette solution containing 130 mM Cs-gluconate, 10 mM EGTA, 5 mM HEPES, 10 mM NaCl, 4.5 mM ATP-Mg, and 0.1 mM GTP, adjusted to pH 7.35 with NaOH. The external solution contained: 160 mM NaCl, 2 mM $CaCl_2$, 10 mM glucose, 5 mM HEPES and 3 mM CsCl, adjusted to pH 7.35 with NaOH. The pipette resistance was 8 - 10 MΩ. Lowering the pipette resistance increased the rundown. With 2-2.5 MΩ electrodes, no spontaneous activity was observed, and 3-5 MΩ electrodes gave short-lived oscillations that seldom lasted longer than 30 seconds.

### *3.4.2 Single cell PCR*

mRNA harvest: mRNA from 1 mL of a P815 mast cell line suspension (ATCC) was harvested using an mRNA extraction kit (RNAeasy kit, MBI). mRNA from morphologically identified ICC and smooth muscle was harvested as follows. Patch pipettes with a resistance of 8-10 MΩ were filled with intracellular solution containing: CsCl 140 mM; HEPES 5 mM; NaCl 10 mM, ATP-Mg 3 mM, GTP 0.1 mM, 40 U RNAse inhibitor (RNAGuard, MBI), pH 7.35. The intracellular solution was drawn up into a syringe, and kept on ice until needed. mRNA was harvested by applying suction to the electrode under visual inspection. The electrode containing the cell contents was removed and the tip was broken into a PCR tube (Perkin Elmer) [27]. The contents of the pipette (approximately 0.5 μL) were expelled by applying positive pressure. Reverse Transcriptase protocol: The following were added to either the cell contents harvested by the patch pipette, or to the mast cell mRNA suspension: 0.5 μg/μL Oligo dT primers (18 dT, Mobix, McMaster University), 0.5 mM four deoxyribonucleoside triphosphates, 10 mM dithiothreitol, 50 mM Tris-HCl (pH 8.0), 75 mM KCl, 3 mM $MgCl_2$. 100 U reverse transcriptase was added (Superscript RT, MBI), and the reaction incubated for one hour at 36°C. Nested PCR: The first PCR reaction was performed by adding the following to the RT reaction mixture: 50 pmol of each outside primer (upstream base pair position 1642: 5'- TGT GAT GGT GCT CAC CTA CA, downstream base pair position 2088: 5'- GAG TCA CGC TTC CTT CTC AA), 200 μM of each deoxyribonucleotide, 1.5 mM $MgCl_2$, 10 mM Tris-HCl pH 8., 50 mM KCl, 2.5 U of Taq polymerase (MBI); and running the reaction for thirty cycles (92°C, 40 sec, 53°C, 40 sec, 72°C, 60 sec) followed

by 15 min of final extension at 72°C in a Perkin Elmer 2400 GeneAmp PCR system. The second PCR reaction was performed on 2 μL of the first PCR product, to which was added: 50 pmol of each inside primer (upstream base pair position 1695: 5'-GGA AGG TTG TCG AGG AGA TA, and downstream base pair position 1952: 5'-CCT TCA GTT CCG ACA TTA GG), 200 uM of each deoxyribonucleotide, 1.5 mM $MgCl_2$, 10 mM Tris-HCl pH 8., 50 mM KCl, 2.5 U of the Taq polymerase; and running the reaction for thirty-five cycles (92°C, 40 sec, 49°C, 40 sec, 72°C, 60 sec) followed by 15 min of final extension at 72°C. Ten microliters of the secondary PCR product was run in parallel with size markers on 1.5% agarose gel stained with ethidium bromide. The *kit* product from the first PCR reaction was 447 bp from cDNA, and approximately 12.9 kbp from genomic DNA. The *kit* product from the second PCR reaction was 258 bp from cDNA, and 614 bp from genomic DNA. Two introns lie in between the inside *kit* primer sets, consisting of a total of 356 bp, accounting for the length difference between cDNA and genomic DNA products in the second PCR reaction [28]. One intron is located between exons 11 and 12, at base pair position 1800, and is 267 bp in length. The other intron is located between exons 12 and 13, at base pair position 1906, and is 89 bp in length. The outside primers surround four introns: the two introns mentioned above, a 99 bp intron at base pair position 1673 between exons 10 and 11, as well as a 12 kbp intron at base pair position 2016 between exons 13 and 14. Thus, a total of approximately 12.4 kbp are contained within these four introns, accounting for the length difference between cDNA and genomic DNA products in the first PCR reaction.

### *3.4.3 Cell isolation*

Smooth muscle cells and ICC were isolated from the proximal small intestine of the mouse [20]. In brief, the isolated external muscle layers were incubated in M199 media (Canadian Life Technologies) with 1mg/ml trypsin for 45 min. Thereafter, incubation occurred in M199 with 1 mg/ml collagenase and 1mg/ml BSA for 20 min. The cells were then released by shaking, centrifuged and plated on rat tail collagen coated coverglass in M199 + 10% fetal bovine serum. The P815 mast cell line was purchased from American Type Culture Collection.

### *3.4.4 Electron microscopy*

EM study of the mouse small intestine cell culture was performed using the "inverted capsule embedding technique" [29]. The cultured cells, grown on glass cover slips, were placed face-upwards in a small Falcon Petri dish and fixed in situ with 2% glutaraldehyde in 0.05M sodium cacodylate buffer, pH 7.4, containing 1.2 mM $CaCl_2$, for 40 min at room temperature. Following fixation, tissue cultures were washed overnight in 0.1 M cacodylate buffer, containing 1.2 mM $CaCl_2$ in 0.05 M sodium cacodylate buffer (pH 7.4), postfixed with 1% $OsO_4$ in 0.05 M sodium cacodylate buffer (pH 7.4) for 40 min at room temperature, stained with saturated uranyl acetate for 30 minutes at room temperature, and dehydrated in graded ethanol and embedded in Epon 812. Thin sections were cut on a Reighert-Jung Ultracut E microtome, stained with lead citrate, and examined in a JEOL-1200 EX Biosystem electron microscope at 80 kV.

## 3.5 Acknowledgements

L. Thomsen was supported by the Carlsberg foundation of Denmark. The Medical Research Council of Canada is gratefully acknowledged for operating grant support, MRC Scientist awards to J.D. Huizinga and D. Andrews, an MRC scholarship to T. Robinson, and an MRC-PMAC scholarship to J. Lee. Electron microscopy was carried out by Dr. Irene Berezin.

## 3.6 Appendix

The contractile nature of the cells is displayed in video format to be accessed at http://www-fhs.mcmaster.ca/huizinga/nature.htm.

## 3.7 References


1. Szurszewski, J.H. in *Physiology of the gastrointestinal tract* (ed Johnson, L.R.) Vol.2, 383-422 (Raven Press, New York, 1987).

2. Huizinga, J.D., Thuneberg, L., Vanderwinden, J.M. & Rumessen, J.J. Interstitial cells of Cajal as pharmacological targets for gastrointestinal motility disorders. *Trends in Pharmacological Sciences* **18**, 393-403 (1997).

3. Thuneberg, L. in *Handbook of Physiology, the gastrointestinal system* (eds Schultz, G.S., Wood, J.D. & Rauner, B.B.) 349-386 (American Physiological Society, Bethesda,U.S.A., 1989).

4. Sanders, K.M. A case for interstitial cells of Cajal as pacemakers and mediators of neurotransmission in the gastrointestinal tract. [Review]. *Gastroenterology* **111**, 492-515 (1996).

5. Faussone-Pellegrini, M.S., Cortesini, C. & Romagnoli, P. Sull'ultrasturttura della tunica muscolare della porzione cardiale dell'esofago e dello stomaco umano con particolare riferimento alle cosiddette cellule interstiziali di Cajal. *Arch. Ital. Anat. Embriol.* **82**, 157-177 (1977).

6. Thuneberg, L., Rumessen, J.J. & Mikkelsen, H.B. Interstitial cells of Cajal - an intestinal impulse generation and conduction system? *Scandinavian Journal of Gastroenterology - Supplement* **71**, 143-144 (1982).

7. Huizinga, J.D., Farraway, L. & Den Hertog, A. Generation of slow-wave-type action potentials in canine colon smooth muscle involves a non-L-type $Ca^{2+}$ conductance. *J. Physiol. (Lond)* **442**, 15-29 (1991).

8. Lecoin, L., Gabella, G. & Le Douarin, N. Origin of the *c-kit* positive interstitial cells in the avian bowel. *Development* **122**, 725-733 (1996).

9. Klüppel, M., Huizinga, J.D., Malysz, J. & Bernstein, A. Developmental origin and Kit-dependent development of the interstitial cells of Cajal in the mammalian small intestine. *Developmental Dynamics* in press(1998).

10. Huizinga, J.D., Thuneberg, L., Kluppel, M., Malysz, J., Mikkelsen, H.B. & Bernstein, A. The *W/kit* gene required for interstitial cells of Cajal and for intestinal pacemaker activity. *Nature* **373**, 347-349 (1995).

11. Ward, S.M., Burns, A.J., Torihashi, S. & Sanders, K.M. Mutation of the proto-oncogene *c-kit* blocks development of interstitial cells and electrical rhythmicity in murine intestine. *J. Physiol. (Lond)* **480**, 91-97 (1994).

12. Komuro, T. & Zhou, D.S. Anti *c-kit* protein immunoreactive cells corresponding to the interstitial cells of Cajal in the guinea-pig small intestine. *J. Auton. Nerv. Sys.* **61**, 169-174 (1996).

13. Vanderwinden, J.M., Rumessen, J.J., Liu, H., Descamps, D., De Laet, M.H. & Vanderhaeghen, J.J. Interstitial cells of Cajal in human colon and in Hirschsprung's disease. *Gastroenterology* **111**, 901-910 (1996).

14. Ward, S.M. & Sanders, K.M. Upstroke component of electrical slow waves in canine colonic smooth muscle due to nifedipine-resistant calcium current. *J. Physiol. (Lond)* **455**, 321-337 (1992).

15. Malysz, J., Thuneberg, L., Mikkelsen, H.B. & Huizinga, J.D. Action potential generation in the small intestine of *W* mutant mice that lack interstitial cells of Cajal. *Am. J. Physiol.* **271**, G387-G399(1996).

16. Der-Silaphet, T.D., Malysz, J., Arsenault, A.L., Hagel, S. & Huizinga, J.D. Interstitial cells of Cajal direct normal propulsive contractile activity in the small intestine. *Gastroenterology* In Press(1998).

17. Lee, H.K. & Sanders, K.M. Comparison of ionic currents from interstitial cells and smooth muscle cells of canine colon. *J. Physiol. (Lond)* **460**, 135-152 (1993).

18. Tokutake, N., Maeda, H., Tokutomi, Y., et al. Rhytmic Cl- current and physiological roles of the intestinal c-kit positive cells . *Pflügers Arch. - Eur. J. Physiol.* **431**, 169-177 (1995).

19. Malysz, J., Richardson, D., Farraway, L., Christen, M.O. & Huizinga, J.D. Generation of slow wave type action potentials in the mouse small intestine involves a non-L-type calcium channel. *Can. J. Phys. Pharm.* **73**, 1502-1511 (1995).

20. Lee, J.C.F., Thuneberg, L., Farraway, L. & Huizinga, J.D. Plasticity in ICC isolated from the mouse small intestine *Dig. Dis. Sci.* **41**, 1904(1996).(Abstract)

21. Thuneberg, L. Interstitial cells of Cajal: intestinal pacemaker cells? *Adv. Anat. Embryol. Cell Biol.* **71**, 1-130 (1982).

22. Liu, L.W.C., Thuneberg, L. & Huizinga, J.D. Cyclopiazonic acid, inhibiting the endoplasmic reticulum calcium pump, reduces the canine colon pacemaker frequency. *J. Pharmacol. Exp. Ther.* **275**, 1058-1068 (1995).

23. Young, H.M., Ciampoli, D., Southwell, B.R. & Newgreen, D.F. Origin of interstitial cells of Cajal in the mouse intestine. *Dev. Biol.* **96**, 97-107 (1996).

24. Nocka, K., Majumder, S., Chabot, B., et al. Expression of *c-kit* gene products in known cellular targets of *W* mutations in normal and *W* mutant mice--evidence for an impaired C-kit kinase in mutant mice. *Genes & Development* **3**, 816-826 (1989).

25. Tomita, T. in *Smooth Muscle* (ed Bulbring, E.) 127-156 (Arnold, London, 1981).

26. Huizinga, J.D., Farraway, L. & Den Hertog, A. Effect of voltage and cyclic AMP on frequency of slow wave type action potentials in colonic smooth muscle. *J. Physiol. (Lond)* **442**, 31-45 (1991).

27. Lambolez, B., Audinat, E., Bochet, P., Crepel, F. & Rossier, J. AMPA receptor subunits expressed by single Purkinje cells. *Neuron* **9**, 247-258 (1992).

28. Gokkel, E., Grossman, Z., Ramot, B., Yarden, Y., Rechavi, G. & Givol, D. Structural organization of the murine c-kit proto-oncogene. *Oncogene* **7**, 1423-1429 (1992).

29. Glauert, A.M. *Fixation, dehydration and embedding of biological specimens* (North-Holland Publishing Company, Amsterdam. New York. Oxford, 1981).

## 3.8 Figure & Legends

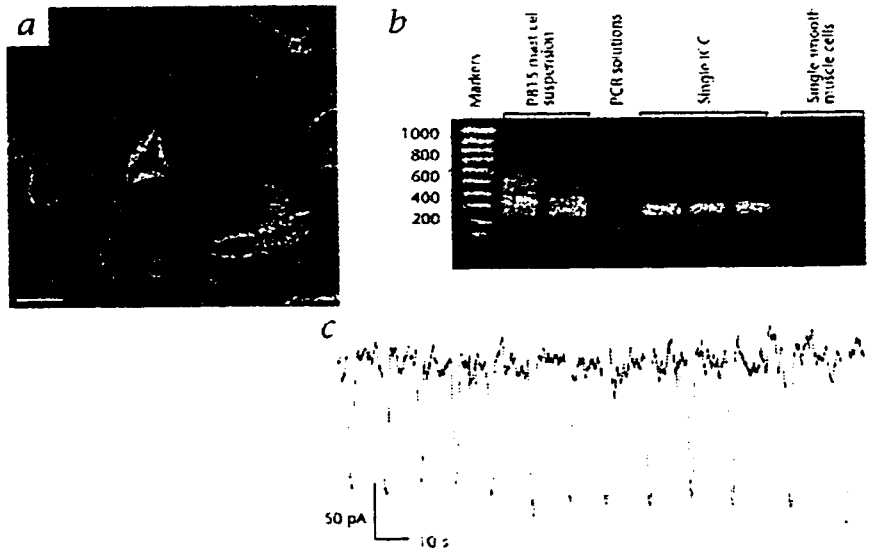


Figure 3-1 Identification and patch clamping of an isolated interstitial cell of Cajal (ICC)

a. A morphologically identified ICC. Magnification bar = 50μm

b. Single morphologically identified ICC revealed the 258 bp *kit* mRNA product on an agarose gel. A cell suspension from a p815 mast cell line also revealed the *kit* mRNA product, as well as other bands, which may be alternatively spliced mRNA products at 525 bp and 348 bp, indicating excision of the 267 bp intron alone, and the 89 bp intron alone, respectively. A faint band at 614 bp may correspond to genomic DNA from the nested primers. The PCR solutions alone were amplified to check for contamination with the *kit* product. Smooth muscle cells did not express *kit* mRNA.

c. Whole cell currents recorded from a morphologically identified interstitial cell

of Cajal, depicts spontaneous current oscillations every 5-10 seconds. This pattern was observed in 24 of 32 cells with a morphology as shown in figure 1A. The holding potential was -30 mV.


Figure 3-2 Electron microscopic analysis of ICC from a 4 day culture of the mouse small intestine

High magnification micrograph showing ultrastructural details of the ICC process. The cell membrane contains caveolae (arrowheads). The cytoplasm is characterised by the presence of numerous electron-dense mitochondria (m) and an aligned group of intermediate filaments (circle). These features distinguish this ICC from other cell types. Magnification bar = 500 nm.

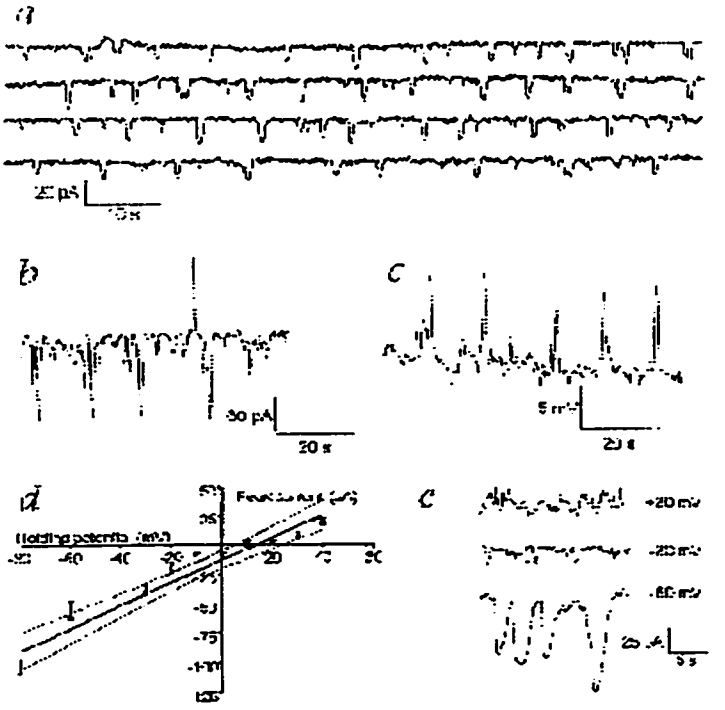

Figure 3-3 Dramatic appearance of a rhythmic spontaneous inward current generated by an ICC identified by light microscopy

a) The holding potential was -80 mV. The duration of the current pulses was 2.4 ± 0.5 s, with a pulse interval of 6.9 ± 0.7 s, which results in a frequency of 6.5 cycles per min. The current amplitude was 100.7 ± 5.2 pA. Note that this activity is recorded at room temperature and that tissue at this temperature generates slow waves at a similar frequency. One current oscillation is shown on an expanded time scale.

b) In the same cell, successive voltage and current clamp recordings were made in the continued presence of 5 μM nifedipine. While voltage clamping the cell to a holding potential of -50mV, a time independent spontaneous rhythmic inward current can be seen to occur at ~ 5 cycles per min (large current oscillations). Switching to current

clamp, it was observed that spontaneous voltage depolarizations occurred also at ~ 5 cycles per min (large voltage oscillations). Occasionally a spontaneous outward current pulse was observed.

c) The linear I/V relationship of the spontaneous inward current reveals that the ion channel carrying the current is not voltage-activated. The reversal potential of +10 mV indicates that the ion channel is conducting a non-specific cationic current. N=6. Dotted lines indicate the average standard error.

d) Current recordings shows a typical experiment with currents recorded at +10, -30 and -60 mV holding potentials

.

# Chapter 4: Smooth Muscle Heterogeneity in the Mouse Small Intestine

Jonathan C.F. Lee and Jan D. Huizinga

Intestinal Disease Research Program, McMaster University, Hamilton, Ontario, Canada

1200 Main Street West, L8N 3Z5

Running title: Smooth muscle cell heterogeneity in the mouse small intestine

Keywords: smooth muscle, ionic currents, electrophysiology, patch clamp

Correspondence address

Jan D. Huizinga
Health Science Center Room 3N5C
(905) 525-9140 ext. 22590
fax: (905) 522-3454
email: huizinga@mcmaster.ca

## 4.a Abstract


1. The intestinal musculature actively propagates the slow waves generated by interstitial cells of Cajal in the Auerbach's plexus, and produces spiking action potentials when appropriately stimulated.
2. It is generally assumed that the muscularis consists of one uniform type of smooth muscle cell. In intact tissue, the smooth muscle syncytium is coupled to produce tissue activities that are summations and/or averages of individual events. By examining intestinal smooth muscle cells in isolation, the different cell types can be documented.
3. After careful examination of whole cell currents, four main cell types were identified by the characteristics of the major outward currents: cells with a fast transient outward current ($I_{to,f}$), cells with a slow transient outward current ($I_{to,s}$), cells with a delayed rectifier-like current ($I_{dr}$), and cells with prominent spontaneous outward currents ($I_{stoc}$).
4. The $I_{to,f}$ component was present in 49% of cells examined and demonstrated full voltage inactivation with a –30 mV prepulse. The IV plots showed a peak chord conductance of 0.7±0.6 nS/pF. The other outward current was sensitive to inhibition by 5 mM TEA.
5. In 31% of cells showed only a fast activating and slow inactivating outward current ($I_{to,s}$). This $I_{to,s}$ had a peak chord conductance of 1.4±0.6 nS/pF and showed only moderate inhibition to 5 mM TEA.

6. In 12% of cells displayed a delayed rectifier-like outward current ($I_{dr}$). This current had a peak chord conductance of 0.8±0.4 nS/pF and was moderately sensitive to inhibition by 5 mM TEA.
7. In the remaining 8% of cells had dynamic STOC activity. The STOC component was blocked completely by 5 mM TEA to reveal a fast activating and strongly inactivating transient outward current.
8. The present study makes it clear that caution must be exercised in examining isolated intestinal smooth muscle cells. Future experiments need to be done in context within each cell type.

## 4.1 Introduction

The circular and longitudinal external muscle layers of the mouse small intestine generate indistinguishable electrical activity. Slow waves, initiated by interstitial cells of Cajal in the Auerbach's plexus area, actively propagate into both muscle layers. In addition, smooth muscle cells themselves generate action potentials when appropriately stimulated, which appear at the plateau phase of the slow waves. During peristaltic activity both muscle layers generate phasic contractile activity.

It was generally assumed that the musculature consists of one uniform type of smooth muscle cell. However, recent reports have challenged this notion (Hara *et al.* 1986; Thornbury *et al.* 1992; Makhlouf & Murthy, 1998). To understand properties of the musculature, one approach is to study smooth muscle cells in isolation. In examining the properties of single cells, it became clear that several distinct cell types collaborate within this musculature. From such observations, the hypothesis emerges that tissue activity comes about through the summation/averaging of the activities of different cell types from being coupled within a syncytium. The objective of the present study was to document the different cell types.

## 4.2 Methods

### *4.2.1 Isolation of Single Smooth Muscle cells*

Adult female mice (20-25g) were sacrificed and an ileal segment was removed. After washing in ECS, the segment was placed in pre-equilibrated M199 media and the tunica muscularis was removed by sharp dissection. Previous examination have shown

the tunica muscularis to be separated along the deep muscular plexus margin. The dissected muscularis was carefully cut into small pieces (~1-2 mm) before it was placed into dissociation solution A + 1 mg/ml trypsin for 15 mins, then 30 mins at 37°C. The supernatant was carefully removed and disscociation solution B + 3 mg/ml collagenase + 1mg/ml BSA was added and allowed to incubate for 15 mins, then 20 mins. The cells were released by shaking. The cell suspension was carefully layered on top of 20% (w/v) Ficoll and spun at 15 g for 15 mins. The cell band located at the interface was removed and plated onto collagen coated coverslips. The cells were maintained in 5% $CO_2$/37°C until needed.

### *4.2.2 Electrophysiology*

Cells were not used beyond 5 days post-isolation because it was impossible to get a stable tight seal with a glass pipette. The cells were continuously perfused with extracellular solution (ECS). Whole cell electrical activity was recorded using conventional disrupted patch. Briefly, the disrupted patch was achieved by sharp suction pulses. Pipettes were made using a Sutter micropipette puller to typical access resistances of 3-5 MΩ. Electrical activity was recorded using the Axopatch 1B amplifier (Axon Instruments, California) and pClamp v6.01 acquisition software. The pipette was lowered onto the cell surface and suction was applied. Upon formation of a tight seal, electrical continuity was made to the interior of the cell by either perforation by disrupting the membrane patch, and then the appropriate whole cell voltage protocols were performed.

A standard voltage clamp protocol was used. Briefly, an appropriate prepulse of either –30 or –100 mV were applied for 500 ms to test for voltage inactivation before the test pulses from –70 to +60 mV was applied for 500 ms. Unless specified, a –100 mV prepulse was used before the test pulses to get the whole cell profiles.

## 4.3 Results

### *4.3.1 Different SMC have different Whole Cell Currents*

In order to ascertain if the variations were from a single distribution, the whole cell currents from 104 different SMC were analyzed for inactivation rates ($\tau$ of inactivation), activation times (time to peak activation of outward currents), takeoff threshold voltages (membrane potential at which there is activation of outward currents) and peak chord conductances.

Histogram plots of binned data showed different distributions (figure 1). The inactivation rates ($\tau$) and activation times showed a skewed distribution toward faster times, while the takeoff voltages and chord conductances showed more of wide spread distribution. Although all distributions consisted of multiple peaks, the distributions of inactivation $\tau$ and chord conductances most clearly showed multiple peaks that suggest of at least 4 different populations. After re-examining the whole cell currents, four main groups were chosen. In Figure 2, the four representative whole cell current groups are shown.

Based on the characteristics of the major outward currents, the following four major cell types were identified:

1. Cells with fast transient outward currents (Figure 2a), 49.0% (51/104 cells). The distinguishing feature of this group is the presence of a fast activating (fastest t <15 ms) and inactivating (fastest $\tau$ <100ms) transient outward current ($I_{to,f}$). This current is exposed once other currents are blocked with TEA. Cells with the fast $I_{to,f}$ frequently have other outward currents that show slower inactivation ($\tau$ >150 ms).
2. Cells with a slow transient outward current (Figure 2b), 31% (32/104 cells). A slow transient outward current, ($I_{to,s}$) is predominant with an inactivation $\tau$ >150 ms. Small differences in the properties of slow transient outward currents, such as the activation rates, may suggest the presence of more than one $I_{to,s}$.
3. Cells with a predominant delayed rectifier current (Figure 2c) 12.% (13/104 cells). In this group, the predominant outward current was a slow activating ($\tau$ ~ 25ms) current with little or very slow inactivation ($\tau$ ~ 600 ms), a delayed rectifier-like current ($I_{dr}$). Frequently, the inward $Ca^{2+}$ current, $I_{ca}$ is present.
4. Cells with prominent spontaneous transient outward current ($I_{STOC}$) activity (Figure 2d), 8% (8/104 cells).

These cells generally have a fast activating ($\tau$ <10 ms) and fast inactivating ($\tau$ < 100 ms) outward current. The STOCs are only slightly affected or not affected at all by application of intracellular $Ca^{2+}$ chelators. These cells exhibit hyperpolarizations when not under voltage clamp as well as spontaneous rhythmic contractions. Other smooth

muscle cells can have STOC activity that disappears once $Ca^{2+}$ chelators in the pipette solution are allowed to diffuse in the cytoplasm (disrupted patch configuration).

### *4.3.2 SMCs with $I_{to,f}$*

Cells with a fast transient outward current were easily recognized since the $I_{to,f}$ has a lower voltage threshold than the other outward currents, and would be expressed at more hyperpolarized potentials (figure 3). The typical voltage threshold for $I_{to,f}$ was -44±10 mV. Since $I_{to,f}$ was seen to have significant inactivation, maximal activation of $I_{to,f}$ was promoted by a prepulse of -100 mV for 500 ms prior to the test pulses in order to remove prior voltage inactivation.

In all cells with $I_{to,f}$ present, $I_{to,f}$ was completely inactivated with a -30 mV prepulse, also for 500 ms, before the test pulses. In order to reveal the currents inactivated by the -30 mV prepulse, the whole cell currents with the -100 mV prepulse were subtracted from the currents with -30mV prepulse. The subtraction currents show that $I_{to,f}$ was not the only current inactivated - frequently a slower inactivating current ($I_{to,s}$) (19/36 cells) and/or a delayed rectifier-like current ($I_{dr}$) (8/36 cells) were also inactivated. Because of the overlap in inactivation ranges between different outward currents, solely using inactivating voltage prepulses can not be used for isolating $I_{to,f}$.

Typical chord conductances found by I/V plots of peak currents were normalized with cell capacitance to yield a peak chord conductance for Ito,f of 0.7±0.6 pS/pF (n=51). After voltage inactivation was allowed to proceed to steady state, $I_{to,f}$ was found not to

inactivate completely but settled to a steady state outward current that was 24% of the peak current.

Using TEA to isolate $I_{to,f}$ (figure 4), the $I_{to,f}$ had a highly variable peak current with an average normalized amplitude of 39±37 pA/pF and activated with an average time to peak activation of 5.4±3.1 ms (n=25). The inactivation was relatively rapid with $\tau$ of 28.4±18.3 ms such that 76±16% of the peak current was removed by inactivation.

The outward currents blocked by TEA can be visualized by subtracting the control whole cell currents by the currents remaining after the addition of the TEA. The inhibition by TEA was observed to be fully reversible. The TEA sensitive outward currents were further examined using the currents elicited by a standard +30 mV test pulse and had slower activation and inactivation than $I_{to,f}$. These currents had a normalized amplitude of 56±47 pA/pF and an average time to full activation of 20±9 ms. These currents showed slow inactivation with an average $\tau$=238±93 ms and inactivated 54±20% from peak amplitudes. The I/V plots showed $I_{to,s}$ had an average takeoff at -33± 12 mV and a chord conductance density of 1.3±0.7 nS/pF.

### *4.3.3 SMCs with $I_{to,s}$*

The whole cell currents in this category have slower inactivation rates than $I_{to,f}$ ($\tau$ at +30 mV > 150 ms). The fast activating, slow inactivating transient outward current ($I_{to,s}$) represented approximately 31% (32/104) of cells examined (figure 5). The I/V relationship revealed the average takeoff to be -38±10 mV with a peak chord

conductance of 1.4±0.6 nS/pF. The average time to full activation was 13±7 ms for the standard +30 mV test pulse. The peak current was seen to have a high degree of variability and had an average normalized peak amplitude of 64±37 pA/pF. The current inactivated 38±14% with $\tau$=474±205 ms with the standard +30 mV test pulse. With the -30 mV prepulse, $I_{to,s}$ were inactivated on average by 54±20%. With 5 mM TEA, $I_{to,s}$ was inhibited by 71±25% (n=4) (figure 6).

### *4.3.4 SMCs with $I_{dr}$ component*

Certain cells were found to have even slower activating outward currents than $I_{to,s}$ (12% (13/104) cells examined) (figure 7). They showed rounded peaks and little or no inactivation, very similar to the delayed rectifier currents found in other smooth muscle cells. This delayed rectifier-like current ($I_{dr}$) activated to peak at 43±18 ms with a typical normalized amplitude of 37±20 pA/pF. Only 38% (5/13) of the cells with only $I_{dr}$ present had significant inactivation over time (500 ms test pulse) with $\tau$=381±195 ms during the +30 mV test pulse. There was only slight inactivation such that only 17±8% of the peak current was inactivated at the +30 mV test pulse. This current was found to be sensitive to voltage inactivation since a -30 mV prepulse typically inactivated the peak currents by 56±15%. The typical takeoff voltages were -33±11 mV and $I_{dr}$ would activate to a peak chord conductance of 0.8±0.4 nS/pF.

The $I_{dr}$ can be blocked with 5 mM TEA to result in 48±32% inhibition (n=6) of the peak currents (figure 8). The inhibition by TEA was readily reversible upon washout.

### *4.3.5 SMCs with $I_{stoc}$*

Although small outward current oscillations can be seen in all smooth muscle cells, certain cells (8% or 8/104 cells) were observed to have large outward current oscillations which increased dramatically in frequency and amplitude when the cell was depolarized (>-20 mV) (figure 9). These outward current oscillations are known as STOCs - spontaneous transient activations of $I_{K,Ca}$ in response to quantal releases of $Ca^{2+}$ from intracellular stores. It was interesting to note that even in the presence of high concentrations of $Ca^{2+}$ chelators in the pipette solution (10 mM EGTA), not all STOC activity could be sequestered.

Cells with STOCs have at least two major outward currents. One outward current would be the $Ca^{2+}$ activated K current ($I_{K,Ca}$), responsible for the STOCs. The other current was a fast activating and slow inactivating transient outward current. The $I_{K,Ca}$ was difficult to characterize because transitory oscillating nature of STOC activity. Fortunately, $I_{K,Ca}$ can be easily blocked by TEA (figure 10).

A fast activating, slow inactivating component had a normalized peak current amplitude of 60.7±15.3 pA/pF and a time to peak activation of 6±4 ms. The IV plots revealed the voltage takeoff to be -37±12 mV with a peak chord conductance of 1.6±0.9 nS/pF. This outward current inactivated 87±22% during the +30 mV test pulse and was almost completely inactivated by a -30 mV prepulse.

## 4.4 Discussion

Some variability in whole cell currents was expected due to experimental conditions. But larger variability can arise from true differences that exist natively in the single cells from which whole cell currents are derived (Michelakis *et al.*, 1997). The objective of this study was to address the large variability seen between cells examined. Obvious differences between smooth muscle cells were not seen. Under the phase contrast microscope, isolated single smooth muscle cells appear morphologically similar. Differences in size and shape can be attributed simply to different states of contraction. Other variabilities were seen as different functional activities. After isolation, a small population of SMCs (<5%) was observed to spontaneously and rhythmically contract. Initial recording with whole cell patch clamp showed some SMCs (<5%) to have spontaneous electrical activity in the form of spiking depolarizations or spontaneous hyperpolarizations from STOC activity. Since the functional ability of smooth muscle cells are determined by its ionic membrane currents, the differential expression of these currents can reflect their different functions.

Pooling all cell current recordings together, the distributions of rates of inactivation and chord conductances were very suggestive of multiple populations. An examination of whole cell recordings from the smooth muscle layers of the mouse small intestine has revealed at least four different groups of whole cell currents. The four main groups were: 1) cells containing a prominent $I_{to,f}$ with other currents; 2) cells with a slower inactivating $I_{to,s}$; 3) cells with only a slower activating and inactivating $I_{dr}$; 4) cells

with prominent STOC activity. Each major current was found to have distinctive kinetics and sensitivity to TEA.

The different cell types observed in the present study in the mouse small intestine could be related to cells coming either from the circular or longitudinal muscle. The motility patterns from longitudinal and circular smooth muscle have been observed to be different (Sarna, 1993). Functional heterogeneity has been suggested in different smooth muscle layers of the external smooth muscle layers (Hara *et al.* 1986; Thornbury *et al.* 1992; Makhlouf & Murthy, 1997). In intact tissue, both spiking and slow wave activity can be recorded in circular or longitudinal muscle layers. In isolated smooth muscle layers, the longitudinal muscle layer show fast spiking activity while the circular muscle layer can show slower spiking activity and/or slow wave activity if the ICC layer was intact (Lui *et al.*, 1993, Hara *et al.* 1986). Makhlouf & Murthy (1997) has shown that the circular and longitudinal smooth muscle layers use different signalling cascades in response to CCK-A stimulation. Upon activation by CCK-A, the circular smooth muscle layer transduces the excitatory signal mostly through the PLC-$IP_3$/DAG pathway leading to IICR type initiation of contraction. Conversely, the longitudinal smooth muscle layer mobilizes the $PLA_2$-AA pathway leading to CICR triggering of contraction. The differences seen between circular and longitudinal muscle would suggest the smooth muscle cells from each layer should be different. Differences in the behavior of intracellular $Ca^{2+}$ stores have been observed in bronchus versus tracheal smooth muscle (Sieck *et al.*, 1997).

The demonstration of smooth muscle cell heterogeneity between different external smooth muscle layers cannot be easily investigated in the mouse intestine because the external smooth muscle layers cannot be reliably separated. It is also very unlikely that this would be the case since both layers generate the same type of electrical activity when intact tissue is examined. This contrasts with colonic tissue where even in intact tissue, differences can be observed throughout the circular muscle layer and in particular between the circular and longitudinal muscle layer (Faussone-Pellegrini, 1985; Smith *et al.* 1987; Liu *et al.* 1997).

Besides dissimilarities in function seen in different organs of the gastrointestinal system, some functional heterogeneity can be seen within the same organ, such as the small intestine (Siegle *et al.*, 1990; Halayko *et al.*, 1997). The composition of smooth muscle have been suggested to be different at various regions of the small intestine since smooth muscle show differential expression of cytoplasmic isoactins from duodenum to ileum (Liddell *et al.* 1993). In other smooth muscle systems, smooth muscle have been shown to show different aspects of functional heterogeneity in vasculature (Archer, 1996; Dempsey *et al.*, 1997; Frid *et al.*, 1994) and in airway (Ma *et al.*, 1997; Minshall *et al.*, 1997; Siech *et al.*, 1997; Stephens *et al.*, 1998). Although there are information of smooth muscle heterogeneity within different smooth muscle organs, there is a paucity of information on differences in smooth muscle within the thickness of the same region of the smooth muscle organ. This aspect of smooth muscle heterogeneity remains to be adequately addressed (Eddinger *et al*, 1997).

The presence of different intestinal smooth muscle cell types within the same region makes adds an extra degree of difficulty in characterizating each isolated cell. Ideally, investigation into individual differences can be achieved by examining single cells in intact tissue, such that the differences can be correlated with its histological location. Due to experimental reasons, patch clamp studies in smooth muscle require single cells. In the mouse, it is extremely difficult to accurately separate the distinct layers of the tunica muscularis. In larger animals (rats, guinea pigs, *etc.*) it is possible to separate layers, and would therefore be the logical choice for future studies. Continuing experiments where the *tunica muscularis* will be fully dispersed, a large N number is needed in order to characterize, first, the different types of cells present, and second, the different currents present in each cell type.

From the whole cell current profiles, it is possible to ascribe some functional aspects to them. As this study suggests, most SMCs (49%) display multiple outward currents, well suited to be an all-purpose, generic smooth muscle cells. The minority have more specific currents with less variety, which can be interpreted for more specific tasks. The majority of SMCs ($I_{to,f}$) were found to have a complex mixture of outward currents with little or no significant voltage activated inward currents. This would suggest these cells are largely inexcitable by voltage but are probably important in wave shaping and in the overall control of excitability. Cells with less complicated outward currents ($I_{to,s}$ & $I_{dr}$) would be expected to have lower involvement in controlling excitatory events than in controlling overall excitability. It was noticed that predominantly cells containing $I_{dr}$ also have significant $I_{Ca}$. Therefore, only a minority of smooth muscle cells have significant

voltage gated $Ca^{2+}$ influx. Another population of smooth muscle cells have predominantly $Ca^{2+}$-activated K currents. Similar results have been seen in vascular smooth muscle cells from the rat pulmonary artery (Archer *et al.*, 1996). Dispersed smooth muscle cells from the conduit pulmonary artery media showed three electrophysiologically distinct cell types. One cell type had $Ca^{2+}$-activated K currents dominant while another had a delayed-rectifer K current dominant. The third cell type showed outward currents from both groups-$K_{Ca}$ and $K_{DR}$. While it has been shown in systemic and pulmonary arteries that phenotypically and physiologically distinct populations of cells can exist within the same arterial segment (Archer *et al.*, 1996; Frid *et al.*, 1994; Wohrley *et al.*, 1995), similar studies have not been done in intestinal smooth muscle. Thus, this study is the first to present results in support of heterogeneity within the same intestinal segment, similar to the arrangement seen in arterial smooth muscle.

Contraction in intestinal smooth muscle is associated with an elevation in intracellular $Ca^{2+}$ (Makhlouf & Murthy, 1997) - this elevation result from extracellular $Ca^{2+}$ influx. The smooth muscle cells with prominent inward $Ca^{2+}$ currents can serve as sensitive "triggers" to depolarizing stimuli. Alternatively, another source for intracellular $Ca^{2+}$ elevation would be release from $Ca^{2+}$ stores, which appear as another minority of smooth muscle cells that is reflected by dynamic STOC activity. In general, all smooth muscle cells are ultimately capable of auto-excitation and contraction in that they all can mechanically contract with sufficient excitation.

The present study makes it clear that pharmacological studies on currents observed in single cells cannot be done simply on any cell in isolation. To be meaningful, whole cell profiles have to be assessed before pharmacological experiments in context with each cell type. The existence of multiple distinct smooth muscle types suggests that there is a functional subspecialization within the external smooth muscle layers of the gut, and that each smooth muscle cell type may have a specific functional role as dictated by their different whole cell currents.

## 4.5 Bibliography

ARCHER, S.L. (1996). Diversity of phenotype and function of vascular smooth muscle cells. *Journal Laboratory Clinical Medicine* **127**, 524-529.

ARCHER, S.L., HUANG, J.M.C., REEVE, H.L., HAMPL, V., TOLAROVA, S., MICHELAKIS, E.D., WEIR, G.K., (1996). Differential distribution of electrophysiologically distinct myocytes in conduit and resistance arteries determine their response to nitric oxide and hypoxia. *Circulation Research* **78**, 431-442.

EDDINGER, T.J., MEER, D.P. (1997). Smooth muscle heterogeneity: Does the striated muscle model apply? *Canadian Journal of Physiology & Pharmacology* **75**, 861-868

FAUSSONE PELLEGRINI, M. S. (1985). Ultrastructural peculiarities of the inner portion of the circular layer of the colon. II. Research on the mouse. *Acta Anat.(Basel)* **122**, 187-192.

FRID, M., MOISEEVA, E., STENMARK, K. (1994). Multiple phenotypically distinct smooth muscle cell populations exist in the adult and developing bovine pulmonary arterial media *in vivo*. *Circulation Research* **75**, 669-681.

HALAYKO, A.J., RECTOR, E., STEPHENS, N.L. (1997). Characterization of molecular determinants of smooth muscle cell heterogeneity. *Canadian Journal of Physiology & Pharmacology* **75**, 917-929.

HARA, Y., KUBOTA, M. & SZURSZEWSKI, J. H. (1986). Electrophysiology of smooth muscle of the small intestine of some mammals. *Journal of Physiology - London* **372**, 501-520.

LIDDELL, R.A., SYMS M., McHUGH, K.M. (1993). Heterogeneous isoactin gene expression in the adult rat gastrointestinal tract. *Gastroenterology* **105**, 347-356.

LIU, L. W. C., FARRAWAY, L., BEREZIN, I. & HUIZINGA, J. D. (1997). Interstitial cells of Cajal: Mediators of communication between longitudinal and circular muscle cells of canine colon. *Cell & Tissue Research*

LIU, L.W.C., HUIZINGA, J.D. (1993). Electrical coupling of circular muscle to longitudinal muscle and interstitial cells of Cajal in canine colon. *Journal of Physiology – London* **470**, 445-461

MA, X., LI, W., STEPHENS, N.L. (1997) Heterogeneity of airway smooth muscle at tissue and cellular levels. *Canadian Journal of Physiology & Pharmacology* **75**, 930-935

MAKHLOUF, G. M. & MURTHY, K. S. (1997). Signal transduction in gastrointestinal smooth muscle. [Review] [92 refs]. *Cellular Signalling 1997 May-Jun;9(3-4):269-76* 269-276.

MICHELAKIS, E.D., REEVE, H.L., HUANG, H.M., TOLAROVA, S., NELSON, D.P., WEIR, E.K., ARCHER, S.L. (1997). Potassium channel diversity in vascular smooth muscle cells. *Canadian Journal of Physiology & Pharmacology* **75**, 889-897.

SARNA, S.K. (1993). Gastrointestinal longitudinal muscle contractions. *American Journal of Physiology* **265(1 Pt 1)**, G156-64

SIECK, G.C., KANNAN, M.S., PRAKASH, Y.S. (1997). Heterogeneity in dynamic regulation of intracellular calcium in airway smooth muscle cells. *Canadian Journal of Physiology & Pharmacology* **75**, 878-888

SIEGLE S.M., BUHNER, S., SCHEMANN, M., SCHMID, H.R., EHRLEIN, H.J. (1990). Propagation velocities and frequencies of contractions along the canine small intestine. *American Journal of Physiology* **258(5 Pt 1)**, G738-44.

SMITH, T. K., REED, J. B. & SANDERS, K. M. (1987). Interaction of two electrical pacemakers in muscularis of canine proximal colon. *American Journal of Physiology* **252**, C290-C299.

STEPHENS, N.L., HALAYKO, A.J. (1998). Airway smooth muscle contractile, regulatory and cytoskeletal protein expression in health and disease. *Comparative Biochemistry & Physiology-B: Biochemistry & Molecular Biology* **119:3**, 415-424.

THORNBURY, K. D., WARD, S. M. & SANDERS, K. M. (1992). Outward currents in longitudinal colonic muscle cells contribute to spiking electrical behavior. *American Journal of Physiology* **263**, C237-C245.

WOHRLEY, J., FRID, M., MOISEEVA, E., ORTON, E., BELKNAP, J., STENMARK, K. (1995). Hypoxia selectively induces proliferation in a specific subpopulation of smooth muscle cells in the bovine neonatal pulmonary arterial media. *Journal of Clinical Investigations* **96**, 273-281

## 4.6 Figures & Legends

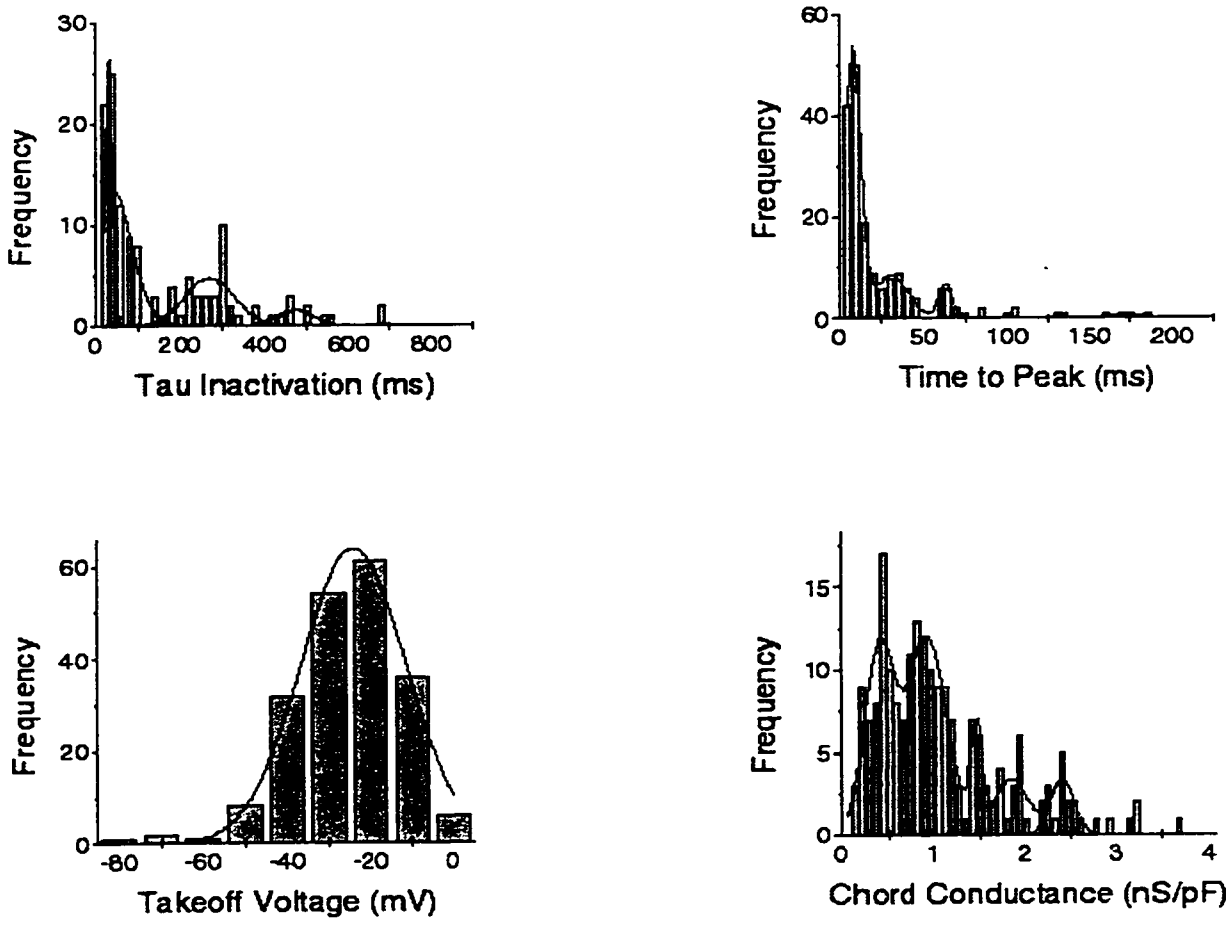


Figure 4-1 Distributions of different whole cell current parameters

Various whole cell current parameters were measured from 104 smooth muscle cells and plotted as frequency distributions. Distributions were fitted by the least squares method.

A. All whole cell currents examined showed some form of voltage inactivation as assessed by either by a -30 mV prepulse or by examining the whole cell currents for time dependent inactivation. From the currents evoked by a –100 mV prepulse to

remove inactivation and a +30 mV test pulse, the time dependent inactivation was fitted to give a tau ($\tau$) value. The frequency distribution of tau inactivation values do not follow a normal distribution. Up to 4 distinct Gaussian distributions can be fitted to correspond to means of 30±14 ms, 39±93 ms, 269±117 ms, and 472±87 ms.

B. The time from the start of the test pulse to the peak current amplitude was measured and plotted as a frequency distribution. Up to 4 distinct Gaussian distributions can be fitted with corresponding means of 8±9 ms, 30±21 ms, 63±8 ms, and 173±24 ms.

C. From the standard protocol of a –100 mV prepulse and varying test pulses from –70 mV to +60 mV, the current-voltage (IV) relationship can be plotted. The voltage point that produces active current was taken to be the takeoff voltage. The frequency distribution of takeoff voltages was uninformative because it corresponded to a single normal distribution with the center at –20±10 mV.

D. Again from the IV plots, chord conductances were normalized with cell capacitances and plotted as a frequency distribution. Up to 5 distinct Gaussian distributions can be fitted with the means at 413±318 pS/pF, 929±422 pS/pF, 1.5±.0.1 nS/pF, and 2.4±0.3 nS/pF.

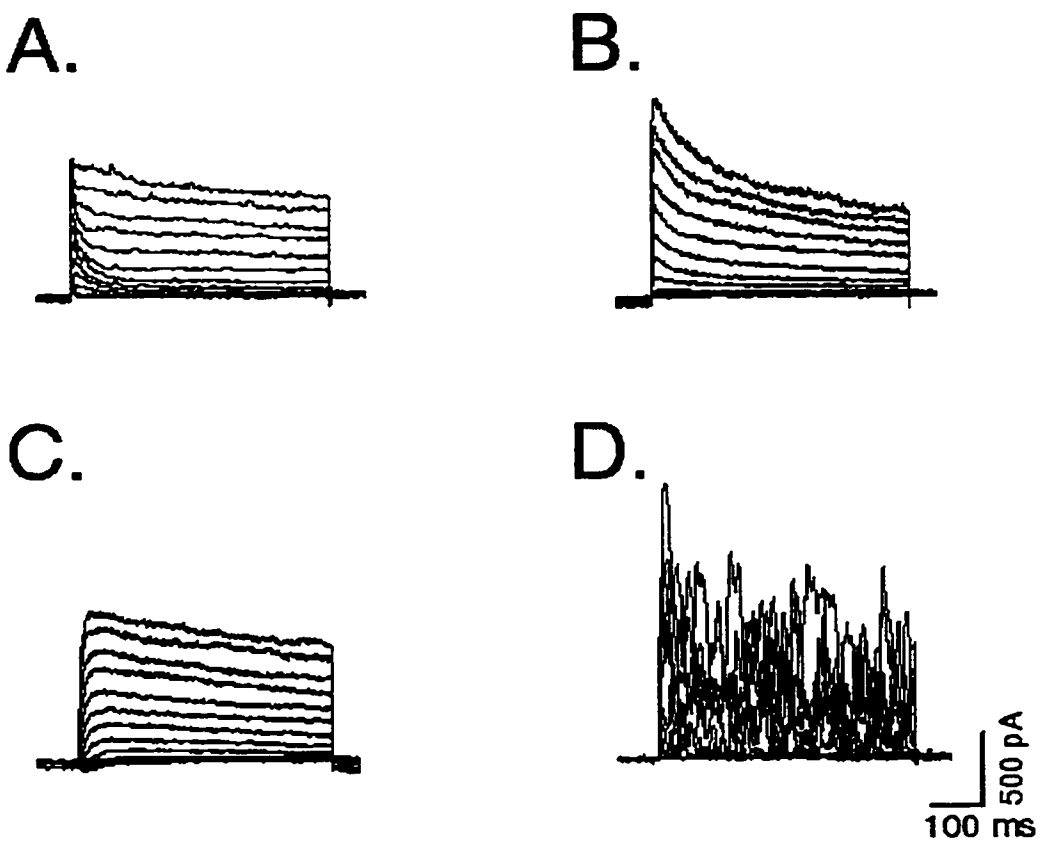


Figure 4-2 Whole cell current profiles of four main smooth muscle cell types

Using a standard voltage protocol of a –100 mV prepulse and test pulses from –70 to +60 mV, whole cell currents were evoked in different single smooth muscle cells. Four main cell types can be identified from their whole cell current profiles.

A. Cells with a fast transient outward current ($I_{to,f}$). Usually buried within another outward current, the distinctive fast activating and inactivating transient outward current can be seen.

B. Cells with a slow transient outward current ($I_{to,s}$). The slow monoexponential inactivation of this outward current suggests the presence of only one dominant outward current.

C. Cells with a delayed rectifier-like outward current ($I_{dr}$). The dominant outward current is slow activating and very slow inactivating.

D. Cells with spontaneous outward current oscillations ($I_{stoc}$). While all smooth muscle cells show some form of STOCs, the cells of this type have prominent STOCs of high amplitude and frequency. Another important distinguishing characteristic is that STOC activity could not be abolished by up to 10 mM EGTA in the pipette.

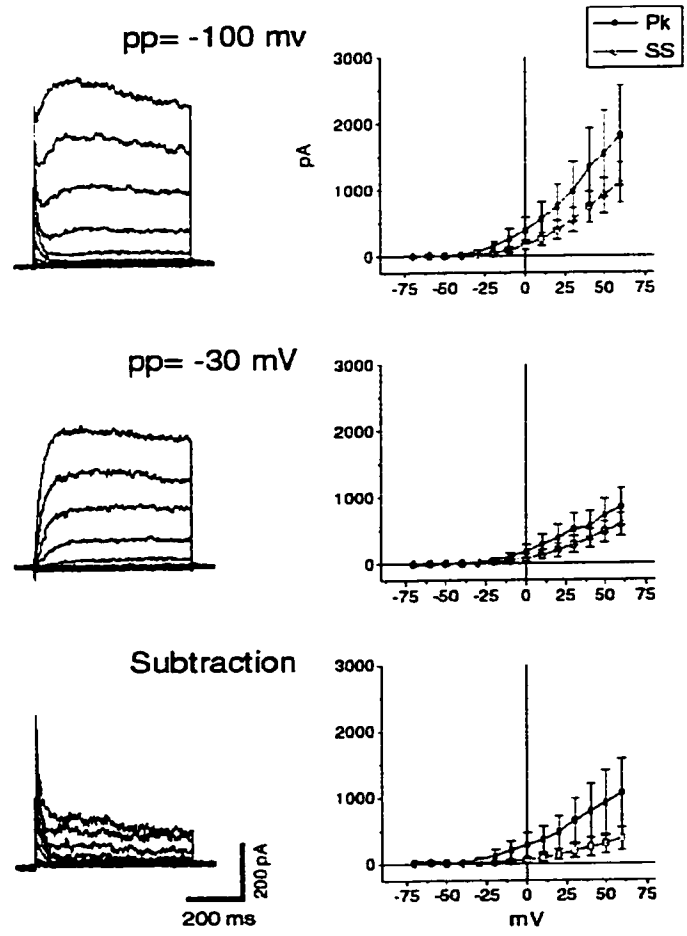


Figure 4-3 Voltage sensitivity of SMCs with $I_{to,f}$

With a prepulse of –100 mV, voltage inactivation would be removed and the full whole cell currents would be expressed. In 49% (51/104 cells), the whole cell current profile shows a prominent $I_{to,f}$ component. This $I_{to,f}$ component was fully inactivated by a –30 mV prepulse, leaving a slower activating and inactivating outward current. The IV plots show $I_{to,f}$ typically has a lower voltage threshold and significant voltage inactivation, as seen by the large differences between peak and steady state currents. The $I_{to,f}$ had a peak chord conductance of 0.7±0.6 nS/pF while the other outward current had a peak chord conductance of 1.2±0.7 nS/pF.

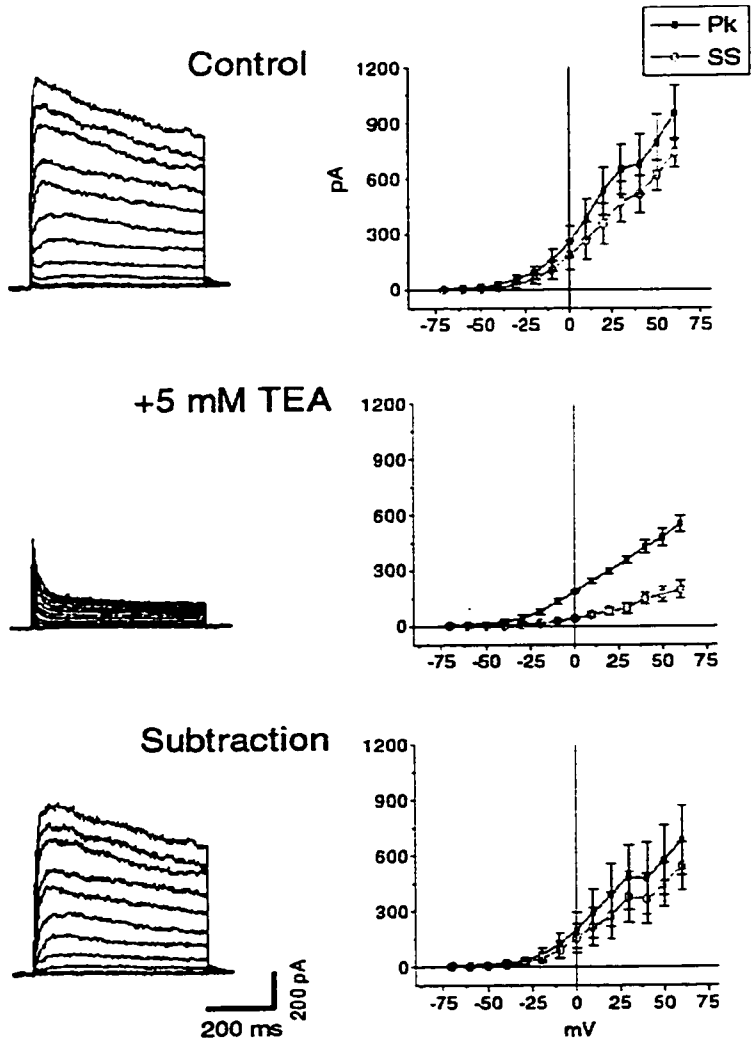


Figure 4-4 TEA sensitivity of SMCs with $I_{to,f}$

The addition of 5 mM TEA abolished the slower activating/inactivating component leaving only $I_{to,f}$. Subtraction of the Control currents with the currents resistant to 5 mM TEA ($I_{to,f}$) produced only the slow activating/inactivating outward current component. This slow activating/inactivating component does inactivate slightly with the –30 mV prepulse, as seen by the comparison of the currents with TEA sensitivity

(current figure) with the currents obtained by inactivating with a –30 mV prepulse (figure 3). Therefore, the –30 mV prepulse is not sufficient to isolate $I_{to,f}$.

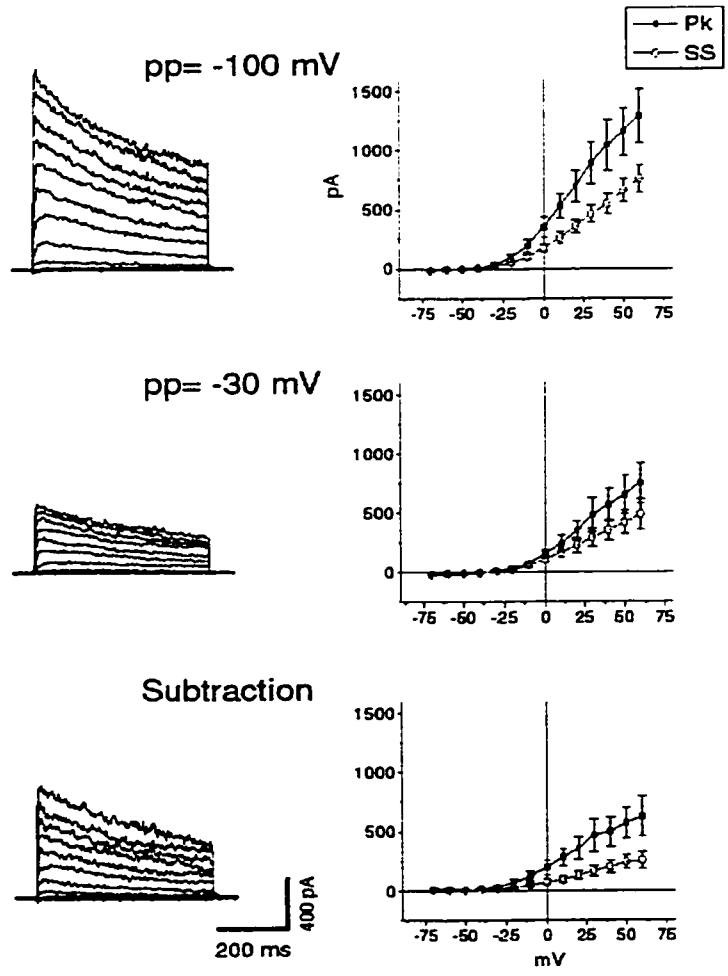


Figure 4-5 Voltage sensitivity of SMCs with $I_{to,s}$

In 31% (32/104) of cells examined have a fast activating/slow inactivating outward current that was significantly reduced by the –30 mV prepulse on average by 54±20% at +30 mV test pulse. For the peak currents expressed, the chord conductance corresponded to 1.4±0.6 nS/pF. Both the subtracted currents and currents remaining after the –30 mV prepulse could be fitted with mono-exponential inactivation decays, suggesting both are made up of one population of outward currents. Another important indication is that all IVs had similar takeoff points (typically -33±12 mV).

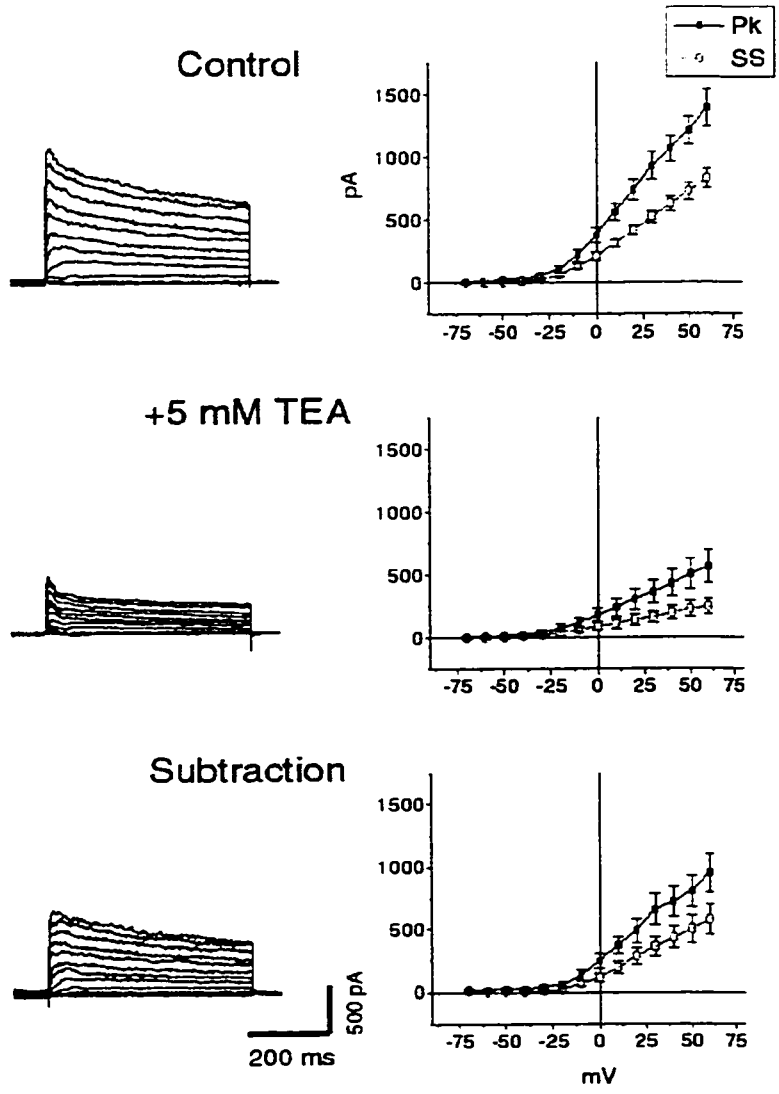


Figure 4-6 TEA sensitivity of SMCs with $I_{to,s}$

The addition of 5 mM TEA blocked 71±25% of the dominant $I_{to,s}$. In this cell, the initial time course of $I_{to,s}$ was influenced by the inward $Ca^{2+}$ current. The presence of the inward $I_{Ca}$ could not be assessed properly without completely blocking the outward currents.

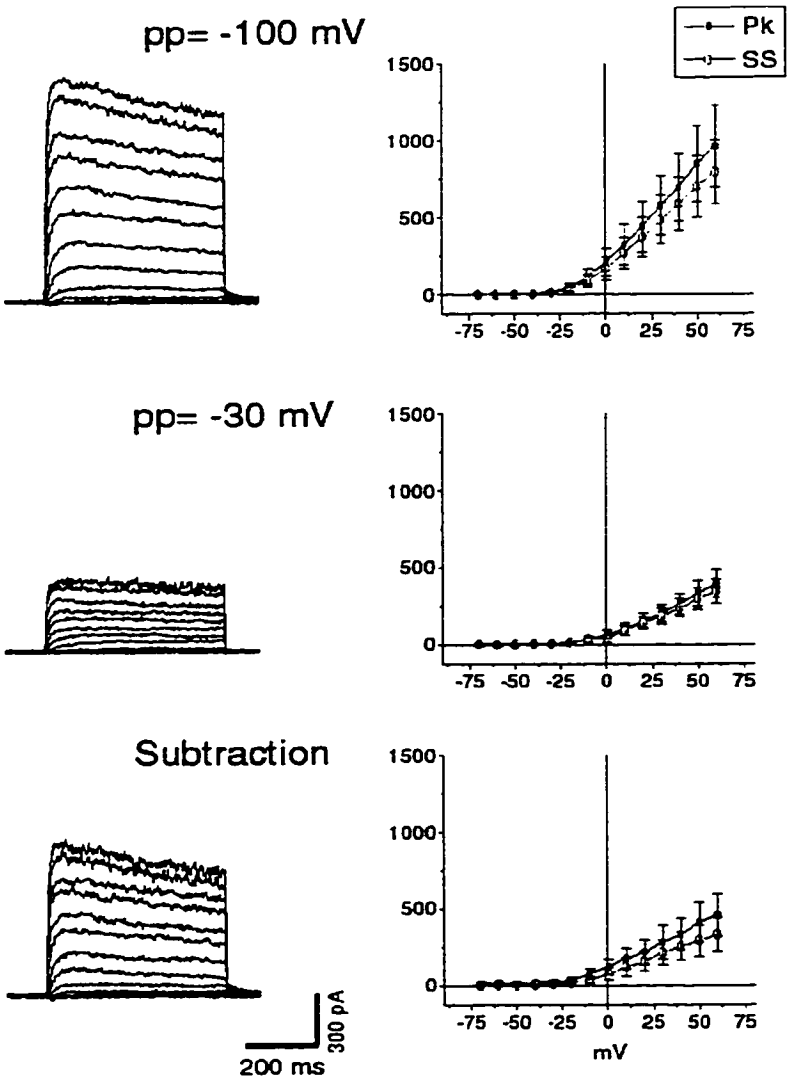


Figure 4-7 Voltage sensitivity of SMCs with $I_{dr}$

In 12% (13/104) of cells examined displayed a slow activating and very slow inactivating outward current that resembled the classical delayed rectifier current. These cells with a delayed rectifier-like outward currents ($I_{dr}$) showed a peak chord conductance of 0.8±0.4 nS/pF and have typical takeoff voltages of –33±11 mV. The –30 mV prepulse on average inactivated the peak currents by 56±15%.

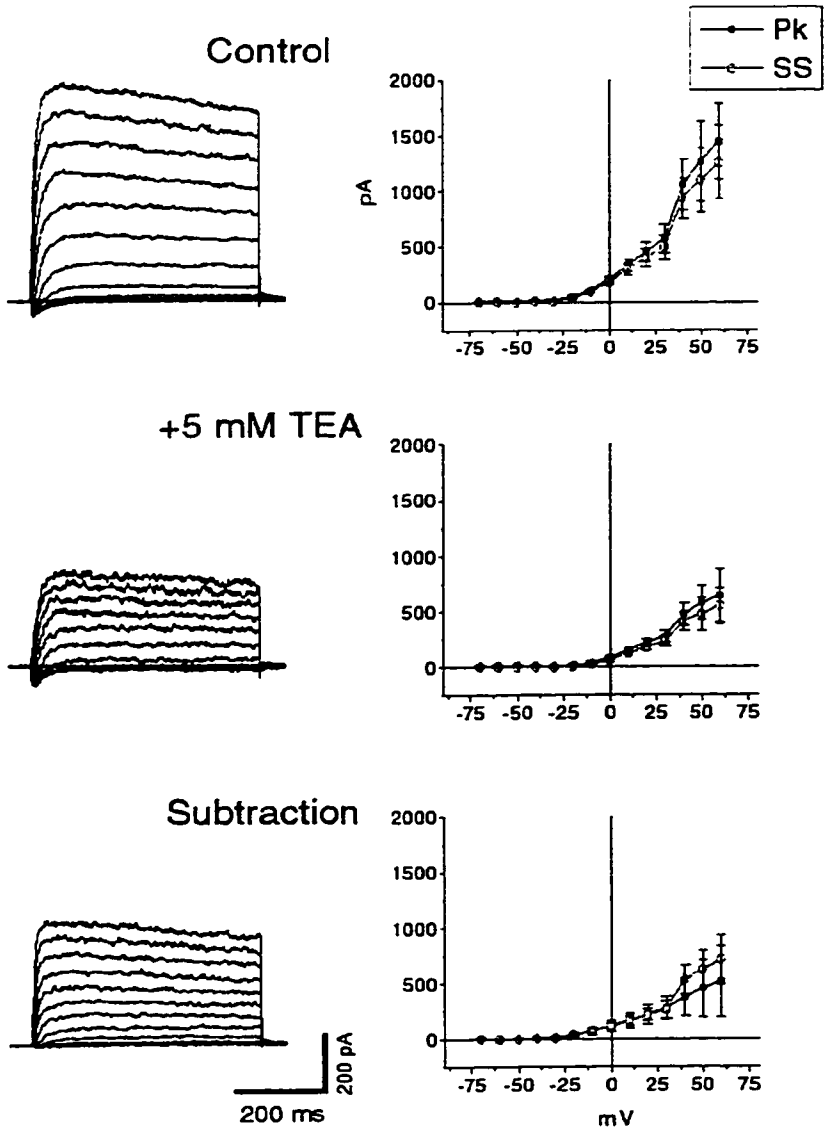


Figure 4-8 TEA sensitivity of SMCs with $I_{dr}$

Frequently, the inward $I_{Ca}$ can be seen with cells containing $I_{dr}$. Because the outward currents are slow to activate, the fast inward currents can be seen before they are masked by the larger outward currents. The $I_{dr}$ was inhibited with 5 mM TEA by 48±32%.

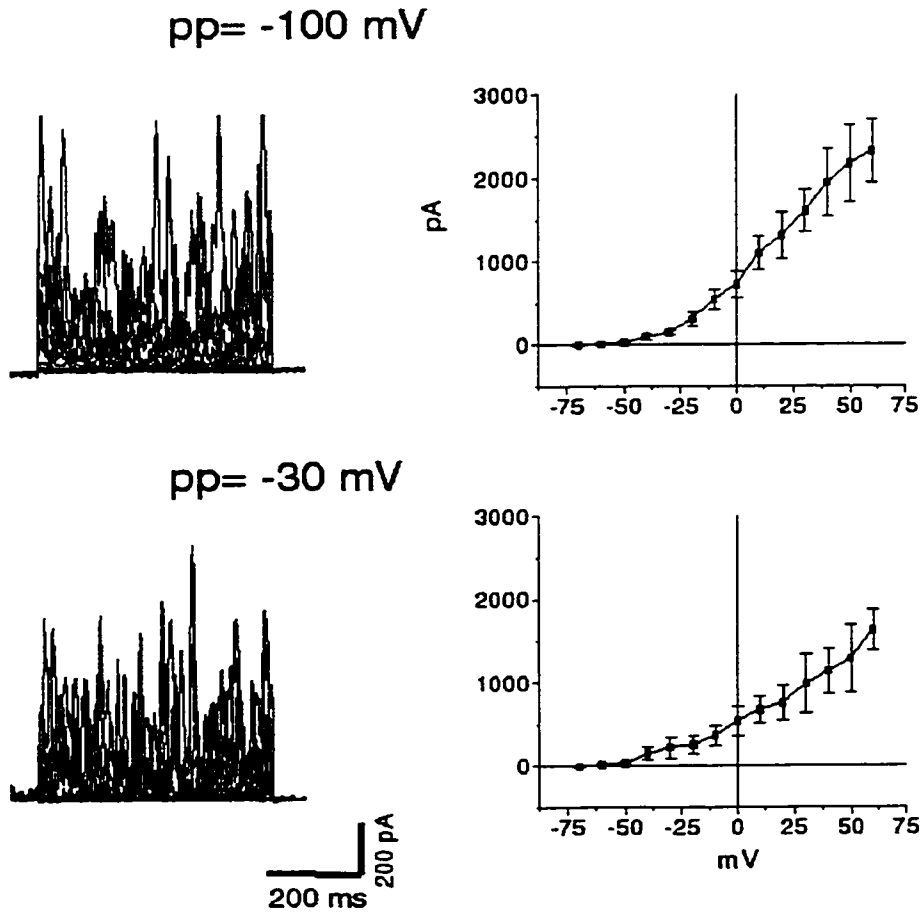


Figure 4-9 Voltage sensitivity of SMCs with $I_{stoc}$

Prominent spontaneous outward current oscillations (STOCs) can be seen in 8% (8/104) of cells examined. STOC activity was highly variable in amplitude and frequency between different cells. Because of the variable nature of the STOCs, only the peak currents were used to make the IV plots. The peak outward currents gave a chord conductance of 1.6±0.9 nS/pF and a voltage takeoff of –53±12 mV. The STOC activity can be voltage inactivated since the –30 mV prepulse reduced the amplitude of peak currents by 66±24% during the +30 mV test pulse.

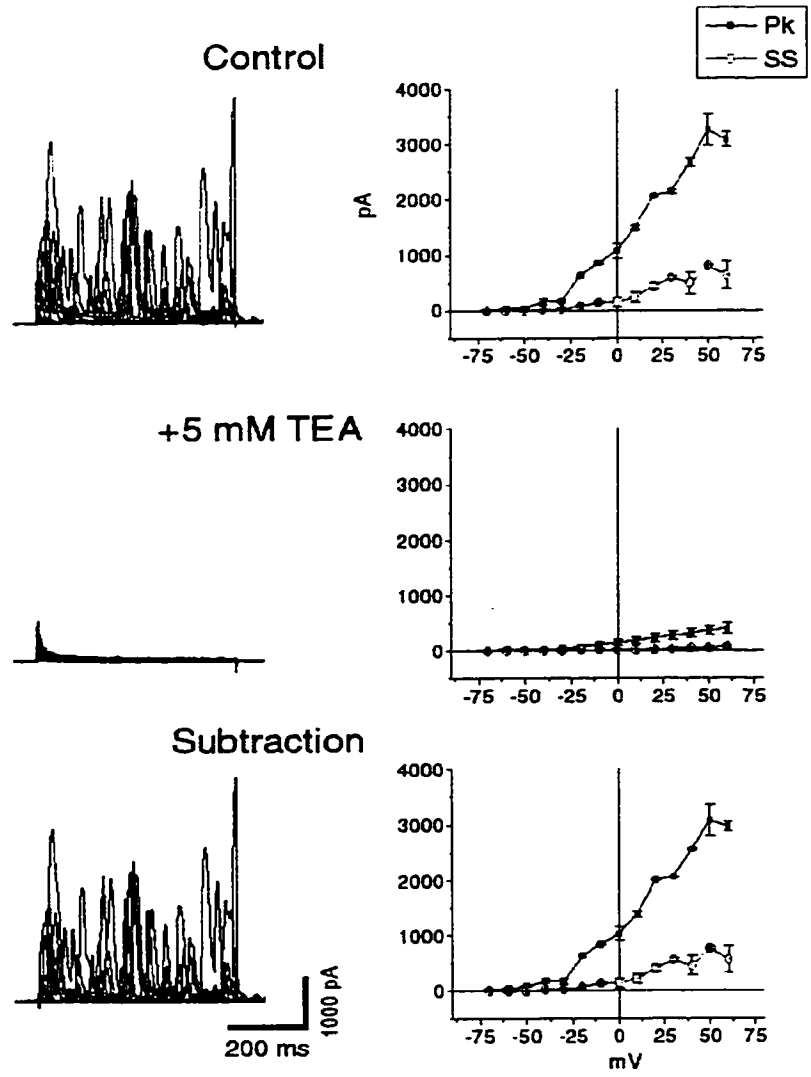


Figure 4-10 TEA sensitivity of SMCs with $I_{stoc}$

STOC activity was abolished completely by 5 mM TEA, leaving a small amplitude fast activating/inactivating transient outward current with a peak chord conductance of 0.8±0.5 nS/pF and had a voltage takeoff of –37±12 mV. This TEA resistant outward current inactivated 87±22% over 500 ms of the +30 mV test pulse and was mostly inactivated by a –30 mV prepulse.

# Chapter 5: Characterization of two transient outward currents in the adult mouse small intestine

**Jonathan CF Lee, *Carlos Barajas-López, and Jan D. Huizinga**

Intestinal Disease Research Program, McMaster University, Hamilton, Ontario L8N 3Z5, Canada

*Current affiliation: Department of Anatomy and Cell Biology, Queen's University, Kingston, Ontario, Canada

Running title: Transient outward currents in smooth muscle

Keywords: Potassium channel, electrophysiology, patch clamp

Correspondence address

Dr. Jan D. Huizinga
McMaster University
HSC-3N5C
1200 Main Street West
Hamilton, ON L8N 3Z5
Canada

Phone: (905) 525-9140 x22590
Fax: (905) 522-3454
E-mail: huizinga@mcmaster.ca

## 5.a Abstract


1. Adult mouse small intestine smooth muscle cells possess two different transient outward currents ($I_{to}$) that can be identified by their rates of inactivation. The fast inactivating Ito has a faster average rate of inactivation ($\tau$ < 100 ms) than the slow inactivating $I_{to}$ ($\tau$ > 150 ms).
2. The chord conductance for the fast $I_{to}$ is smaller than the slow $I_{to}$ (0.5±0.1 nS/pF vs. 1.3±0.1 nS/pF respectively). The inactivation processes can be fitted by mono-exponentials to give averaged $\tau$'s of the fast and slow $I_{to}$'s of 44±1 ms and 229±4 ms respectively.
3. Simultaneous plots of voltage dependent activation and inactivation processes reveal a voltage range where window currents are possible. The voltage window range for the fast $I_{to}$ was -56 to -36 mV (20 mV range) vs. slow $I_{to}$ range at -42 to +5 mV (47 mV range).
4. The latencies for recovery from inactivation was different between the two $I_{to}$'s. The fast $I_{to}$ recovers more quickly from inactivation than the slow $I_{to}$ with taus of recovery from inactivation of $\tau$(fast Ito) = 11±4 ms vs. $\tau$(slow $I_{to}$) = 42±16 ms. Thus, the slow $I_{to}$ requires ~ 4x more time to recover from voltage inactivation than the fast $I_{to}$.
5. The effect of different rates of depolarization on Ito activation were examined. The plots of peak currents evoked by different rates of depolarization could be described by inverse exponential relationships. The fast $I_{to}$ has a larger response to fast rates of

depolarizations by having $\tau$=2±1 mV/ms with maximal activation (95% complete) at 5 mV/ms. The slow $I_{to}$ had $\tau$=14±9 mV/ms with maximal activation (95% complete) at 42 mV/ms.

6. Intestinal smooth muscle cells exhibit relatively slow slow-wave activity and fast action potentials. The fast $I_{to}$ will be most effective in inhibiting action potentials. Since both $I_{to}$ have substantial substained currents, both would still contribute throughout the duration of the slow wave. The prolonged depolarization caused by the plateau of the slow wave will allow expression of the window currents and allow both $I_{to}$ to contribute in different ways.

## 5.1 Introduction

A transient potassium outward current was first identified by Connor and Stevens (Connor & Stevens, 1971) in neurons of the sea slug *Anisodoris*. This current inactivates rapidly and has been named the rapidly inactivating K current, or $K_A$. According to inactivation kinetics, various types of transient K currents appear to exist. In some neurons, activation of these currents is fast enough to participate in the repolarization phase of the action potential. These currents might also serve as a damper in the interspike interval to space successive action potentials (Bielefeld *et al.* 1990). Similar transient K currents have been observed in smooth muscle preparations from artery (James *et al.* 1995), vein (Beech & Bolton, 1989), bladder (Smith *et al.* 1998), and intestine (Ohya *et al.* 1987).

In the mouse small intestine, the musculature generates two major electrical activities: the slow wave and the superimposed spike-like action potentials. The slow wave occurs at a frequency of 40-60 cpm at 37°C with a rate of rise of the slow wave upstroke (-V/-t) of ~0.1 mV/ms. Spike action potentials are superimposed on the plateau of the slow waves and occur at a frequency of ~300 cpm and have an average rate of rise of ~5 mV/ms (Malysz *et al.* 1995). Both the slow wave and spike action potentials occur well within the voltage activation range of transient outward currents, suggesting that transient outward currents may play a role in influencing the major intrinsic activities in the mouse small intestine.

Our objective was to characterize transient outward currents in the smooth muscle cells from the mouse small intestine as part of our general objective to elucidate the

cellular and electrophysiological basis of control of excitation in this tissue (Huizinga, Thuneberg, Vanderwinden & Rumessen, 1997) using different voltage-clamp protocols which include square pulse protocols and ramps. Our observations indicate the presence of at least two types of transient outward currents with different kinetic properties.

Part of these results were previously published in abstract form (Lee, Barajas-López & Huizinga, 1997). [Jan, can you verify this? I don't remember this abstract]

## 5.2 Methods

### *5.2.1 Isolation of single smooth muscle cells*

An adult female mouse (20-25g) was sacrificed and an ileal segment removed. After simple washing, the segment was placed in pre-equilibrated M199 cell media and the muscularis externa was removed by separation along the deep muscular plexus margin. The dissected muscularis was cut into small pieces (~1-2 mm) and added into dissociation solution A + 1 mg/ml trypsin for 15 mins, then 30 mins at 37°C. The supernatant was carefully removed and then dissociation solution B + 3 mg/ml + 1 mg/ml BSA was added and allowed to incubate for 15 mins, then 20 mins. The cells were released by shaking. The cell suspension was carefully layered on top of 20% (w/v) Ficoll and spun at 15 g for 15 mins. The cell band located at the interface was removed and plated onto collagen coated coverslips. The cells were maintained in 5% $CO_2$/37°C until needed.

### *5.2.2 Electrophysiology*

Cells were not used beyond 5 days post-isolation because stable tight seals were more difficult to obtain. The cells were continuously perfused with extracellular solution (ECS). Whole cell electrical activity was recorded using the nystatin perforated patch. This was achieved by adding 2 mg/ml nystatin in the intracellular solution (ICS). Pipettes were made using a Sutter micropipette puller to typical tip resistance of 3-5 MΩ. Electrical activity was recorded using the Axopatch 1B amplifier (Axon Instruments, California) and pClamp v5.2 acquisition software. Different voltage protocols were performed to assess different kinetic aspects of whole cell currents.

### *5.2.3 Analysis*

Data analysis was done by the Axon pClamp v6.1 utilities and by Microcal Origin graphing/fitting program. Fitting was done by chi-square reduction by Simplex and Levenberg-Marquardt algorithms. Goodness of fit was assessed both by chi-square minimization and by visual inspection. Data are shown as average ± S.E.M.

### *5.2.4 Solutions, with concentrations in mM*

ECS (Extracellular solution): NaCl 125.0, KCl 5.0, $MgCl_2$ 1.2, $NaH_2PO_4$ 1.2, Glucose 11.0, $NaHCO_3$ 4.0, $CaCl_2$ 2.0, HEPES 10.0, pH 7.35.

ICS (Intracellular solution): K-Methanesulfonate 129.0, NaCl 5.0, MgAcetate 2.0, $CaCl_2$ 1.0, EGTA 11.0, HEPES 10.0, pH=7.25.

Solution A: NaCl 134.0, KCl 3.0, Taurine 5.0, EDTA 5.0, $MnCl_2$ 2.0, HEPES 10.0, pH 7.40.

Solution B: NaCl 133.0, KCl 3.0, Taurine 5.0, CaCl2 0.1, $MgCl_2$ 2.0, Glucose 10.0, HEPES 10.0, pH 7.35.

M199 media: 1X M199 media, $NaHCO_3$ 26.0 mM, Glutamine 2.0, Penicillin 0.25 mg/ml, FBS 10%.

Drugs: Verapamil and nifedipine were dissolved in 70% EtOH as $10^{-2}$ M stock solutions. CPA was dissolved in DMSO as $5X10^{-2}$ M stock solution.

Chemicals and drugs were purchased from Sigma-Aldrich Canada Ltd.

M199 culture media was obtained from Gibco-Life Sciences Canada.

## 5.3 Results:

### *5.3.1 General properties of whole cell outward currents*

Outward potassium currents were recorded from 104 intestinal smooth muscle cells by using step depolarizations from –70 to +60 mV, usually from a holding potential of –50 to –70 mV. In 51 out of 104 cells, a fast activating and inactivating transient outward current ($I_{to}$) can be seen as a component of the total outward currents. The other outward currents which showed either slower or no inactivation could be completely inhibited by the $K^+$ channel blocker TEA (Fig. 1A and 1B). The only outward current remaining after the application of 60 mM TEA was $I_{to}$, an outward current that activated quickly to peak amplitude (less than 25 ms) and inactivated to 24±16% (n=51) of the peak currents (as assessed by a test pulse of +30 mV).

The peak $I_{to}$ was always prominent when the holding potential was set to -100 mV, but was small or masked by other outward currents when the holding potential was set to -30 mV (Fig. 2). Therefore, to fully express $I_{to}$, a prepulse of -100 mV for at least 500 ms was applied before the test pulses in order to remove any inactivation imposed at the typical holding potentials (-50 to -70 mV).

The transient outward currents remaining after 60 mM TEA could be further distinguished into two populations by their rates of inactivation and the presence of significant peak currents after a -30 mV prepulse (Fig. 2). The standard voltage protocol for expressing whole cell currents was to give a -100 mV prepulse (500 ms), followed by step test pulses from -70 to +60 mV from holding potentials of -50 to -70 mV. The transient outward currents expressed with the standard voltage protocol had either "fast" inactivation (Fig. 2A), in that the $I_{to}$ temporally inactivated to a steady state in less than 150 ms, or "slow" inactivation where $I_{to}$ needed greater than 150 ms to inactivate to steady state (Fig. 2B). The transient outward currents showing "fast" inactivation were designated as "fast $I_{to}$". Similarly, the transient outward currents showing "slow" inactivation were designated as "slow $I_{to}$". Another method to classify the transient outward current was by using a -30 mV prepulse instead of the -100 mV prepulse for the standard voltage protocol. The fast $I_{to}$ completely inactivated, while the slow $I_{to}$, peak currents can still be seen, indicating incomplete voltage inactivation by the -30 mV prepulse.

### *5.3.2 Voltage dependent activation and inactivation of $I_{to}$*

The two different transient outward currents were distinguished according to their electrophysiological properties. Fast inactivation was seen in 28 cells (55%), and slow inactivation was seen in 23 cells (43%) out of a total of 51 cells. Both transient outward currents were very fast activating (activation to peak current < 10 ms). I/V plots of elicited peak currents against imposed membrane voltages gave similar takeoffs for the fast and slow inactivating $I_{to}$ at -43±13 mV and -45±7 mV respectively (Fig. 3). From the I/V plots, the chord conductances were 0.5±0.1 nS/pF for the fast $I_{to}$, and 1.3±0.1 nS/pF for the slow $I_{to}$. The steady state currents also had similar takeoff points.

The relative amount of steady state currents (SS) remaining after temporal inactivation was compared to the peak currents (Pk) evoked at the same potentials (Fig. 3C). This SS/Pk ratio shows the relative amount of inactivation for the given voltage. For the fast $I_{to}$, the SS/Pk ratio increases linearly with increasingly positive voltages, but always has the SS/Pk ratio lower than the slow $I_{to}$. Thus, the relative amount of inactivation was decreasing with depolarization for the fast $I_{to}$. For the slow $I_{to}$, the SS/Pk ratio increased and leveled off at 0.4 (40% of steady state currents remained relative to the peak currents) at potentials positive than -10 mV. The relative amount of inactivation for the slow $I_{to}$ initially decreases but then settles to a steady level after -10 mV depolarization. Overall, since the SS/Pk ratios were always higher for the slow $I_{to}$ (i.e. the slow $I_{to}$ always have more steady state currents remaining relative to the peak currents than for the fast $I_{to}$), the slow $I_{to}$ shows a lesser degree of inactivation than the fast $I_{to}$.

### *5.3.3 The voltage dependency of Inactivation*

The time dependent inactivation from peak current to steady state was best described for both populations by mono-exponential fits (Fig. 4A and 4B). The time constant for the inactivation, $\tau$ (time when 66% of inactivation is completed), was plotted against the imposed voltages (Fig. 4C). The fast $I_{to}$ had an average $\tau$ = 44±1 ms while the slow $I_{to}$ had an average $\tau$ = 229±4 ms over all voltages. The wide margin between the $\tau$'s validates the grouping of the $I_{to}$ into two populations of fast and slow inactivating currents.

The voltage dependency of inactivation was explored using the double pulse (prepulse) protocol (Fig. 5). The membrane potential was allowed to settle to steady state inactivation before a test pulse was given in order to assess the level of inactivation that had occurred. With increasing levels of depolarization in the first pulse, the inactivation decreased the peak current according to a Boltzman distribution. Two distinct voltage ranges for inactivation were observed (Fig. 5B and 5C). The values for 5% and 95% thresholds were estimated from values derived from successful fits of the data. The fast inactivating $I_{to}$ has $V_h$= -78 mV and k=14, and started inactivating (5% threshold) at -120 mV and completely inactivated (95% threshold) at -36 mV (Fig. 5B). The slower inactivating $I_{to}$ had $V_h$ = +33 mV and k =13, and displays 5% threshold = -70 mV and 95% threshold = +5 mV (Fig. 5C).

### *5.3.4 Simultaneous voltage activation and inactivation of $I_{to}$*

Conversion of peak currents to conductances corresponded to Boltzman distributions with a half activation potential ($V_h$)= -12.1±2.8 mV, slope factor (k) = 15.0 for the fast $I_{to}$, and $V_h$= 6.8±1.9 mV, k =16.7 for the slower inactivating $I_{to}$. Considering the 5% and 95% activation points to full conductance, the fast inactivating $I_{to}$ started activating (5%) at -56.3 mV and reach full conductance (95% complete) at +32.1 mV. Similarly, the slow $I_{to}$ started activating (5%) at -45.1 mV and reached full activation (95%) at +56.1 mV.

Both the activation and inactivation processes were plotted together against the imposed membrane potential. The degree of overlap between activation and inactivation processes determines the amount of "window" $I_{to}$ available at any membrane potential. Figure 6 shows the ranges for "window" currents for both populations of $I_{to}$ using 5% threshold of activation and 95% threshold for inactivation. Since both fast and slow $I_{to}$ activated in approximately the same ranges, the differences in inactivation were the main determinants of the differences in window currents. The voltage range for the fast $I_{to}$ window currents were from -56 to -36 mV (Fig. 6A). The slow $I_{to}$ had a larger voltage range for windows currents that extended from -42 to +5 mV (Fig. 6B). The fast $I_{to}$ had little overlap between the activation and inactivation processes such that when it activated, inactivation had already removed 72.0% of the total current. For the slow $I_{to}$, there was substantial overlap such that at activation, only 2.8% of the total current had been inactivated; hence the slow $I_{to}$ window currents will be significantly more available for this current.

### *5.3.5 Latencies for recovery from inactivation*

To assess the time needed for recovery from inactivation, a three pulse latency protocol was used (Fig. 7A). The first voltage pulse was used to maximally inactivate the current, followed by a hyperpolarizing pulse of varying durations to remove the inactivation, and the last pulse was used to elicit the test current in which the peak amplitude would reflect the degree of inactivation still present. A plot of the peak currents from the test pulse against the duration (or latency) spent recovering from inactivation (duration of the second pulse) reveals a mono-exponential relationship (Fig. 7B and 7C). The fast $I_{to}$ recovered more quickly from inactivation with $\tau$ =11±4 ms and was complete (95%) at 32 ms. In contrast, the slow $I_{to}$ had a $\tau$ = 42±16 ms with complete recovery (95%) at 126 ms. Therefore, the slow $I_{to}$ required ~4 times longer to recover from inactivation than the fast $I_{to}$ and would be unlikely to recover completely from fast events with very high frequency (>480 cpm).

### *5.3.6 The effect of depolarization rate on $I_{to}$ activation*

Although the above experiments examined activation and inactivation processes in detail, they may not reflect activity during continuously changing potentials. This is important since *in vivo* cellular membrane potential changes are not instantaneous and step-wise, but have definite rates of depolarization. To examine how $I_{to}$ would behave under different rates of change in membrane potential (*dV/dt*), voltage ramps with

different velocities were used (Fig. 8A). Fast rates of depolarization (>10 mV/ms) evoked peak currents that approached the maxima, limited only by the rate of activation of $I_{to}$ itself. A plot of the peak current evoked by the ramps of the same voltage ranges (-150 to +60 mV) against ramp velocity revealed a mono-exponential relationship which were different between the fast and slow $I_{to}$ (Fig. 8B and 8C). The fast $I_{to}$ demonstrated a significantly faster response to depolarization with $\tau$ =2±1 mV/ms and approached its maximum (95%) at 5 mV/ms (Fig. 8B). The slow $I_{to}$ had a slower response with $\tau$ =14±9 mV/ms with maximal activation (95%) at 42 mV/ms (Fig. 8C). Therefore, the slow $I_{to}$ requires very fast events (~9 times faster than the fast $I_{to}$) in order to be maximally activated.

Since a depolarization rate of 42.54 mV/ms is clearly unphysiological, the slow $I_{to}$ would not be fully activated under normal rates of depolarization. Considering the rates of depolarization of slow waves and spiking activity to be approximately 1 mV/ms and 5 mV/ms respectively, only the fast $I_{to}$ would maximally respond to spiking events while both currents would respond to slow wave type depolarizations.

### *5.3.7 Pharmacology*

Both currents were revealed by their insensitivity to 60 mM TEA (n=32) (Fig. 8A). Both $I_{to}$'s were also insensitive to 5 mM 4-AP (n=3). The $I_{to}$'s were blocked by $Cs^+$ (n=7), and to 1 mM quinine or quinidine (n=3) (Fig. 8B). Unfortunately, these blockers are non-specific and cannot be used to selectively block $I_{to}$.

## 5.4 Discussion

The transient outward currents revealed by TEA were shown to consist of two major groups that differed markedly in electrophysiological properties. Both $I_{to}$ activated in approximately the same voltage range (~ -50mV) and showed similar peak evoked currents but different chord conductances. The inactivation profiles showed the fast $I_{to}$ to be inactivated at more hyperpolarized potentials than the slow $I_{to}$. The fast $I_{to}$ had little overlap between the activation/inactivation curves while the slow $I_{to}$ had considerable overlap. This was interpreted to result in having more slow $I_{to}$ available (not inactivated) at a given voltage than the fast $I_{to}$. The latencies for recovery from inactivation revealed that the slow $I_{to}$ required ~4 times longer latencies than the fast $I_{to}$. To illustrate the importance of the differences in latencies, the fast $I_{to}$ can withstand depolarizing events with frequencies up to 1875 cpm and still be able to recover from inactivation while the slow $I_{to}$ can only sustain events with frequencies up to 476 cpm. The voltage ramp analysis showed the fast $I_{to}$ responded better to fast rates of depolarization and was attenuated sharply by slow rates in comparison with the slow $I_{to}$. All results are consistent with having two distinct populations of transient outward currents.

### *5.4.1 Functional consequences of $I_{to}$ expression*

The amount of $I_{to}$ that can be evoked was dependent on both the voltage and the rate of depolarization; and hence the two major electrical activities in the intestine, slow waves and action potentials, will be affected differently. We predict that the $I_{to}$ in the

mouse small intestine will, similar to $I_A$ , provide transient inhibition to excitatory electrical activity. From their kinetic properties, they can modulate only specific excitatory events. For example, the ramp analysis demonstrated that the $I_{to}$ would be effective in inhibiting relatively fast depolarizing events. If the depolarizing event outlasts the time for inactivation, the excitatory event would only be opposed by the steady state current remaining because $I_{to}$ has temporally inactivated. The increased response of $I_{to}$ to fast velocities and its relatively short latencies for recovery from inactivation suggests that it could modulate the frequency of fast electrical events. Thus, in essence, the $I_{to}$ provides a frequency filter such that only events that are large enough (high amplitude), fast enough (high rate of depolarization) and long enough (long duration) and frequent enough (high frequency) would overcome the inhibitory influence of $I_{to}$. Fast events with high frequency would essentially be damped up to the point at which $I_{to}$ can no longer recover from inactivation. Action potentials superimposed on slow waves can easily reach 400 cpm so that the slow $I_{to}$ may indeed set the limit for this frequency.

It is likely the fast $I_{to}$ would be more involved with inhibiting spiking activity while both the fast and slow $I_{to}$ would influence the slow wave type depolarizations. The slow wave type depolarizations are special in that they arise from a fast upstroke and have a relatively long duration of depolarization (plateau) before repolarizing. The long duration would effectively inactivate the transient outward currents, and thus allow for easier occurrences of spiking activity at the plateaus of the slow waves. But, since the plateau typically occurs at -40 to -30 mV, there would still be significant contributions

from "window" currents. Therefore, transient outward currents, and especially fast $I_{to}$, would be responsible for modulating the threshold for spiking activity.

### *5.4.2 Comparisons with other $I_{to}$'s in smooth muscle*

Transient outward currents have been described in other tissues, but the remarkable variability in properties makes it imperative that they have to be examined carefully within each tissue of interest. Within the gastrointestinal system, transient outward currents were identified in opossum esophageal circular muscle (Akbarali *et al.* 1995), newborn rat ileum (Smirnov *et al.* 1992), guinea pig proximal colon (Vogalis & Sanders, 1991), and dog colon (Farrugia *et al.* 1993) and human jejunal circular muscle (Duridanova *et al.* 1997). These currents differed from the currents described here in that they were sensitive to 4 mM 4-AP, whereas in our preparations, 5 mM 4-AP did not affect the mouse intestinal $I_{to}$. Insensitivity to 4-AP was also reported for transient outward currents in guinea pig gastric antrum (Noack *et al.* 1992). Most reported high concentrations (up to 10 mM) of 4-AP to block $I_{to}$ (Bielefeld *et al.* 1990; Hisada *et al.* 1990), while some show selective block with micromolar concentrations of quinine (Farrugia *et al.* 1993; Duridanova *et al.* 1997). It is clear that characteristics as well as the pharmacology of transient outward current is diverse in the various tissues (Hisada *et al.* 1990; Imaizumi *et al.* 1990; McFadzean & England, 1992).

The presence of two distinct transient outward currents in different smooth muscle cell populations suggests they perform different roles. Currently, the lack of

specific inhibitors for $I_{to}$ in the mouse small intestine prevents evaluation of the currents in tissue.

## 5.5 Acknowledgments

The authors wish to thank Laura Farraway for preparation of the cells, David Richardson and John Malyz for the data relating to intact tissue.

## 5.6 References

AKBARALI, H. I., HATAKEYAMA, N., WANG, Q. & GOYAL, R. K. (1995). Transient outward current in opossum esophageal circular muscle. *American.Journal.of.Physiology.* **268**, Pt 1):G979-87.

BEECH, D. J. & BOLTON, T. B. (1989). A voltage-dependent outward current with fast kinetics in single smooth muscle cells isolated from rabbit portal vein. *Journal.of.Physiology.* **412**, 397-414.

BIELEFELD, D. R., HUME, J. R. & KRIER, J. (1990). Action potentials and membrane currents of isolated single smooth muscle cells of cat and rabbit colon. *Pflugers Archiv.-.European.Journal.of.Physiology.* **415**, 678-687.

CONNOR, J. A. & STEVENS, C. F. (1971). Voltage clamp studies of a transient outward membrane current in gastropod neural somata. *J.Physiol.(Lond)* **213**, 21-30.

DURIDANOVA, D. B., GAGOV, H. S., DAMYANOV, D. & BOEV, K. K. (1997). Two components of potassium outward current in smooth muscle cells from the circular layer of human jejunum. *General.Physiology.&.Biophysics.* **16**, 49-58.

FARRUGIA, G., RAE, J. L., SARR, M. G. & SZURSZEWSKI, J. H. (1993). Potassium current in circular smooth muscle of human jejunum activated by fenamates. *American.Journal.of.Physiology.* **265**, Pt 1):G873-9.

FARRUGIA, G., RAE, J. L. & SZURSZEWSKI, J. H. (1993). Characterization of an outward potassium current in canine jejunal circular smooth muscle and its activation by fenamates. *Journal.of.Physiology.* **468**, 297-310.

HISADA, T., KURACHI, Y. & SUGIMOTO, T. (1990). Properties of membrane currents in isolated smooth muscle cells from guinea-pig trachea. *Pflugers Archiv.-.European.Journal.of.Physiology.* **416**, 151-161.

HUIZINGA, J.D., THUNEBERG, L., VANDERWINDEN, J.M. & RUMESSEN, J.J. (1997). Interstitial cells of Cajal as pharmacological targets for gastrointestinal motility disorders. *Trends in Pharmacological Sciences* **18**, 393-403.

IMAIZUMI, Y., MURAKI, K. & WATANABE, M. (1990). Characteristics of transient outward currents in single smooth muscle cells from the ureter of the guinea-pig. *Journal.of.Physiology.* **427**, 301-324.

JAMES, A. F., OKADA, T. & HORIE, M. (1995). A fast transient outward current in cultured cells from human pulmonary artery smooth muscle. *American.Journal.of.Physiology.* **268**, Pt 2):H2358-65.

LEE, J.C.F., BARAJAS-LÓPEZ, C. & HUIZINGA, J.D. (1997). Characterization of transient outward currents in smooth muscle cells of the mouse small intestine. *American Journal of Physiology* ***in preparation.***

MALYSZ, J., RICHARDSON, D., FARRAWAY, L., CHRISTEN, M. O. & HUIZINGA, J. D. (1995). Generation of slow wave type action potentials in the mouse small intestine involves a non-L-type calcium channel. *Can.J.Physiol.Pharmacol.* **73**, 1502-1511.

MCFADZEAN, I. & ENGLAND, S. (1992). Properties of the inactivating outward current in single smooth muscle cells isolated from the rat anococcygeus. *Pflugers Archiv.-.European.Journal.of.Physiology.* **421**, 117-124.

NOACK, T., DEITMER, P. & LAMMEL, E. (1992). Characterization of membrane currents in single smooth muscle cells from the guinea-pig gastric antrum. *Journal.of.Physiology.* **451**, 387-417.

OHYA, Y., KITAMURA, K. & KURIYAMA, H. (1987). Cellular calcium regulates outward currents in rabbit intestinal smooth muscle cell. *American.Journal.of.Physiology.* **252**, Pt 1):C401-10.

SMIRNOV, S. V., ZHOLOS, A. V. & SHUBA, M. F. (1992). A potential-dependent fast outward current in single smooth muscle cells isolated from the newborn rat ileum. *Journal.of.Physiology.* **454**, 573-589.

SMITH, R. D., EISNER, D. A. & WRAY, S. (1998). The effects of changing intracellular pH on calcium and potassium currents in smooth muscle cells from the guinea-pig ureter. *Pflugers Archiv.-.European.Journal.of.Physiology.* **435**, 518-522.

VOGALIS, F. & SANDERS, K. M. (1991). Characterization of ionic currents of circular smooth muscle cells of the canine pyloric sphincter. *Journal.of.Physiology.* **436**, 75-92.

## 5.7 Figures & Legends

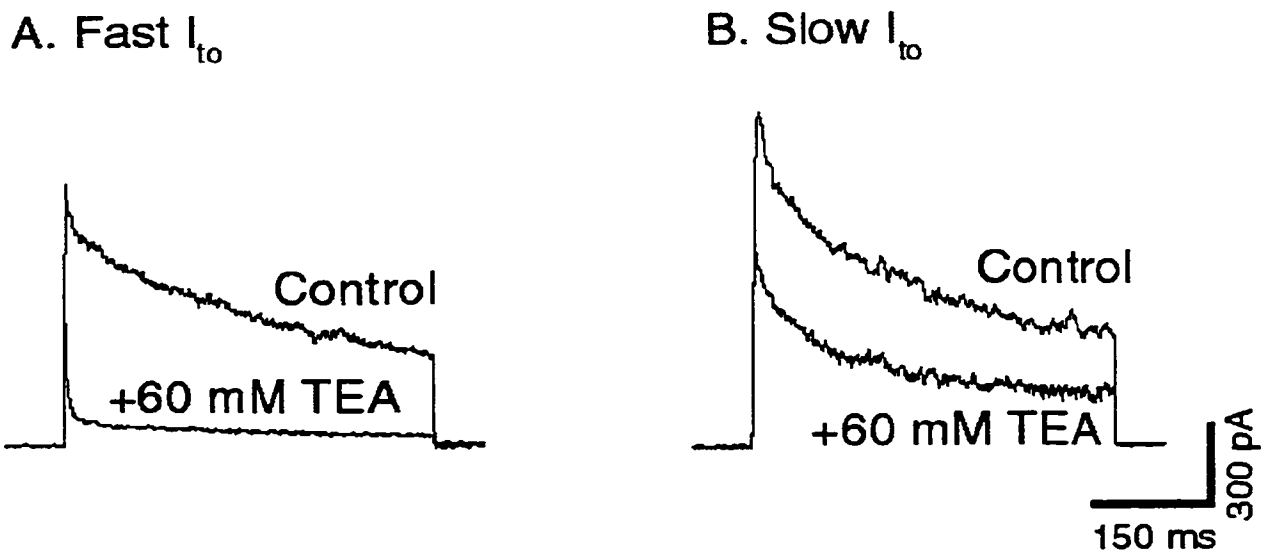


Figure 5-1 Transient outward currents isolated by 60 mM TEA.

Whole cell currents were evoked by a voltage step to +30 mV from a holding potential of -50 mV. With the addition of 60 mM TEA, transient outward currents were expressed. The transient outward currents were either **A.** fast inactivating ($\tau$ = 42 ms) or **B.** slow inactivating ($\tau$ = 174 ms). A sustained component was present in both.

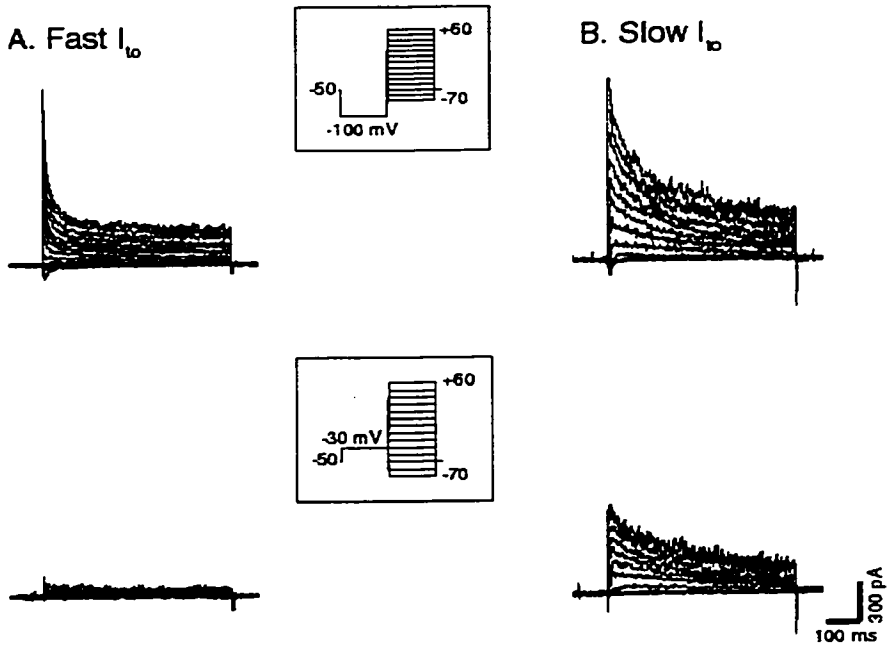


Figure 5-2 Voltage dependent transient outward currents have different inactivation kinetics.

In the presence of TEA (60 mM), the transient outward currents ($I_{to}$) were evoked. Also, the inward $Ca^{2+}$ currents could be seen at the beginning of the test pulse when L-type calcium channel blockers were not applied. Because the $I_{to}$ is sensitive to voltage inactivation, a -100 mV prepulse was given for 500 ms before the test pulses from -70 to +60 mV were given, as seen for the top figures. The bottom figures were the result of changing the prepulse to -30 mV, and demonstrating the sensitivity of the transient outward currents to voltage inactivation. **A.** In 56% of cells with a transient outward current that exhibited fast inactivation (peak $\tau$ <100 ms) and with sensitivity to voltage inactivation; this current was designated as the "fast" $I_{to}$. **B.** In 44% of the cells with

much slower inactivation (peak $\tau$ >150 ms) and less sensitive to voltage inactivation; this current was designated as the "slow" $I_{to}$.

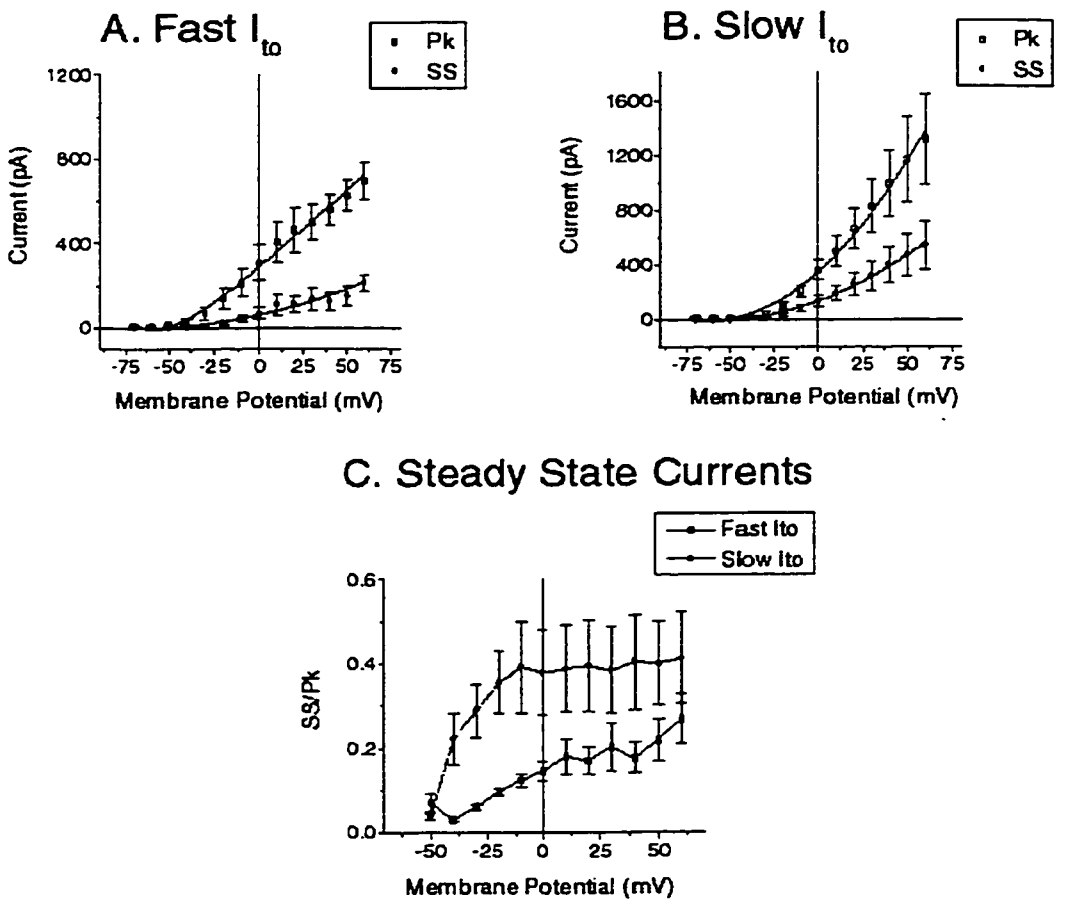


Figure 5-3 Current-voltage (IV) plots of the different transient outward currents.

Expressed are the peak currents (Pk) as well as the sustained, steady state currents (SS) for the **A.** fast $I_{to}$, and **B.** slow $I_{to}$. Both the peak and steady state currents showed similar thresholds for activation and can be seen to develop monophasically. The slow $I_{to}$ had a higher peak chord conductance than the fast $I_{to}$ (1.31±0.06 nS/pF vs. 0.54±0.13 nS/pF respectively). **C.** A plot of the steady state current to peak current ratio (SS/Pk) showed that the SS/Pk ratio increased proportionally with voltage for the fast $I_{to}$, but the SS/Pk ratio levels off at ~ −10 mV for the slow $I_{to}$.

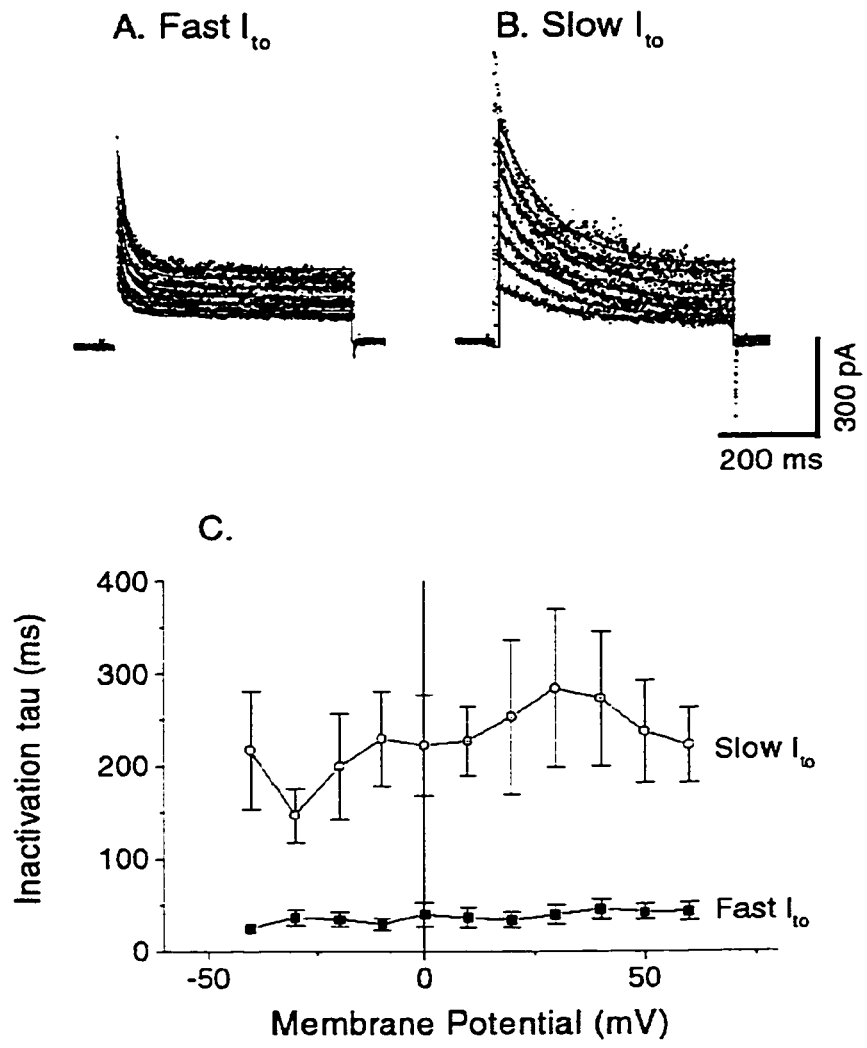


Figure 5-4 Inactivation rates of the fast $I_{to}$ and slow $I_{to}$.

Inactivation rates were fitted as mono-exponentials over the voltage ranges at which temporal inactivation can be seen. Representative mono-exponential fits were superimposed on data points obtained from voltages steps 0 mV to +60 mV for the **A.** fast $I_{to}$ and **B.** slow $I_{to}$. **C.** Although the inactivation process was clearly voltage dependent, the rate of inactivation did not change significantly over the observed voltage

range. The slow $I_{to}$ inactivation rate was ~5.3 times slower than the fast $I_{to}$ inactivation rate (comparing $\tau$ (slow $I_{to}$) = 228.7±3.7 ms with $\tau$ (fast $I_{to}$) = 43.5±0.9 ms).

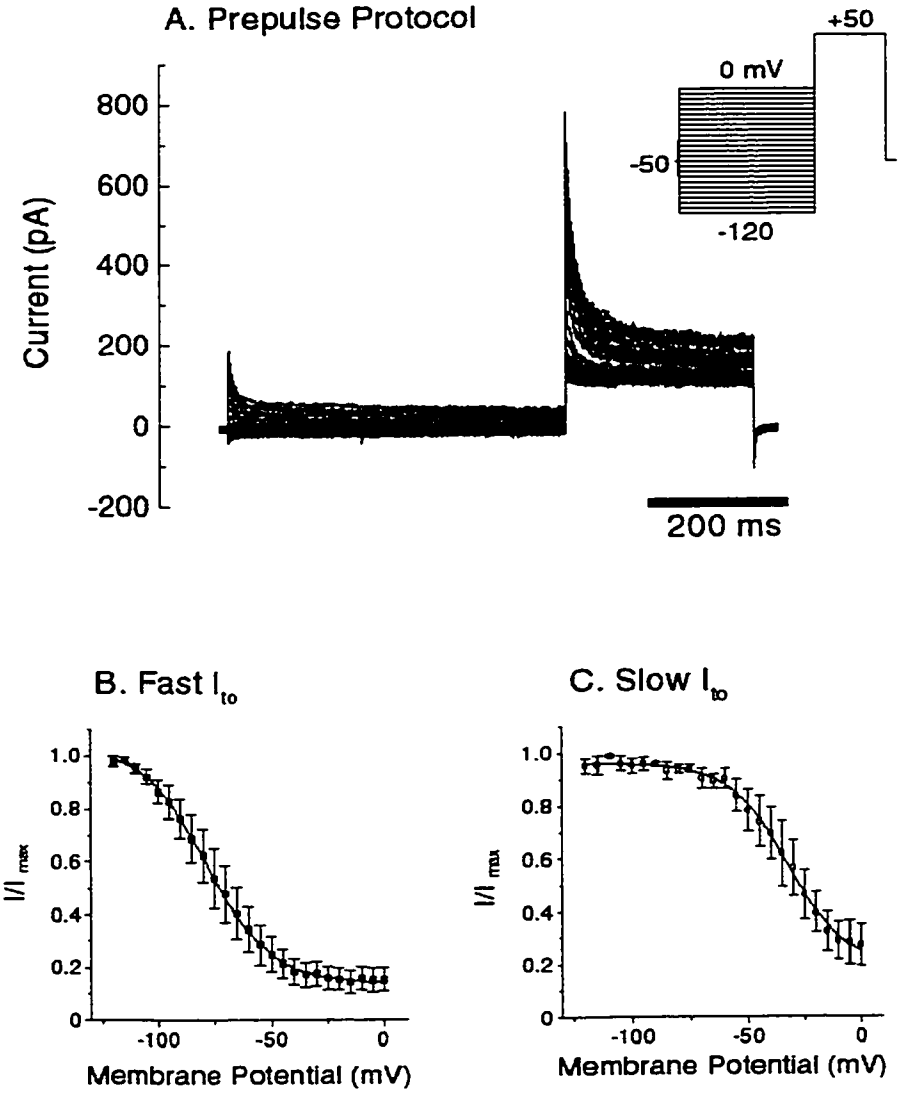


Figure 5-5 Voltage dependent inactivation process as assessed by the double voltage pulse protocol.

**A.** From a holding potential of -50 mV, voltage pulses from -120 to 0 mV were given for 500 ms before the test pulse of +50 mV was given. As seen with the currents elicited in the first pulse, the inactivation process has settled to steady state. The peak amplitude from the test pulse can be seen to decrease with increasingly positive first

pulses, as expected with voltage dependent inactivation. This voltage dependent inactivation of the transient outward currents was shown as plots of normalized peak currents ($I/I_{max}$) to the corresponding voltages of the first pulse. The data was fitted with the Boltzman equation to obtain the half inactivation voltage ($V_h$) and slope factor (k). **B.** The fast $I_{to}$ had $V_h$= -78±1 mV and k=14 . **C.** The slow $I_{to}$ had $V_h$= -33±1 mV and k=13.

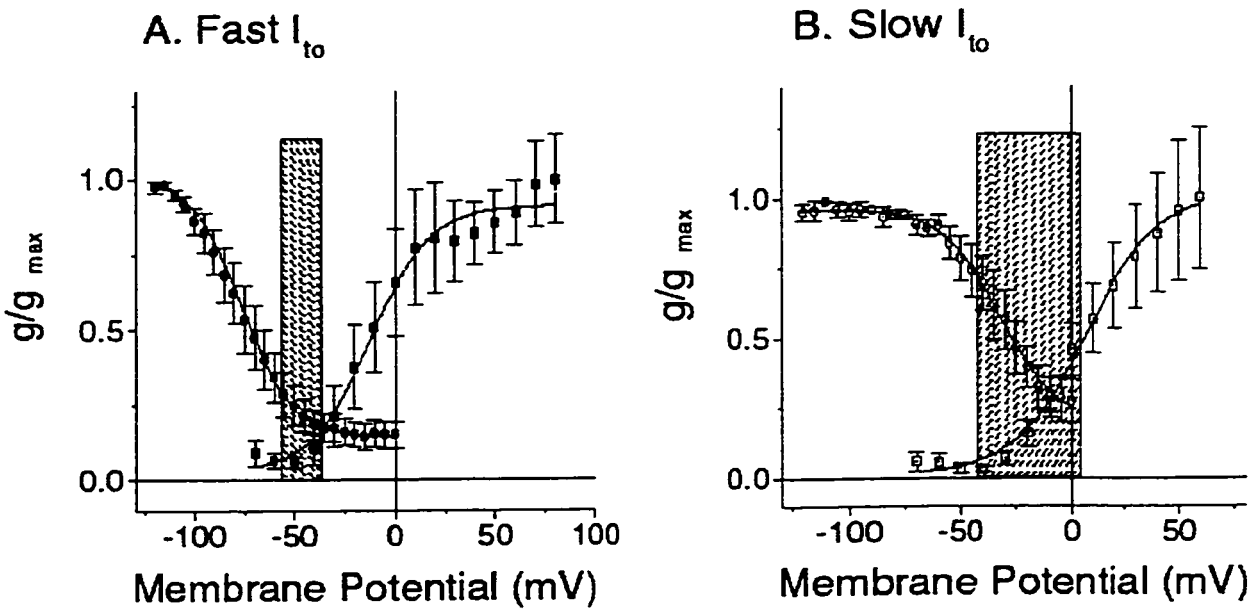


Figure 5-6 Simultaneous plots of activation and inactivation processes reveal differences in the window currents.

Both activation and inactivation processes were normalized as conductances and expressed as ratios relative to the maximum values. Since both the fast and slow $I_{to}$ show similar takeoff for activation, the main difference in the voltage behavior between the two transient outward currents was the inactivation voltage dependency. The voltage range for window currents was expressed as the threshold for activation (5% point) to completion of inactivation (95% point). **A.** The voltage range for window currents in the fast $I_{to}$ was -56 to -36 mV. **B.** The slow $I_{to}$, the window currents were between -42 to +5 mV. Therefore, the slow $I_{to}$ has significantly more window current relative to the fast $I_{to}$.

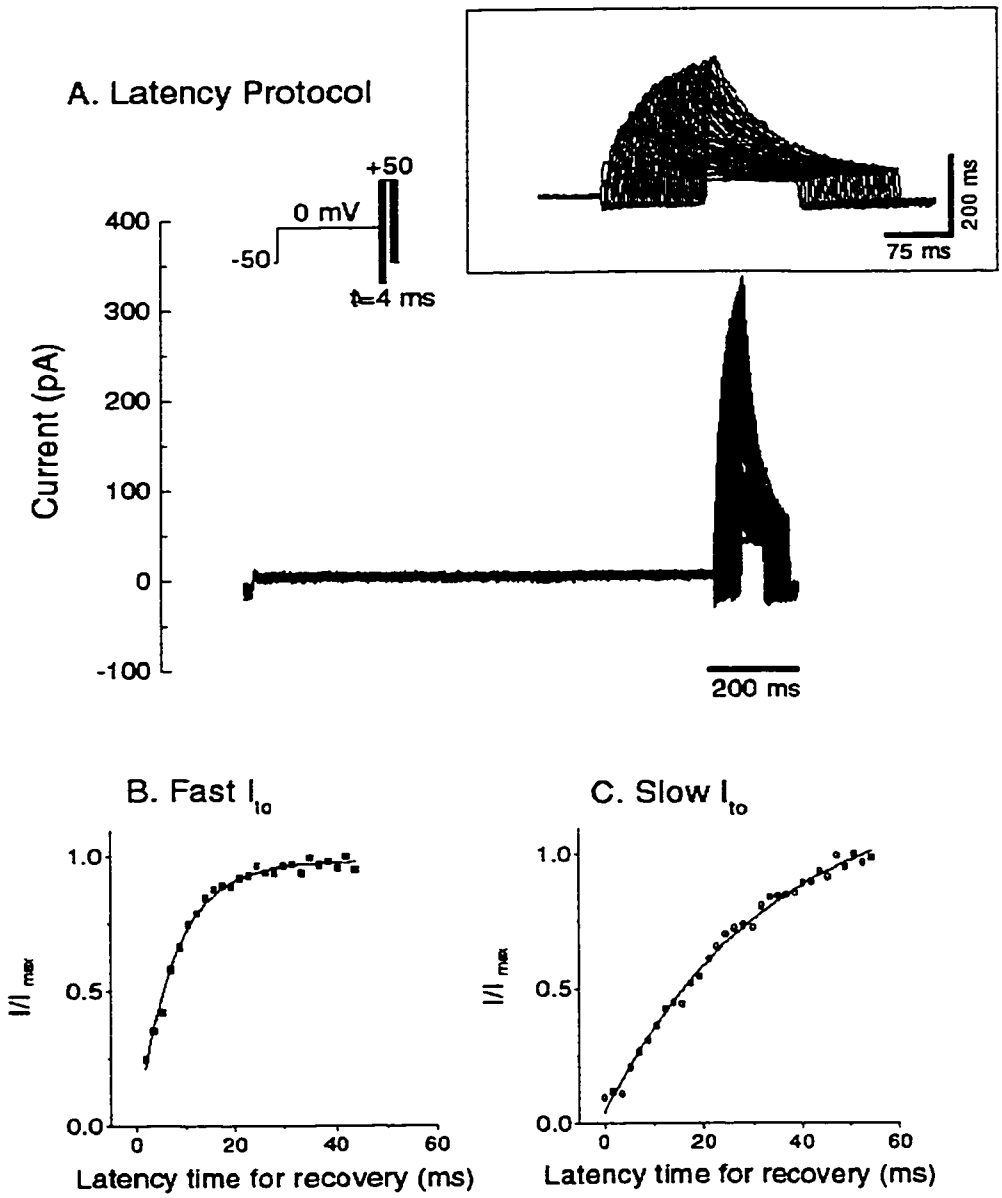


Figure 5-7 The latency for recovery from inactivation as assessed by the three pulse experiment.

**A.** Briefly, from a holding potential of -50mV, the first inactivating pulse (0mV, 500 ms) was given, followed by a second recovery pulse of -100mV with increasing durations ($\Delta t$=4 ms). The final third test pulse of +50 mV was given to assess the amount

of recovery during that duration. As the duration increases, the peak current elicited by the test pulse can be seen to increase in a monophasic manner, as seen in the insert. The peak currents from the test pulses were normalized and plotted against the time spent recovering from 0 mV inactivation (duration of second pulse). The data was fitted according to an inverse exponential relationship to obtain the tau ($\tau$) value. **B.** The fast $I_{to}$ recovered more quickly from inactivation with $\tau$=11±4 ms. **C.** The slow $I_{to}$ was slower to recover with $\tau$=42±16 ms.

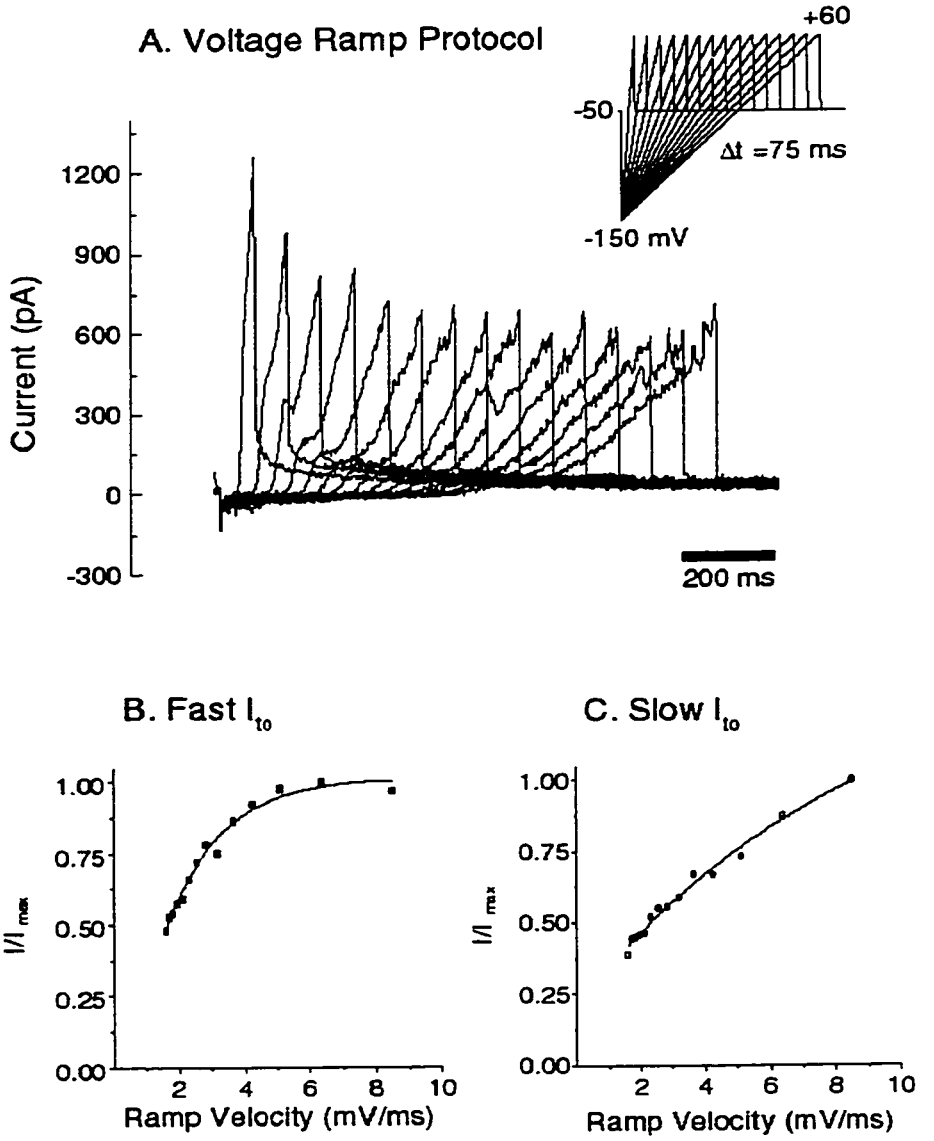


Figure 5-8 The response of $I_{to}$ to different rates of depolarization as assessed by voltage ramps.

**A.** Briefly, ramps from -150 to +60 mV with increasing durations ($\Delta t$=75 ms), and therefore different depolarization rates, were given. All ramps had the same range of depolarization (-150 to +60 mV) so that differences between ramps are due solely to the rates of the ramps. Peak currents can be seen to decrease exponentially. The peak currents

from each ramp was normalized and plotted against ramp depolarization rate. The data was fitted with an inverse exponential relationship to arrive at a tau ($\tau$) for the fit. **B.** The fast $I_{to}$ responded better to fast depolarization rates with $\tau$=2±1 mV/ms and was maximally expressed (95% complete) at 4.61 mV/ms. **C.** The slow $I_{to}$ had $\tau$=14±9 mV/ms and was maximally expressed (95% complete) at a higher depolarization rate of 42 mV/ms.

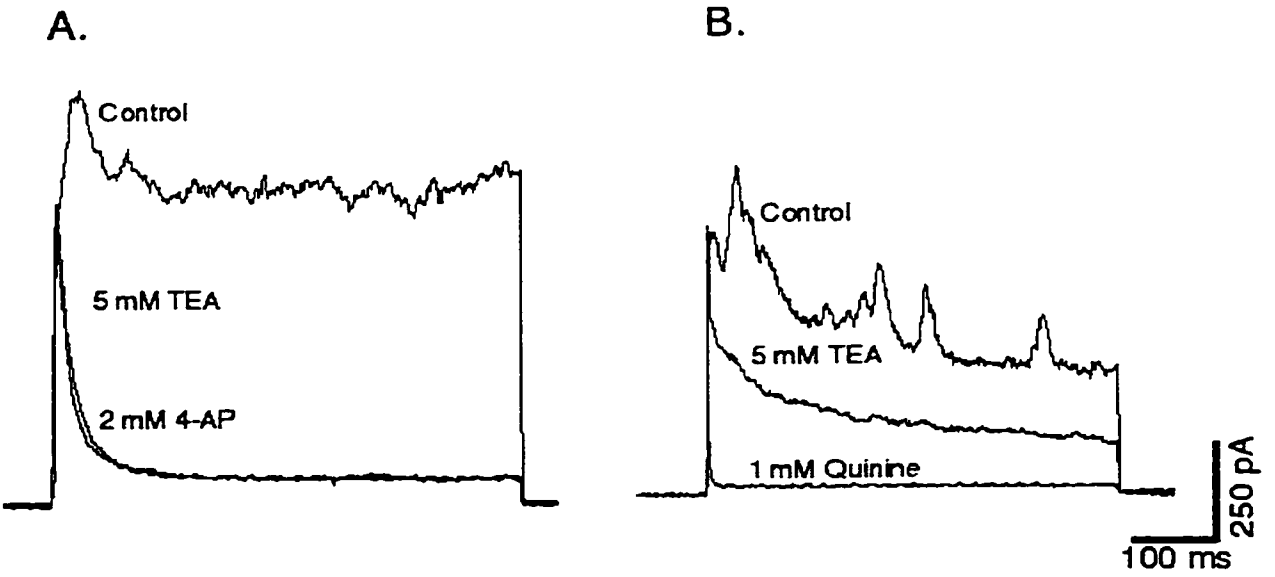


Figure 5-9 Pharmacology of $I_{to}$

**A.** After blocking the other outward currents with 5 mM TEA to reveal $I_{to}$, additional application with 2 mM 4-AP does not block this current further. **B.** After the addition of 5 mM TEA, 1 mM quinine almost completely abolishes this current.

# Chapter 6: Properties of Intracellular $Ca^{2+}$ Stores in Mouse Intestinal Smooth Muscle Cells as Assessed by STOC Activity

Jonathan C.F. Lee, and Jan D. Huizinga

McMaster University, Hamilton, Ontario, Canada

1200 Main Street West, L8N 3Z5

Running title: Properties of Intracellular $Ca^{2+}$ Stores in Intestinal SMC

Keywords: intracellular $Ca^{2+}$ stores, STOCs, smooth muscle

Correspondence address

Jan D. Huizinga
Health Sciences Centre Room 3N5C
905 -525 9140 ext. 22590
fax: 905 522 3454
email: huizinga@mcmaster.ca

## 6.a Abstract


1. In smooth muscle cells, spontaneous transient outward currents (STOCs) represent the transitory activation of $Ca^{2+}$ activated K channels in the cell membrane by elevations in intracellular [$Ca^{2+}$]. Therefore, when the membrane potential can be clamped by whole cell patch clamp, the expression of STOCs would represent primarily intracellular $Ca^{2+}$ cycling events.
2. STOCs have been recorded in isolated adult mouse small intestinal smooth muscle cells as whole cell spontaneous voltage and current oscillations.
3. Spontaneous voltage oscillations from STOCs were observed in a minority of smooth muscle cells (25% of all cells examined). These cells had depolarized membrane potentials which averaged –21.7±8.6 mV and expressed prominent oscillatory hyperpolarizations with an average amplitude and frequency of –13.7±9.5 mV and 133.8±94.5 cpm, respectively. The recovery of a spontaneous hyperpolarization follows a mono-exponential decay with $\tau$=68.7±36.6 ms.
4. In voltage clamped cells, STOCs can be seen to have a voltage dependency. Both STOC amplitude and frequency was strongly voltage dependent and showed a biphasic relationship with the transition point at ~0mV. The current to voltage (IV) plot can be fitted with two distinct conductances of 5.0±0.4 nS and 10.3±1.7 nS. Similarly, the frequency to voltage plot had two different rates of change: 2.6±0.4 cpm/mV and 7.2±0.6 cpm/mV. The other parameters showed weak voltage dependency such that the average durations, time to peak, and $\tau$ of recovery were

22.8±9.0 ms, 8.0±1.2 ms, and 15.4±3.5 ms.

5. STOCs were shown to be carried by $BK_{Ca}$ by its complete block with TEA, iberiotoxin, and penitrem A.
6. STOCs are not dependent on the entry of extracellular $Ca^{2+}$ since blockade of $Ca^{2+}$ channels by either 0.1 mM $Cd^{2+}$, or various L-type $Ca^{2+}$ channel blockers diltiazem, nifedipine, and pinaverium bromide failed to significantly affect any STOC parameter.
7. STOCs are dependent on intracellular $Ca^{2+}$ store activity because interference with normal $Ca^{2+}$ cycling by 3 μM CPA or 1 μM ryanodine specifically inhibits STOC activity.
8. Single channel recordings from cell-attached patches report a large outward conductance channel with moderate to long open states that correspond to $BK_{Ca}$. The average conductance of this channel was 186.3±26.4 pS. At the maximal whole cell conductance shown by STOCs at HP>0mV, each STOC event would potentially by made up of 55±9 $BK_{Ca}$ channels.
9. Based on these observations, predictions about the kinetic characteristics of the intracellular $Ca^{2+}$ stores in the adult mouse small intestine smooth muscle can be made.

## 6.1 Introduction

In all muscle cells, there are special arrangements between the sarcolemma and $Ca^{2+}$ stores sacroplasmic reticulum (SR) membranes that initiate and/or contribute to excitation/contraction (EC) coupling. The structures and the mechanism of EC coupling are different between different muscle systems. In smooth muscle cells, certain regions of the $Ca^{2+}$ stores SR form unique junctional spaces by closely apposing the sarcolemma membrane and leaving a narrow cytoplasmic space where $Ca^{2+}$ diffusion is restricted (Kohda *et al.* 1997). This "superficial buffer barrier" space allows for transient elevations in intracellular $Ca^{2+}$ within the superficial restricted space without increasing intracellular $Ca^{2+}$ to the deep cytoplasmic space and contractile apparatus. Therefore, events originating from the deep cytoplasmic space (central SR, general cytoplasmic space) react to an integration of $Ca^{2+}$ signals before a cellular $Ca^{2+}$ dependent effect is initiated. In contrast, events originating from the superficial cytoplasmic space are subjected less to $Ca^{2+}$ signal processing and probably reflects the actual SR $Ca^{2+}$ release events (Nelson *et al.* 1995), (Mironneau *et al.* 1996). Spontaneous transient outward currents (STOCs) are well established (Benham & Bolton, 1986), (Nelson & Quayle, 1995) to be periodic activation of $K_{Ca}$ in the plasma membrane in direct response to membrane depolarizations and local increases in $[Ca^{2+}]_i$. If membrane voltage can be controlled by voltage clamping, such as with whole cell patch clamp, these STOCs could be used as endogenous indicators of intracellular $Ca^{2+}$ elevations, especially of the superficial

cytoplasmic space where $Ca^{2+}$ levels cannot be measured by calcium indicator dyes (Kohda *et al.* 1997).

In this paper, STOC activity was analyzed as relating to intracellular $Ca^{2+}$ cycling in mouse small intestinal smooth muscle. Both spontaneous (current clamp) and voltage clamp STOC oscillations will be shown, followed by kinetic analysis and pharmacology. Single channel recordings from cell attached patches will be used to determine $BK_{Ca}$ conductance in this cell type. Finally, a simple model of intracellular $Ca^{2+}$ handling leading to STOC generation in the mouse small intestine smooth muscle will be presented.

## 6.2 Methods

### *6.2.1 Dissection of the external musculature from small intestine*

Adult female mice (20-25g) were sacrificed and a small intestine segment averaging 10 cm was removed proximal to the ileocaecal junction. The mesentery was carefully removed and the small intestine segment was placed in pre-equilibrated M199 media. Subsequently, the segment was opened flat by cutting along the mesenteric line. The segment was pinned flat with the mucosa facing the dissecting dish and the muscularis externae was carefully removed by sharp dissection. Examination of the strip of muscularis externae by electron microscopy revealed that the muscularis externae was separated along the deep muscular plexus region. The deep muscular nerve plexus was retained on the submucosal layer and was absent from the stripped muscle tissue. The

dissected muscularis externae was carefully cut into small pieces (~1-2 mm in length) in preparation for enzymatic dissociation.

### *6.2.2 Enzymatic Dissociation*

The muscularis externae was washed briefly in solution A before incubating at 37°C in solution A + 1mg/ml trypsin for 15 min first, then for 30 min. The supernatant was carefully removed and replaced with solution B + 3mg/ml collagenase + 1mg/ml BSA for 15 min, and then for 20 min more. The cells were then released by shaking. The cell suspension was layered on a 20% (w/v) Ficoll cushion and spun at 15 g for 15 min. The cell band located at the interface was transferred to a new container and resuspended with M199 media to the desired density. This cell suspension was plated into Falcon petri dishes with collagen coated coverslips glued to the bottoms. The cells were maintained in 5% $CO_2$/37°C until ready for use.

### *6.2.3 Electrophysiology*

Cells were not used beyond 5 days post-isolation because it became nearly impossible to form a tight seal with a glass pipette without enzyme pre-treatment. The cells were continuously bathed with extracellular solution (ECS) at room temperature. Electrical activity in SMC was recorded using whole cell patch clamp technique (Neher and Sakmann). Pipettes were made using a Sutter micropipette puller to typical access resistances of 3-5 MΩ. The pipette was filled with ICS and inserted into the headstage of

the patch amplifier (Axopatch 1B, Axon Instruments, Calif.). The pipette was quickly lowered onto the cell surface and suction was applied. Upon formation of a tight seal (~2-5 GΩ), the patch was disrupted using sharp suction to proceed to whole cell recording. Initially, the patch amplifier was switched over to current clamp to get a reading of the membrane potential. Holding potentials for voltage clamp were chosen from observations of the membrane potential in current clamp. Results were acquired by Axotape (v1.2, Axon Instruments, Calif.) sampling at 50 Hz using the TM-1 DMA interface.

### *6.2.4 Solutions*

Solutions, with concentrations in mM

ECS (Extracellular solution): NaCl 125.0, KCl 5.0, MgCl2 1.2, $NaH_2PO_4$ 1.2, Glucose 11.0, $NaHCO_3$ 4.0, $CaCl_2$ 2.0, HEPES 10.0, pH 7.35

ICS (Intracellular solution): K-Methanesulfonate 118.0, $MgCl_2$ 2.0, $CaCl_2$ 1.0, EGTA 9.0, BAPTA 2.0, $Na_2ATP$ 2.0, GTP 0.1, $Na_2$Phosphocreatine 3.0, Glucose 5.0, HEPES 10.0, pH=7.25

Solution A: NaCl 134.0, KCl 3.0, Taurine 5.0, EDTA 5.0, $MnCl_2$ 2.0, HEPES 10.0, pH 7.40

Solution B: NaCl 133.0, KCl 3.0, Taurine 5.0, $CaCl_2$ 0.1, $MgCl_2$ 2.0, Glucose 10.0, HEPES 10.0, pH 7.35

M199 media: 1X M199 media, $NaHCO_3$ 26.0 mM, Glutamine 2.0, Penicillin 0.25 mg/ml, FBS 10%

Drugs: Verapamil, nifedipine, diltiazem, pinaverium-Br, and Bay K 8644 were dissolved in 70% EtOH as $10^{-2}$ M stock solutions.

CPA was dissolved in DMSO as $5X10^{-2}$ M stock solution

Chemicals and drugs were purchased from Sigma-Aldrich Canada Ltd.

Media was obtained from Gibco-Life Sciences Canada

## 6.3 Results

### *6.3.1 Spontaneous Hyperpolarizations from STOCs in Smooth Muscle Cells*

Smooth muscle cells were patched in the whole cell configuration and spontaneous voltage activity was recorded in current clamp mode (figure 1). Isolated SMCs were seen to have depolarized resting membrane potentials which averaged -21.7±8.6 mV. In a minority of cells (25%, 26/104), spontaneous hyperpolarizations from STOCs can be seen. Among the cells which showed STOC activity, the majority of these cells had the STOC activity disappear, presumably from the $Ca^{2+}$ buffering of the intracellular pipette solution. The voltage oscillations occurred with an average amplitude of -13.7±9.5 mV and frequency of 133.8±94.5 cpm. On an expanded time scale, the voltage oscillation can be seen to have a fast takeoff followed by a slower monophasic recovery. The average time to peak amplitude and duration was 40.4±13.2 ms and 170.9±79.1 ms respectively. If the recovery process can be fitted as a mono-exponential function, the average $\tau$ for recovery was found to be 68.7±36.6 ms.

### *6.3.2 Spontaneous Transient Outward Currents (STOCs)*

In voltage clamped cells, applying a typical whole cell protocol (from a holding potential of -50 mV, test pulses of 500 ms from -70 to +60 mV was applied) produced multiple STOCs superimposed on other voltage activated currents (figure 2a). Cells with STOCs typically have an underlying transient outward current that remains even after STOCs are completely blocked with TEA. STOC activity can be more easily visualized with depolarizing potentials. The appearance of each current oscillation was heterogeneous and exclusive (i.e. discrete events). With voltage clamp, the membrane potential could be set to different potentials (figure 2b). Starting at approximately HP= –60 mV, individual STOC events can be discerned from baseline noise. With increasing depolarization, STOCs become prominent. Prolonged depolarizations above HP= -30mV were not attempted often since they usually lead to contraction, and subsequent loss of the tight seal.

Average amplitudes of STOC events were plotted against holding potentials for current-voltage (IV) plots (figure 3a). The IV plot appeared biphasic and could be fitted with two different linear regressions to yield a fitted minor chord conductance of 5.0±0.4 nS and a maximum chord conductance of 10.3±1.7 nS. The point of transition was approximately at HP=0mV.

The voltage dependency of the frequency of STOCs was found to be also biphasic and could be fitted with two different linear regressions (figure 3b). The slower voltage dependency ($d$Freq/$d$V=2.6±0.4 cpm/mV) occurred at the hyperpolarized potentials before a greater voltage dependency can be seen at holding potentials >0 mV

($d$Freq/$d$mV=7.2±0.6 cpm/mV). The parameters of duration and time to peak were found to be weakly voltage dependent. The duration change over voltage (dDur/dV) was inversely proportional such that the duration of the STOC event decreased with depolarization (figure 3c). The negative linear trend was small and corresponded to a linear regression of 0.069±0.018 ms/mV (r= -0.86). If the durations were assumed not to be voltage dependent, the duration would average 22.8±.9.0 ms over all voltages. The parameter of time to peak showed a positive dependency with increasing depolarization (figure 3d). A linear regression revealed a relative change of the time to peak against voltage ($dT_{peak}/dV$) to be 0.030±0.006 ms/mV (r=0.86). Since the relative change over voltage was small, the time to peak can be averaged to 8.0±1.2 ms over the entire voltage range examined (-40 to +60 mV). After a STOC event has peaked, the recovery time was roughly 10 times longer than the rise time. Frequently in the larger STOC events, the recovery can be seen to follow a mono-exponential course. After fitting for an inverse mono-exponential relationship, the $\tau$ for recovery was plotted against holding potential (figure 3e). The $\tau$ for recovery was found to be variable over the different holding potentials and was difficult to ascertain its voltage dependency. Linear regression yields a low correlation coefficient (r= -0.15). Assuming the rate of recovery does not change significantly with voltage, the average $\tau$ for recovery over all voltage ranges would be 15.4±3.5 ms.

### *6.3.3 Pharmacology*

As expected, $BK_{Ca}$ channel blockers TEA, iberiotoxin and penitrem A inhibited STOC activity. In the whole cell configuration, TEA was observed to directly block outward currents along with STOC activity to leave a small transient outward current (figure 4a). In another cell, 10 mM procaine was observed to inhibit STOCs and a significant portion of the outward currents (figure 4b). A specific toxin blocker of $BK_{Ca}$, iberiotoxin, inhibited STOC activity (figure 5a). Smaller amplitude STOC events can still be seen, indicating the oscillatory release of $Ca^{2+}$ from intracellular stores have not been affected. Penitrem A, an alkaloid blocker of $BK_{Ca}$, also inhibited STOC activity strongly without significantly depolarizing the membrane potential (figure 5b). Collectively, the inhibition of STOCs by TEA, iberiotoxin, and penitrem A suggests that STOCs are openings of $BK_{Ca}$ channels.

### *6.3.4 Extracellular $Ca^{2+}$ not necessary for STOC activity*

The entry of extracellular $Ca^{2+}$ can be blocked by several ways. The non-specific $Ca^{2+}$ channel blocker, $Cd^{2+}$, did not affect STOC activity (figure 6a). The addition of L-type $Ca^{2+}$ channel blockers diltiazem, nifedipine, and pinaverium bromide also failed to affect any STOC parameter (figure 6b).

Conversely, the entry of extracellular $Ca^{2+}$ increased the amplitude, duration and frequency of STOCs. The entry of extracellular $Ca^{2+}$ was encouraged by the addition of Bay K8644, a L-type $Ca^{2+}$ channel opener. In whole cell voltage clamp, +30 mV (500

ms) test pulses evokes typical whole cell outward currents. In certain cells, the addition of Bay K8644 not only increases the outward whole cell currents expressed, but can evoke STOC activity (figure 6a). In cells exhibiting intrinsic STOC activity, the addition of 5 μM Bay K8644 quickly increased STOC occurrence and amplitude. On average, STOC frequency increased 230% of control, along with STOC amplitude and duration to 123% and 68% respectively (n=3). The only parameters that did not change significantly were the time to peak amplitude and the rates of recovery.

### *6.3.5 STOC activity depends on Intracellular $Ca^{2+}$ store activity*

STOCs represent openings of $BK_{Ca}$ that are activated by discharges of $Ca^{2+}$ from intracellular stores. The addition of procaine, a blocker of CICR release, blocked whole cell outward currents in a similar fashion as TEA (figure 4b). The addition of 10 mM procaine inhibited spontaneous voltage oscillations and depolarized the cell by 8.6±2.1mV, indicative more of direct block of $BK_{Ca}$ than specific inhibition of CICR (figure 4c). Other agents, such as cyclopiazonic acid (CPA) and ryanodine, showed the involvement of intracellular stores better. Spontaneous hyperpolarizations caused from STOCs can be reversibly blocked with CPA, an inhibitor of the sarcoplasmic/endoplasmic reticulum $Ca^{2+}$-ATPase (SERCA) (figure 8). Ryanodine has been found to be both an activator and inhibitor of CICR depending on the concentration (Ehrlich *et al.* 1994). In these cells, even 1 μM ryanodine caused irreversible block of STOC activity and subsequent depolarization (figure 9). The specific inhibition of STOC

activity by CPA and ryanodine strongly suggests the participation of intracellular $Ca^{2+}$ stores.

### *6.3.6 $BK_{Ca}$ Single Channel Recording*

In the cell attached patch configuration, outward currents from single channels could be recorded with a voltage ramp (figure 9). The pipette potential was ramped from -100 to 0 mV for 1 s. At negative pipette potentials, single channel events can be seen to increase in amplitude and frequency correspondingly to the voltage applied. These single channels have a large conductance corresponding to $BK_{Ca}$ (186.3±26.4 pS). From the IV plot of whole cell STOCs, the maximum chord conductance of 10.3±1.7 nS would be made up on average of 55±9 $BK_{Ca}$ single channels per average STOC event.

## 6.4 Discussion

### *6.4.1 Adult mouse intestinal smooth muscle intracellular stores*

It has been well established that most smooth muscle cells, if not all, have some form of intracellular $Ca^{2+}$ stores (Gordienko *et al.* 1998), (Laporte & Laher, 1997), (Sieck *et al.* 1997), (Sims *et al.* 1997), (Sims *et al.* 1996), (Kasai *et al.* 1995). The properties of the mouse intestinal smooth muscle cell $Ca^{2+}$ stores, and especially their relationship with STOCs (Bolton & Imaizumi, 1996) are not well known. Mouse mutant models in which motility is driven primarily by myogenic mechanisms instead of ICC pacemakers (Malysz *et al.* 1996) offer new insights into different contributions to motility. Both

myogenic and ICC dependent motility are sensitive to pharmacological agents that interfere with intracellular $Ca^{2+}$ handling. Understanding intracellular $Ca^{2+}$ handling in intestinal smooth muscle is an important step to how it affects and interacts with other pacemaking mechanisms, and ultimately to motility.

Our results show the adult mouse small intestine smooth muscle contains at least a CICR $Ca^{2+}$ store that can spontaneously release $Ca^{2+}$ as oscillations. These oscillatory releases of $Ca^{2+}$ are transduced as STOCs. The voltage dependency of STOC activity are contributed by voltage dependent $Ca^{2+}$ entry, likely from $Ca^{2+}$ channels, and by the voltage dependency of the $BK_{Ca}$ channels themselves. The amplitude of STOCs was observed to increase with depolarization in a biphasic manner, with an initial lower conductance of 5.0±0.4 nS (<0 mV) to a higher conductance of 10.3±1.7 nS (>0 mV). The frequency of STOCs also showed a biphasic voltage dependency; at membrane potentials up to 0 mV, the relative rate of change of frequency by voltage ($d$Freq/$d$mV) was 2.6±0.4 cpm/mV, while at membrane potentials more depolarized that 0 mV showed $d$Freq/$d$mV=7.2±0.6 cpm/mV. Both parameters of amplitude and frequency of STOCs in response to depolarization must be interpreted with the considerations that $BK_{Ca}$ itself is sensitive to both membrane voltage and local $[Ca^{2+}]_i$ (Benham *et al.* 1986). Assuming the intracellular $Ca^{2+}$ stores themselves are not directly voltage sensitive (addition of $Cd^{2+}$ and/or L-type $Ca^{2+}$ channel blockers do not affect STOC activity), the responses of amplitude and frequency to depolarization would depend on the combination of the detection limit of $BK_{Ca}$ at that membrane potential and possible $Ca^{2+}$ channel activation. At hyperpolarized membrane potentials, $BK_{Ca}$ may not be sensitive enough to be

activated by every $[Ca^{2+}]_i$ oscillation. As the $Ca^{2+}$ sensitivity of $BK_{Ca}$ increases with depolarization, STOCs would show a more accurate activation by intracellular $Ca^{2+}$ oscillations. Also, the entry of extracellular $Ca^{2+}$ through voltage activated $Ca^{2+}$ channels will contribute to increasing cytoplasmic $[Ca^{2+}]_i$, which will lead to increases in STOC amplitude and frequency. Therefore, the biphasic nature of STOC amplitude and frequency that occurs at ~0mV can be explained in part by the voltage activation of $Ca^{2+}$ channels, and by the change in activation kinetics of $BK_{Ca}$ at those potentials.

The parameters that were not expected to be voltage sensitive were the duration and time to peak of the STOC events. Both the duration and time to peak amplitude was weakly dependent on voltage. Neither parameter showed biphasic behavior as demonstrated by amplitude or frequency. The rates of deactivation can be seen more clearly in spontaneous voltage oscillations to be mono-exponential decays while spontaneous outward currents show more complex patterns. From the STOCs that showed mono-exponential decay, it was difficult to ascertain if the $\tau$ of deactivation was voltage dependent.

STOCs were sensitive to inhibition by $BK_{Ca}$ blockers TEA, iberiotoxin, and penitrem A (Knaus *et al.* 1994). In whole cell experiments, 10 nM iberiotoxin blocked 15% of the outward whole cell current as well as reducing the amplitude of STOCs accordingly. Others have found that iberiotoxin does not block effectively when applied at the cellular level (Garcia *et al.* 1991). Surprisingly, procaine was found to block outward currents and STOCs to a similar degree as TEA (Benham *et al.* 1985; Ohya *et al.*

1987). The complete block of STOCs by TEA, iberiotoxin, and penitrem A shows STOCs are carried by $BK_{Ca}$.

As shown by other groups, smooth muscle STOCs are not dependent on extracellular $Ca^{2+}$ for activity (Benham & Bolton, 1986; Ohya *et al.* 1987). However, STOC activity can be stopped by depleting the internal $Ca^{2+}$ stores, possibly by long term exposure to a $0Ca^{2+}$ environment. Elevations in cytoplasmic [$Ca^{2+}$] have been shown to stimulate $BK_{Ca}$ activity and intracellular $Ca^{2+}$ cycling (Carl & Sanders, 1989; Ehrlich *et al.* 1994). Therefore, the increase in STOC activity from increasing extracellular $Ca^{2+}$ entry probably uses both direct $Ca^{2+}$ activation of $BK_{Ca}$ as well as indirect activation of intracellular $Ca^{2+}$ stores.

The complete inhibition of STOCs by specific agents, CPA (Suzuki *et al.* 1992) and ryanodine (Sakai *et al.* 1988), known to interfere with intracellular $Ca^{2+}$ handling verifies intracellular stores involvement. CPA acts specifically to block the SERCA $Ca^{2+}$-ATPase resulting in inhibition of reuptake of $Ca^{2+}$ back into the SR and eventually depleting the $Ca^{2+}$ stores. The relatively fast inhibition of STOCs with CPA suggests that simply inhibiting the reuptake of $Ca^{2+}$ is enough to stop the oscillatory release of $Ca^{2+}$. Ryanodine acts on the ryanodine sensitive $Ca^{2+}$ release channel in the SR membrane (Muraki *et al.* 1992). Others have found that low concentrations of ryanodine can activate RyR while higher concentrations block RyR (Garcia *et al.* 1990). In the mouse, even 1 μM ryanodine was enough to irreversibly block STOC activity. Ryanodine has been observed to cause irreversible inhibition of STOC activity in other single smooth muscle cell preparations (Sakai *et al.* 1988; Bolton & Lim, 1989; Nelson & Quayle, 1995).

### *6.4.2 Predicted parameters of intracellular $Ca^{2+}$ stores*

Once the kinetic parameters of STOCs are found, a simple model of the mouse small intestine smooth muscle $Ca^{2+}$ stores can be presented. In rat posterior cerebral artery smooth muscle cells, an unitary $Ca^{2+}$ event can be observed by $Ca^{2+}$-indicators in the superficial part of the cytoplasmic spaces as "sparks" (Nelson *et al.* 1995). These sparks have rise times of 20 ms and half time of decay of 50 ms. The STOCs rise times found (8.0±1.2 ms) were faster than those observed for sparks. The average $\tau$ of deactivation was 15.4±3.5 ms, again faster than those observed for sparks. Differences in the kinetic properties of STOCs and sparks may be from tissue (intestinal vs. arterial) and/or species differences (mouse intestine vs. rat cerebral artery) in intracellular $Ca^{2+}$ handling. The $Ca^{2+}$ release event would be expected to have the following properties: the mouse $Ca^{2+}$ release channel(s) would be expected to have rise times faster than 8.0 ms and deactivate faster than 15.4 ms. STOC activity requires a basal concentration of intracellular $Ca^{2+}$ since strong $Ca^{2+}$ buffering abolishes STOC activity (Saunders & Farley, 1991), (Hume & Leblanc, 1989), and $Ca^{2+}$ entry is not required for continued activity (Ohya *et al.* 1987). Excitation from either depolarization or $Ca^{2+}$ entry can increase $Ca^{2+}$ release activity-the mechanisms are inter-related such that depolarization alone cannot increase $Ca^{2+}$ release activity but is transduced by $Ca^{2+}$ entry. In circumstances when $[Ca^{2+}]_i$ can be elevated without depolarization (opening of L-type $Ca^{2+}$ channels by Bay K8644 or release by $IP_3$ stores), $Ca^{2+}$ release events are increased not only in amplitude, but also in frequency (Gordienko *et al.* 1998), (Satoh *et al.* 1997), (Weissberg *et al.* 1989). It has been shown that elevations in cytoplasmic $Ca^{2+}$ in

increases SR RyR open probability and open times in planar lipid bilayers (Herrmann Frank *et al.* 1991). At cytoplasmic $Ca^{2+}$ concentrations below 300nM, the $IP_3R$ $Ca^{2+}$-release receptor is allosterically activated (Ehrlich *et al.* 1994), (Hirose *et al.* 1998). Whatever the source of stimulating $Ca^{2+}$ release, there appears to an upper limit in oscillatory $Ca^{2+}$ release frequency. In the mouse small intestine, the maximal frequency levels at an average of 856 cpm. Just from record traces, the amplitude of STOCs can be seen to fluctuate. It has been suggested that the amplitude of STOCs can be a function of the $Ca^{2+}$ stores load (Kohda *et al.* 1996). Alternatively, distinct STOC amplitudes may arise from $Ca^{2+}$ discharges from distinct $Ca^{2+}$ pools whose discharge amplitude and frequency may be different from each other (Iino *et al.* 1988). Nevertheless, the average amplitude of STOCs in response to voltage agrees more with Nernst-type relationship for $K^+$ conductances than an amplifying regenerative system expect from CICR type stores. From these experiments, the mouse small intestinal smooth muscle $Ca^{2+}$ stores can potentially be "excited" by depolarization or events leading to intracellular $Ca^{2+}$ elevation, but normally functions independent of membrane potential. Depolarization serves more to express the oscillatory $Ca^{2+}$ discharges from intracellular $Ca^{2+}$ stores as STOCs than to modify them.

### *6.4.3 Comparisons with other smooth muscle preparations*

The STOC activity found in mouse small intestinal smooth muscle are consistent with properties found in other smooth muscle preparations (Chen & van Breemen, 1993), (Porter *et al.* 1998), (Cotton *et al.* 1997), (Hamada *et al.* 1997), (Imaizumi *et al.* 1993).

The function of STOCs in intestinal smooth muscle may be the same as for vascular smooth muscle (Nelson & Quayle, 1995)-relaxation and "braking" of depolarizing excitation. In intestinal smooth muscle, oscillations in intracellular $Ca^{2+}$ have been implicated in coordinating spiking events. During a depolarizing event, STOCs are expressed as oscillatory hyperpolarizing events that provides transient inhibition rather than a prolonged inhibition, as expected with a long activating $K^+$ conductance, such as $K_{Dr}$. Because the inhibition is synchronous with $Ca^{2+}$ release from intracellular stores, it provides direct inhibition to excitatory effects dependent on cytoplasmic $Ca^{2+}$ oscillations. In the intestinal smooth muscle, the spiking activity should be influenced by oscillations in intracellular $Ca^{2+}$ (Kohda *et al.* 1997), (Malysz *et al.* 1996), (Iino *et al.* 1993) and modified accordingly with STOC expression. The inhibition of $IK_{Ca}$ has been found to stimulate spiking activity in the colon (Thornbury *et al.* 1992). The transient nature of STOC hyperpolarizations allow for periodic depolarizing events to occur, especially if they are faster than the inter-STOC interval. Collectively, STOC activity may play a major role in modulation of spiking activity and FM (frequency modulation) type inhibition.

## 6.5 Bibliography

BENHAM, C. D. & BOLTON, T. B. (1986). Spontaneous transient outward currents in single visceral and vascular smooth muscle cells of the rabbit. *Journal of Physiology - London* **381**, 385-406.

BENHAM, C. D., BOLTON, T. B., LANG, R. J. & TAKEWAKI, T. (1985). The mechanism of action of $Ba^{2+}$ and TEA on single $Ca^{2+}$-activated $K^+$-channels in arterial and intestinal smooth muscle cell membranes. *Pflügers Archiv - European Journal of Physiology* **403**, 120-127.

BENHAM, C. D., BOLTON, T. B., LANG, R. J. & TAKEWAKI, T. (1986). Calcium-activated potassium channels in single smooth muscle cells of rabbit jejunum and guinea-pig mesenteric artery. *Journal of Physiology* **371**, 45-67.

BOLTON, T. B. & IMAIZUMI, Y. (1996). Spontaneous transient outward currents in smooth muscle cells. *Cell Calcium* **20**, 141-152.

BOLTON, T. B. & LIM, S. P. (1989). Properties of calcium stores and transient outward currents in single smooth muscle cells of rabbit intestine. *Journal of Physiology* **409**, 385-401.

CARL, A. & SANDERS, K. M. (1989). Ca2+-activated K channels of canine colonic myocytes. *American Journal of Physiology* **257**, C470-C480.

CHEN, Q. & VAN BREEMEN, C. (1993). The superficial buffer barrier in venous smooth muscle: sarcoplasmic reticulum refilling and unloading. *British Journal of Pharmacology* **109**, 336-343.

COTTON, K. D., HOLLYWOOD, M. A., MCHALE, N. G. & THORNBURY, K. D. (1997). Outward currents in smooth muscle cells isolated from sheep mesenteric lymphatics. *Journal.of.Physiology.* **503**, 1-11.

EHRLICH, B. E., KAFTAN, E., BEZPROZVANNAYA, S. & BEZPROZVANNY, I. (1994). The pharmacology of intracellular Ca(2+)-release channels. [Review]. *Trends in Pharmacological Sciences* **15**, 145-149.

GARCIA, J., FILL, M., TORO, L. & STEFANI, E. (1990). Functional studies of Ca2+ channels from plasmalemma and sarcoplasmic reticulum membranes in muscle cells. [Review]. *Seminars in Cell Biology* **1**, 255-264.

GARCIA, M. L., GALVEZ, A., GARCIA-CALVO, M., KING, V. F., VAZQUEZ, J. & KACZOROWSKIGJ. (1991). Use of toxins to study potassium channels. [Review]. *Journal of Bioenergetics & Biomembranes* **23**, 615-646.

GORDIENKO, D. V., BOLTON, T. B. & CANNELL, M. B. (1998). Variability in spontaneous subcellular calcium release in guinea-pig ileum smooth muscle cells. *Journal of Physiology - London* **507**, 707-720.

HAMADA, H., DAMRON, D. S., HONG, S. J., VAN WAGONER, D. R. & MURRAY, P. A. (1997). Phenylephrine-induced Ca2+ oscillations in canine pulmonary artery smooth muscle cells. *Circulation Research.* **81**, 812-823.

HERRMANN FRANK, A., DARLING, E. & MEISSNER, G. (1991). Functional characterization of the $Ca^{2+}$-gated $Ca^{2+}$ release channel of vascular smooth muscle sarcoplasmic reticulum. *Pflügers Archiv - European Journal of Physiology* **418**, 353-359.

HIROSE, K., KADOWAKI, S. & IINO, M. (1998). Allosteric regulation by cytoplasmic Ca2+ and IP3 of the gating of IP3 receptors in permeabilized guinea-pig vascular smooth muscle cells. *Journal.of.Physiology.* **506**, 407-414.

HUME, J. R. & LEBLANC, N. (1989). Macroscopic K+ currents in single smooth muscle cells of the rabbit portal vein. *Journal of Physiology - London* **413**, 49-73.

IINO, M., KOBAYASHI, T. & ENDO, M. (1988). Use of ryanodine for functional removal of the calcium store in smooth muscle cells of the guinea-pig. *Biochemical & Biophysical Research Communications* **152**, 417-422.

IINO, M., YAMAZAWA, T., MIYASHITA, Y., ENDO, M. & KASAI, H. (1993). Critical intracellular Ca2+ concentration for all-or-none Ca2+ spiking in single smooth muscle cells. *EMBO Journal.* **12**, 5287-5291.

IMAIZUMI, Y., MURAKI, K., HENMI, S. & WATANABE, M. (1993). Physiological functions and regulation of K+ and Cl- channels in single smooth muscle cells. [Review] [Japanese]. *Nippon Yakurigaku Zasshi - Folia Pharmacologica Japonica* **101**, 153-167.

KASAI, Y., TSUTSUMI, O., TAKETANI, Y., ENDO, M. & IINO, M. (1995). Stretch-induced enhancement of contractions in uterine smooth muscle of rats. *Journal.of.Physiology.* **486**, 373-384.

KNAUS, H. G., MCMANUS, O. B., LEE, S. H., SCHMALHOFER, W. A., GARCIA-CALVO, M., HELMS, L. M., SANCHEZ, M., GIANGIACOMO, K., REUBEN, J. P., SMITH, A. B.,3RD & ET AL (1994). Tremorgenic indole alkaloids potently inhibit smooth muscle high-conductance calcium-activated potassium channels. *Biochemistry* **33**, 5819-5828.

KOHDA, M., KOMORI, S., UNNO, T. & OHASHI, H. (1996). Carbachol-induced [Ca2+]i oscillations in single smooth muscle cells of guinea-pig ileum. *Journal.of.Physiology.* **492**, 315-328.

KOHDA, M., KOMORI, S., UNNO, T. & OHASHI, H. (1997). Characterization of action potential-triggered [Ca2+]i transients in single smooth muscle cells of guinea-pig ileum. *British.Journal.of.Pharmacology* **122**, 477-486.

LAPORTE, R. & LAHER, I. (1997). Sarcoplasmic reticulum-sarcolemma interactions and vascular smooth muscle tone. *J.Vasc.Res.* **34**, 325-343.

MALYSZ, J., THUNEBERG, L., MIKKELSEN, H. B. & HUIZINGA, J. D. (1996). Action potential generation in the small intestine of *W* mutant mice that lack interstitial cells of Cajal. *American Journal of Physiology* **271**, G387-G399.

MIRONNEAU, J., ARNAUDEAU, S., MACREZ-LEPRETRE, N. & BOITTIN, F. X. (1996). Ca2+ sparks and Ca2+ waves activate different Ca(2+)-dependent ion channels in single myocytes from rat portal vein. *Cell Calcium* **20**, 153-160.

MURAKI, K., IMAIZUMI, Y. & WATANABE, M. (1992). Ca-dependent K channels in smooth muscle cells permeabilized by beta-escin recorded using the cell-attached patch-clamp technique. *Pflügers Archiv - European Journal of Physiology* **420**, 461-469.

NELSON, M. T., CHENG, H., RUBART, M., SANTANA, L. F., BONEV, A. D., KNOT, H. J. & LEDERER, W. J. (1995). Relaxation of arterial smooth muscle by calcium sparks [see comments]. *Science* **270**, 633-637.

NELSON, M. T. & QUAYLE, J. M. (1995). Physiological roles and properties of potassium channels in arterial smooth muscle. [Review]. *American Journal of Physiology* **268**, Pt 1):C799-822.

OHYA, Y., KITAMURA, K. & KURIYAMA, H. (1987). Cellular calcium regulates outward currents in rabbit intestinal smooth muscle cell. *American Journal of Physiology* **252**, C401-C410.

PORTER, V. A., BONEV, A. D., KNOT, H. J., HEPPNER, T. J., STEVENSON, A. S., KLEPPISCH, T., LEDERER, W. J. & NELSON, M. T. (1998). Frequency modulation of Ca2+ sparks is involved in regulation of arterial diameter by cyclic nucleotides. *American Journal of Physiology* **274**, Pt 1):C1346-55.

SAKAI, T., TERADA, K., KITAMURA, K. & KURIYAMA, H. (1988). Ryanodine inhibits the Ca-dependent K current after depletion of Ca stored in smooth muscle cells of the rabbit ileal longitudinal muscle. *British Journal of Pharmacology* **95**, 1089-1100.

SATOH, H., HAYASHI, H., BLATTER, L. A. & BERS, D. M. (1997). BayK 8644 increases resting calcium spark frequency in ferret ventricular myocytes. *Heart Vessels* **Suppl**, 12:58-61.

SAUNDERS, H. M. & FARLEY, J. M. (1991). Spontaneous transient outward currents and Ca(++)-activated K+ channels in swine tracheal smooth muscle cells. *Journal of Pharmacology and Experimental Therapeutics* **257**, 1114-1120.

SIECK, G. C., KANNAN, M. S. & PRAKASH, Y. S. (1997). Heterogeneity in dynamic regulation of intracellular calcium in airway smooth muscle cells. *Can.J.Physiol.Pharmacol.* **75**, 878-888.

SIMS, S. M., JIAO, Y. & PREIKSAITIS, H. G. (1997). Regulation of intracellular calcium in human esophageal smooth muscles. *American.Journal.of.Physiology.* **273**, Pt 1):C1679-89.

SIMS, S. M., JIAO, Y. & ZHENG, Z. G. (1996). Intracellular calcium stores in isolated tracheal smooth muscle cells. *American.Journal.of.Physiology.* **271**, Pt 1):L300-9.

SUZUKI, M., MURAKI, K., IMAIZUMI, Y. & WATANABE, M. (1992). Cyclopiazonic acid, an inhibitor of the sarcoplasmic reticulum $Ca^{2+}$-pump, reduces $Ca^{2+}$-dependent $K^+$ currents in guinea-pig smooth muscle cells. *British Journal of Pharmacology* **107**, 134-140.

THORNBURY, K. D., WARD, S. M. & SANDERS, K. M. (1992). Outward currents in longitudinal colonic muscle cells contribute to spiking electrical behavior. *American Journal of Physiology* **263**, C237-C245.

WEISSBERG, P. L., LITTLE, P. J. & BOBIK, A. (1989). Spontaneous oscillations in cytoplasmic calcium concentration in vascular smooth muscle. *American Journal of Physiology* **256**, C951-C957.

## 6.6 Figures & Legends

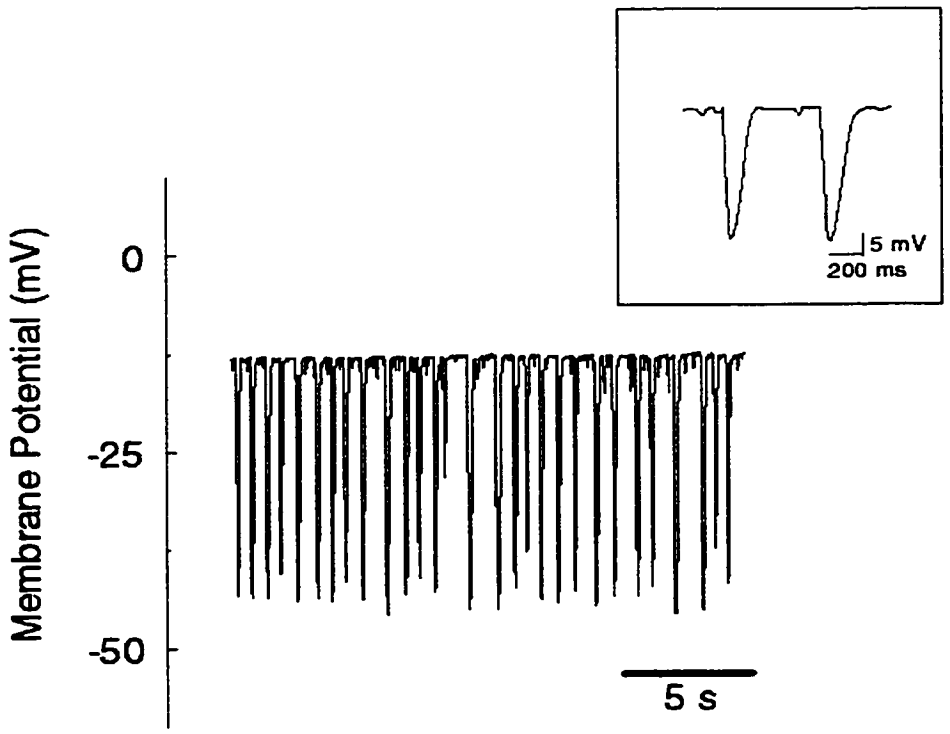


Figure 6-1 Spontaneous voltage oscillations in isolated smooth muscle cells

The resting membrane potential of isolated SMCs were generally depolarized and averaged -21.7±8.7 mV (n=9). Spontaneous hyperpolarizations can show regular or irregular rhythmicity, with variations in frequency and amplitude. On average, the voltage oscillations had a frequency of 133.8±94.5 cpm and an amplitude of –13.7±9.5 mV. On an expanded time scale, the voltage oscillation can be seen to have a fast takeoff followed by a monophasic recovery (insert). The voltage oscillations had an average time to peak of 40.4±13.2 ms and durations of 170.9±79.1 ms. The recovery process could be fitted as monoexponential relationship with an average $\tau$ for recovery of 68.7±36.6 ms.

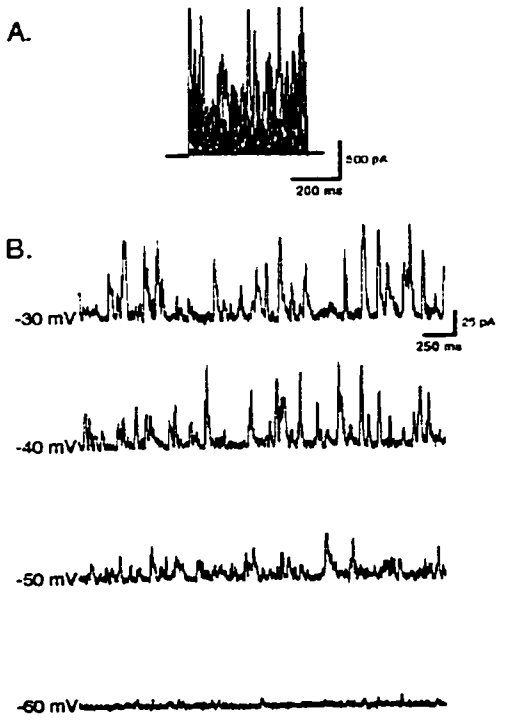


Figure 6-2 Spontaneous current oscillations are voltage dependent

A. Using a voltage clamp protocol of +10 mV steps (500 ms) from -70 to +60 mV from a holding potential of -50 mV, whole cell currents were expressed in smooth muscle cells. Along with the outward currents, spontaneous transient outward currents (STOCs) was seen to superimpose the underlying whole cell currents. Although the amplitude of STOCs can be seen to increase with depolarization, the occurrence of STOCs was not dependent on voltage (i.e. the STOC event was not triggered by voltage).

B. From different holding potentials from -60 to -30 mV, STOCs can be seen to increase in amplitude and in frequency. Spontaneous current oscillations frequently appear more heterogeneous than spontaneous hyperpolarizations.

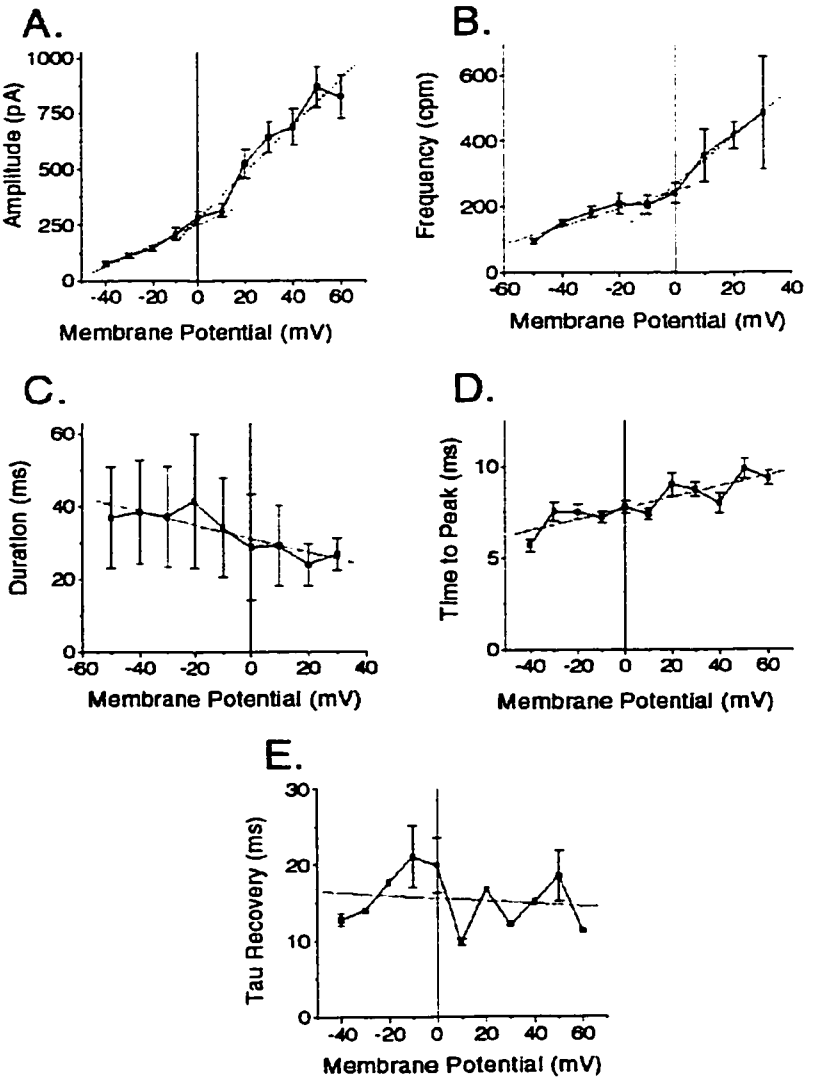


Figure 6-3 The voltage dependency of various STOC parameters: Amplitude, frequency, duration, time to peak, and $\tau$ for recovery

A. The current amplitudes of STOCs were plotted against applied voltage (n=43). The current amplitudes responded biphasically with a vertex approximately at HP=0 mV. Two linear relationships can be fitted – a low chord conductance of 5.0±0.4 nS and a high chord conductance of 10.3±1.7 nS.

B. The frequency of STOC events behaved similarly to current amplitudes towards applied voltage. The frequency appeared biphasic with the vertex at HP=0 mV. Again, two linear relationships can be fitted representing the relative rates of change of frequency to voltage ($d$Freq/$d$mV). The slower $d$Freq/$d$mV corresponded to 2.6±0.4 cpm/mV while at HP>0 mV, dFreq/dmV was 7.2±0.6 cpm/mV.

C. The duration of STOC events showed a negative linear trend (r=-0.86) with a slope ($d$Dur/$d$mV) of -0.19±0.4 ms/mV. Further depolarization can be seen to slowly decrease STOC duration.

D. With increasing voltages, the time to peak amplitude within a STOC event showed a positive linear correlation (r=0.86) which amounted to only a small rate of change of time relative to voltage ($d$T$^{peak}$/$d$V) of 0.03±0.01 ms/mV. Thus, depolarization does slowly decrease the takeoff rate from the resting membrane potential to the peak amplitude such that the time to peak amplitude only increases 0.30 ms per +10 mV increase.

E. On certain STOCs, the recovery can be fitted as a monoexponential process. The $\tau$ for recovery of a STOC event was plotted against the applied voltage. The resulting plot showed a random trend (r=-0.15) with an average time for deactivation of 15.4±3.5 ms. Therefore, the rate of deactivation of a STOC event does not appear to be voltage dependent.

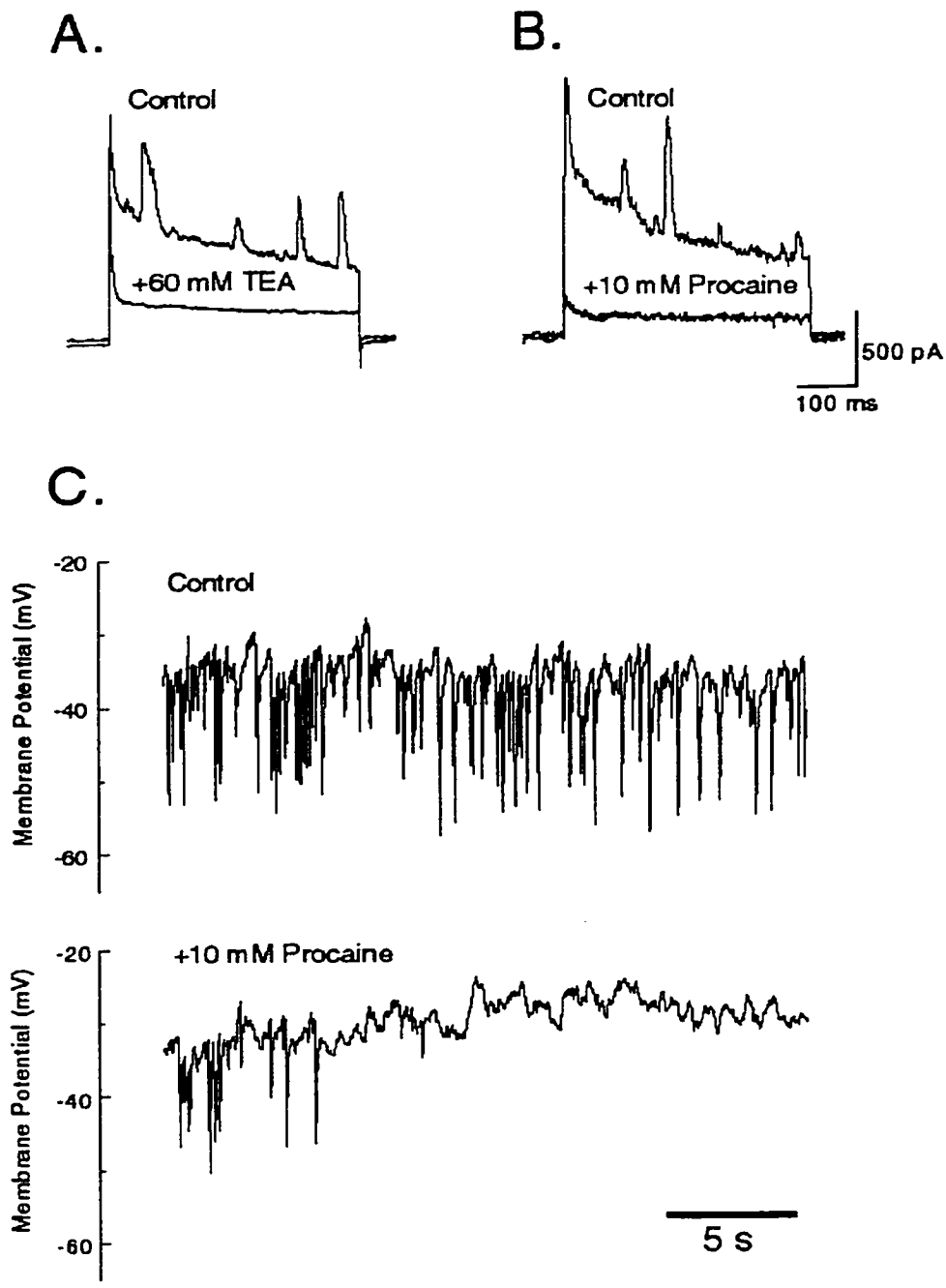


Figure 6-4 STOCs are blocked by TEA or procaine

A. In SMCs where STOCs can be recorded superimposed on whole cell currents, the application of either 60 mM TEA or 10 mM procaine blocked STOCs

completely along with a large portion of outward currents, often leaving only a transient outward current. Whole cell currents were recorded with a +30 mV voltage step for 500 ms.

B. In current clamp mode, typical spontaneous hyperpolarizations from STOC activity was recorded, as shown in the Control. In the same cell, the application of 10 mM procaine quickly abolished the spontaneous hyperpolarizations and depolarized the resting membrane potential an average of 12.9±3.9 mV (n=5). This is more consistent with blockade of K channels rather than specific inhibition of $IP_3R$ $Ca^{2+}$ release.

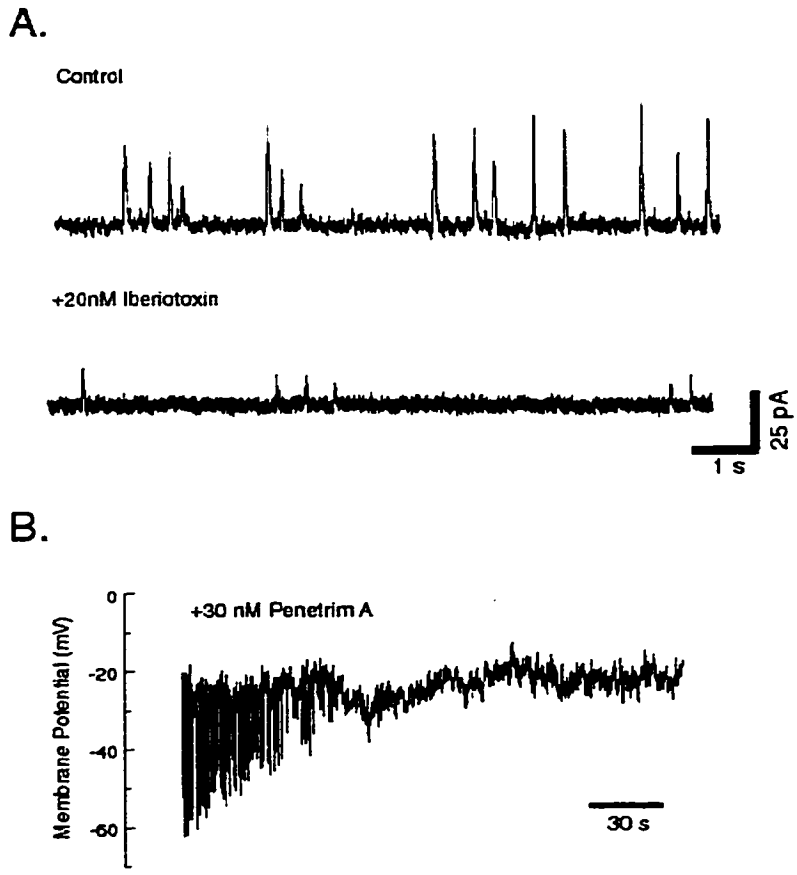


Figure 6-5 STOCs are produced by activation of $BK_{Ca}$

A. Typical spontaneous transient outward current (STOCs) can be seen at a holding potential of -30 mV in the Control trace. After applying 20 nM iberiotoxin, a specific toxin blocker for $BK_{Ca}$, STOCs are inhibited (n=3). Remaining small current oscillations can still be seen from incomplete block of $BK_{Ca}$, indicating intracellular $Ca^{2+}$ cycling has not been affected.

B. In a cell demonstrating spontaneous hyperpolarizations from STOCs, application of 30 nM penitrem A, an alkaloid blocker for $BK_{Ca}$, inhibited STOC activity.

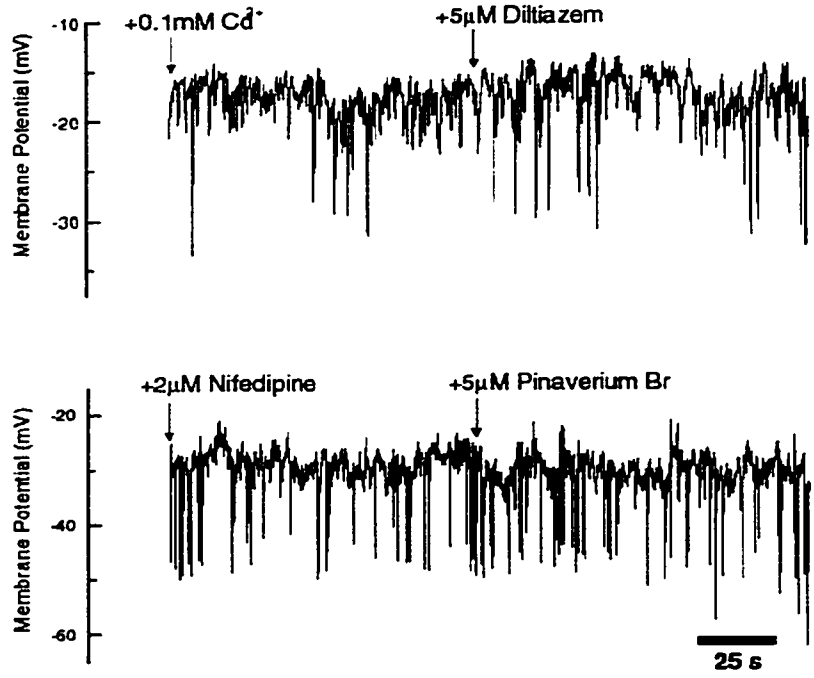


Figure 6-6 STOC activity is not dependent on the entry of extracellular $Ca^{2+}$

A. In cells where typical spontaneous hyperpolarizations from STOC activity were observed, the perfusion with 0.1 mM $Cd^{2+}$ or 5 μM diltiazem did not significantly affect STOC activity (n=2).

B. Again in cells with typical spontaneous hyperpolarizations from STOC activity, the application of dihydropyridines, specifically micromolar amounts of nifedipine and pinaverium bromide, did not affect STOC activity (n=4). Collectively, the lack of effect from typical $Ca^{2+}$ channel blockers suggests STOCs are not dependent on $Ca^{2+}$ entry.

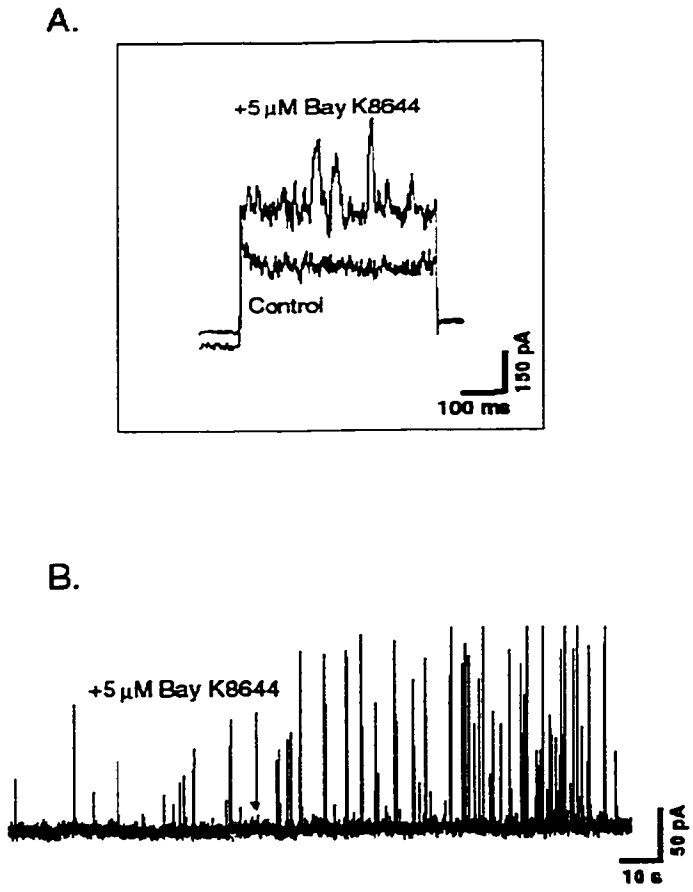


Figure 6-7 STOC activity can be stimulated by $Ca^{2+}$ entry

A. In whole cell voltage clamp, test pulses of +30 mV for 500 ms was given to elicit whole cell outward currents. In a SMC where STOC activity is low, the addition of 5 μM Bay K 8644, a L-type $Ca^{2+}$ channel opener, increased the whole cell outward currents as well as promoted STOC activity.

B. At a holding potential of 0 mV, sporadic STOC activity can be seen. With the addition of 5 μM Bay K 8644, STOC frequency and amplitude can be seen to increase dramatically. Frequently, the application of Bay K 8644 leads to contraction.

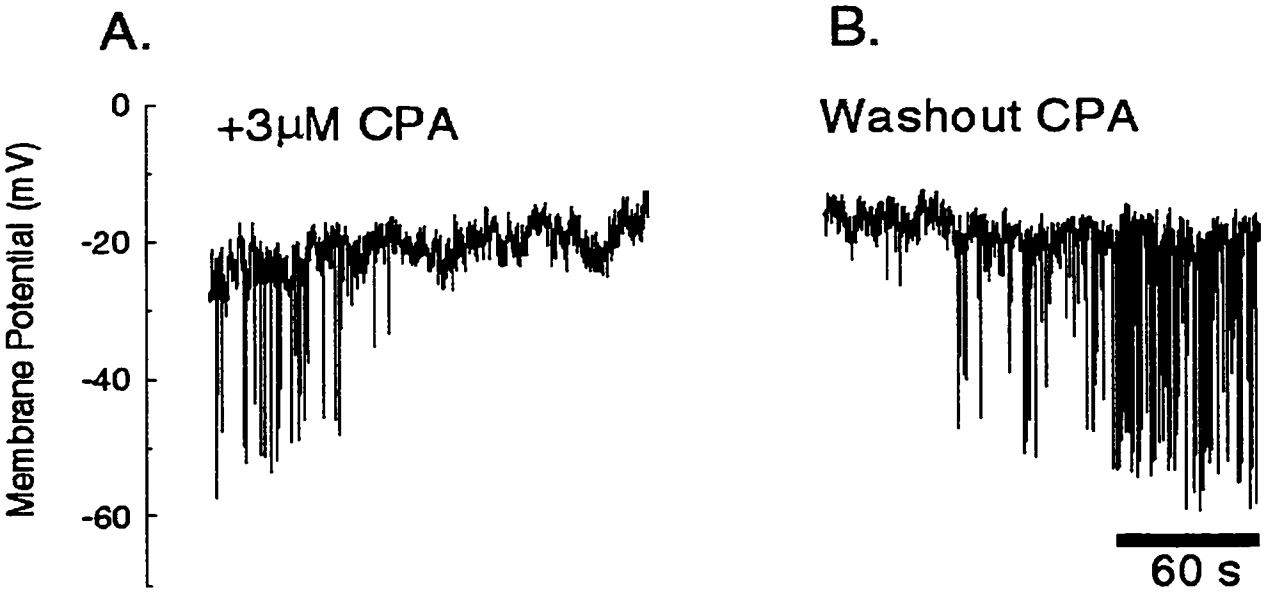


Figure 6-8 STOC activity is dependent on intracellular $Ca^{2+}$ cycling

A. In a cell with typical spontaneous hyperpolarizations from STOC activity, 3 μM CPA, a specific SERCA inhibitor, was added. This caused a fast abolition of STOCs with a small corresponding depolarization.

B. After a long washout (>20 mins), the spontaneous hyperpolarizations returned with increased frequency and amplitude. Further recordings still show the altered frequency and amplitude, indicating that the intracellular $Ca^{2+}$ status did not recover to its control state.

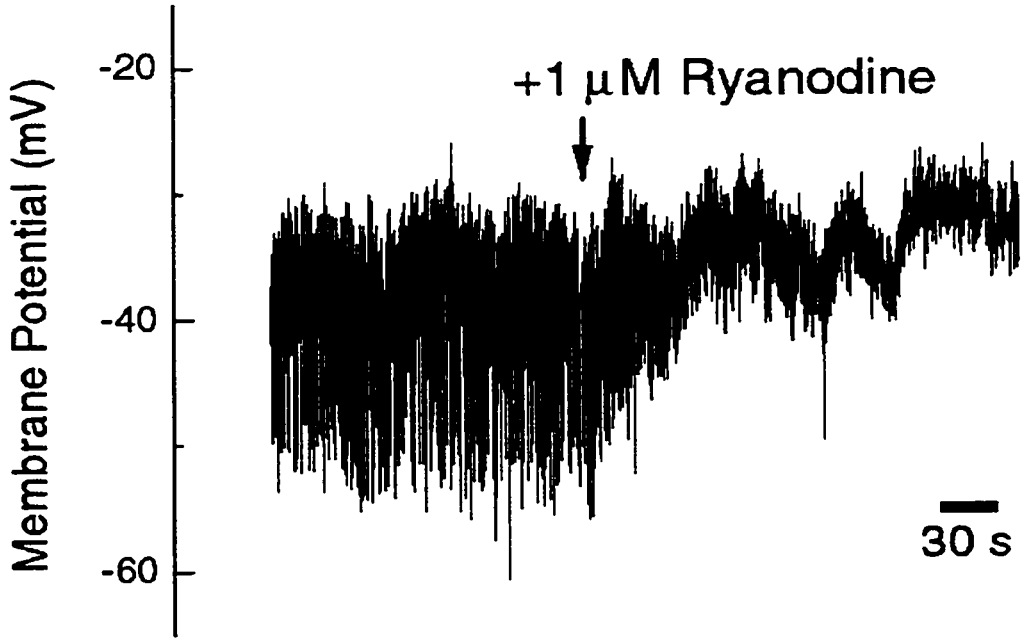


Figure 6-9 STOC activity is dependent on intracellular RyR-$Ca^{2+}$ release channels

In a cell with typical spontaneous hyperpolarizations from STOC activity, 1 μM ryanodine was added. The spontaneous hyperpolarizations were rapidly abolished without any changes in the resting membrane potential (n=2).

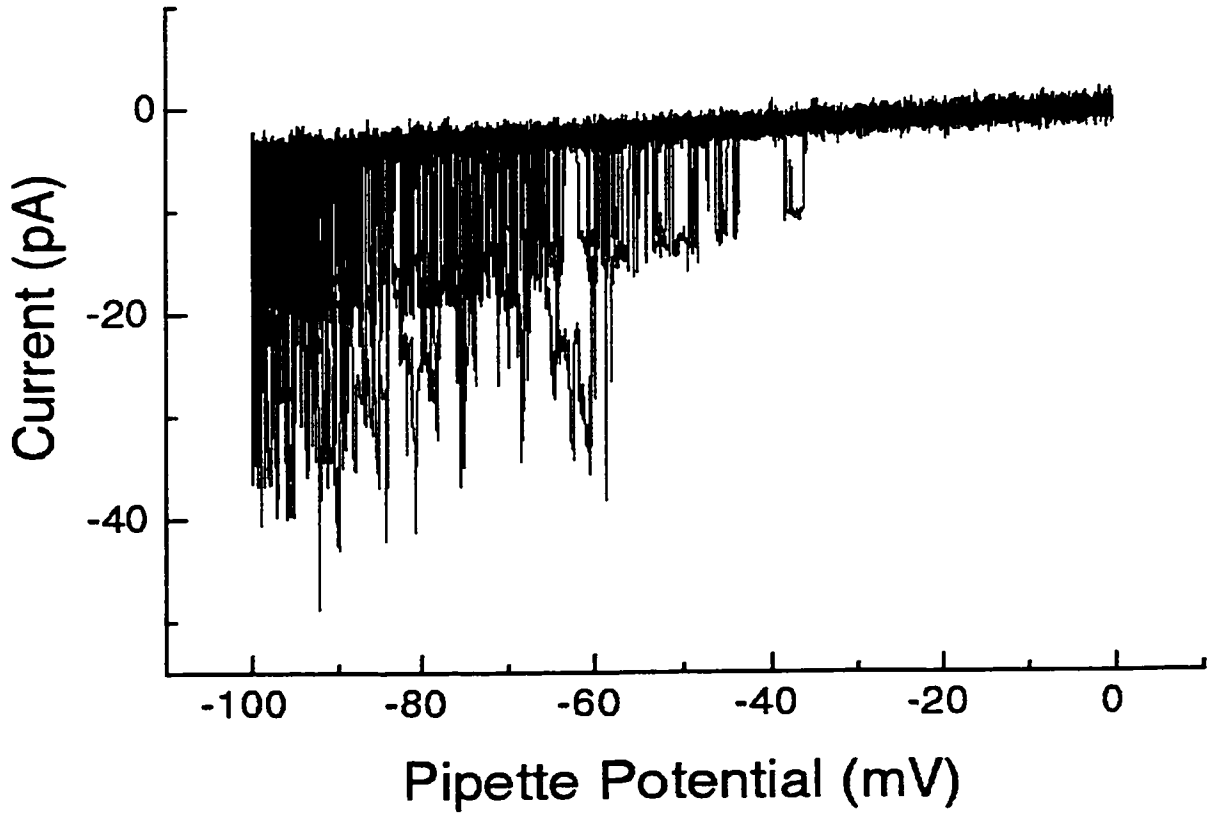


Figure 6-10 Large conductance BKCa single channels can be recorded in membrane patches

In a cell attached patch, at least 4 single $BK_{Ca}$ channels can be recorded with a voltage ramp from -100 to 0 mV. The single channels showed robust activity with moderate open times. Subtracting the slope of the baseline from the single channel amplitude yielded an average conductance of 186.3±26.4 pS.

## Chapter 7: Discussion

The results of my research have suggested several new and different views, which will be discussed separately.

## 7.1 Studies into ICC

### *7.1.1 Comments on "The generation of slow waves is an intrinsic property of interstitial cells of Cajal"*

This chapter shows the results of recording slow wave-like activity from isolated ICC, fulfilling one of the main objectives of research of this thesis. The isolation procedure, short term culture methods, as well as the description of the criteria used to identify single ICC in culture was reported in this paper. Furthermore, simply the ability to record this pacemaker-like activity from isolated ICC represents the successful conclusion in solving the major technical difficulties of this project. The importance of these results is that they show that isolated ICC generates the intrinsic pacemaker-like activity, and that this activity corresponds closely with tissue slow wave activity. This slow wave-like activity was recorded not only as simple voltage oscillations, but more importantly, shown to be driven by active inward currents. These observations verify the hypothesis that slow waves are generated by ionic channel activation and not from other possibilities such as temporary blockade of potassium conductances or oscillations in $Na^+/K^+$ ATPase activity. The slow wave-like activity was shown to be clearly different from action potentials generated by smooth muscle cells.

Two separate groups have reported spontaneous activity from isolated ICC. Langton et al. recorded spontaneous depolarizations from interstitial cells within the

submuscular plexus of the dog colon (Langton *et al.* 1989). The spontaneous activity does not match tissue slow wave activity, especially in its vulnerability to L-type $Ca^{2+}$ channel blockers. The follow-up paper by Lee et al. characterized these interstitial cells to have L-type calcium currents with different kinetics with those found in smooth muscle cells (Lee & Sanders, 1993). Another group, Tokutomi et al., identified cells from the mouse small intestine with positive *c-kit* immunoreactivity (Tokutomi *et al.* 1995). These cells show rhythmic voltage and current fluctuations, which were carried by a $Ca^{2+}$ sensitive chloride conductance. In whole tissue, extracellular $Cl^-$ restriction and $Cl^-$ blockers had little effect on slow wave parameters (Malysz *et al.* 1995). Collectively, it is unlikely the spontaneous activities recorded by either group represent the pacemaker slow wave activity seen in intact tissue. The spontaneous activity that I have recorded has all the characteristics indistinguishable from tissue slow waves. The next paper, "Interstitial cells of Cajal generate a rhythmic pacemaker current" advances the current state of knowledge on ICC by demonstrating the presence of a unique membrane marker, *ckit*, by selective RT-PCR. These results have recently been confirmed by Koh et al. (Koh *et al.* 1998). Thus, the objective of showing single ICC that correspond to ICC seen in the pacemaker region of the small intestine, are capable of intrinsically generating slow wave type activity has been fulfilled.

### *7.1.2 Problems encountered in studying ICC*

All previous ultrastructural studies of ICC and direct consultations with Dr. Thuneberg suggested that ICC would be difficult to isolate. Within the tissue, ICC are

buried within the enteric plexus regions and are intercalated with other interstitial cells, nerve fibers, and with circular smooth muscle cells. The difficulty was compounded by the fact that, in the mouse, the individual smooth muscle layers cannot be separated well by sharp dissection. Fortunately, the mouse small intestine external smooth muscle layers are thin - roughly less than 30 smooth muscle cells in thickness. Also, it was found that with careful dissection of the muscularis externae from the intact intestine, the external smooth muscle layers would separate at the deep muscular plexus region and leave the neural plexus on the inner surface. Thus, this allowed almost pure preparations of myenteric ICC, the origin of slow waves in the small intestine. An isolation procedure was eventually optimized for isolating patchable ICC.

After successfully isolating single cells, the short term culturing system needed to be optimized. Several problems needed to be addressed. First, isolated cells took on rounded shapes after dispersion and needed to recover to near tissue morphologies before they can be recognized. Second, freshly dissociated cells were difficult to patch and had altered electrophysiological properties. This was not surprising given the relatively "harsh" dissociation conditions they had to endure. Thirdly, the number of ICC was expected to be low in relation to all other cells, especially smooth muscle cells. Also, ICC do not appear to grow in isolation, suggesting a prerequisite trophic interaction with other cells in culture. This would mean that the plating density had to be high, which severely limits the accessibility to single ICC. Lastly, during the development of ICC isolation and primary short-term culture procedures, ICC were observed to dedifferentiate in extended culture, not unlike smooth muscle cells. This is consistent with their mesenchymal origins

but complicates long term study with isolated ICC since there is now only a small time window in which to recognize and examine ICC (3-5 days). Thus, ICC can only be examined as primary cultures and only for a short time.

### *7.1.3 Future Directions in the Study of ICC*

The ability to harvest single ICC already suggests several topics for further study. Tim Robinson and Lars Thomsen have been pursuing better characterization of ICC through molecular biological methods. Clearly the task of characterizing ICC will be simplified if a convenient vital marker for ICC can be found. The use of the ACK2 antibody labeling against *ckit* has already been used by Tokutomi *et al.* with limited success (Tokutomi *et al.* 1995). Further optimizations in isolation and/or culturing as to increase ICC yields and working time would greatly help. Once ICC can be conveniently harvested and identified, the monumental task of characterizing the electrophysiological basis of slow wave generation remains.

## 7.2 Studies in SMC

### *Comments on "Heterogeneity of Ionic Cellular Currents in the Mouse Intestinal Smooth Muscle"*

The smooth muscle layers of the gut represent the basic players in motility, responsible for generating the end contractions. All contacting and surrounding cells would play a role in regulating and/or modulating smooth muscle activity. Since all

regulatory signals must be integrated before or at the level of smooth muscle, studies into the electrophysiology of smooth muscle cells are important in understanding the basic *in vivo* activity. The initial objective was to study the ionic currents present in smooth muscle cells and possibly relate them to observed tissue electrical activities. With larger numbers of observations, it was slowly realized that instead of a homogeneous distributions of whole cells currents (i.e. in each SMC, the same family of currents are present in different amplitudes), it became clear that whole cell currents were differentially distributed (i.e. distinct populations of SMC possessing different families of currents). Histological studies on muscularis externae already suggests differences, especially between longitudinal and circular layers (Gabella, 1989). This paper reports on the heterogeneity of whole cell currents examined forming at least four distinct groups. The presence of certain currents was confirmed by single channel recordings.

#### *7.2.1.1 Problems Encountered*

The most glaring problem was that the smooth muscle was completely dispersed, and therefore cannot reveal any clues to their localization nor position within the smooth muscle syncytium. In retrospect, the mouse small intestine was not the ideal tissue to work to demonstrate heterogeneity within the thickness of the tissue since the thinness of the muscularis tunica prevented clear separation of individual layers. It would be difficult using mouse intestinal smooth muscle to relate isolated cells to a specific location within the musculature. Alternatively, the ease in isolating single smooth muscle cells from the

mouse small intestine would be ideal for investigating regional differences of the mouse GI system. In all related investigations, large numbers of observations are needed since there is no convincing way to demonstrate heterogeneity except through statistical means.

#### *7.2.1.2 Future Implications*

The next obvious step was to link the electrophysiological observations to functional and/or histological differences in intact tissue. Individual differences in smooth muscle cell cannot be seen in intact tissue because of electrical coupling, such that electrophysiological studies in whole tissue reflects the summation of the smooth muscle into a syncytium. Clearly different experimental protocols are needed to better study the heterogeneity of smooth muscle cells in the gut.

### *7.2.2 Comments on "Characterization of Transient Outward Currents in Smooth Muscle"*

One specific outward current was targeted and characterized in the paper. The transient outward current was unique in its extreme resistance to common potassium channel blockers and its distinctive fast activation and inactivation kinetics. A novel ramp analysis was used to assess the response to different rates of depolarization. Because a specific blocker for this current could not be found, its effects on tissue electrical activity could not be confirmed. One type of fast transient outward currents ($I_{to}$) is expected to play a major role in limiting excitability to only the plateaus of slow waves.

#### *7.2.2.1 Problems Encountered*

One of the major problems was inherited by a problem mentioned previously - the heterogeneity in the ionic currents in different smooth muscle cells meant that not all cells contained the fast $I_{to}$. Adding to the confusion, the final analysis showed two distinct fast $I_{to}$ with different kinetic properties. In hindsight, experiments would have been done differently if it was known that SMCs responded differently to the common $K^+$ blocker, TEA, used to isolate $I_{to}$. The transient outward currents were easy to isolate because of their extreme resistance to common $K^+$ blocker; by the same virtue, neither the identity of the transient outward currents can be described with pharmacology to $K^+$ blockers nor its effects in tissue can be tested without a specific blocker.

#### *7.2.2.2 Future Implications*

The original intention was to dissect the major outward currents present in SMCs. Already it has revealed itself to be a more complex than first suspected. The discovery of (a) specific blocker(s) for the fast $I_{to}$ responsible for the plateau excitability is important not only to provide validation for the kinetic studies, but represents a major pharmacological target for controlling spiking excitability and hence, motility. The refinement of ramp protocols and analysis will bring new insights into how continuously changing membrane potentials affect ion current activation.

### *7.2.3 Comments on "Properties of Intracellular $Ca^{2+}$ Stores in Mouse Intestinal Smooth Muscle Cells"*

Spontaneous transient outward current oscillations (STOCs) have been seen in a variety of smooth muscle (Benham & Bolton, 1986; Ohya *et al.* 1987; Rusko *et al.* 1990; Zholos *et al.* 1991; Noack *et al.* 1992). Although this suggestion has already been proposed (Bitar *et al.* 1986; Nelson *et al.* 1995), the idea of using STOCs as built-in biosensors for intracellular $Ca^{2+}$ activity has been largely undeveloped. In the SMCs showing STOCs, it was shown that quantal intracellular $Ca^{2+}$ release is triggered mostly from intracellular events rather than transient extracellular $Ca^{2+}$ entry. Although STOCs can be blocked by LCCBs, it was found to be mostly due to direct blockade of $K_{Ca}$ channels. Careful recording of STOC activity can reveal intimate details of intracellular $Ca^{2+}$ stores at the resolution (or better) of current $Ca^{2+}$ imaging techniques.

#### *7.2.3.1 Problems Encountered*

The heterogeneity of SMCs meant not every SMC showed STOC activity and there appeared to be differences in STOC activity within the populations of SMCs that showed STOC activity. The differences in STOC activity (frequency, amplitude, duration, etc.) can possibly reflect differences in intracellular $Ca^{2+}$ cycling. The most obvious weakness was the lack of direct evidence of the actual intracellular $Ca^{2+}$ status. As noted in some reports, STOC activity can represent distinct regions of the cell (sparks) rather than reflect on global $Ca^{2+}$ status. Therefore only simultaneous STOC recording

with $Ca^{2+}$ imaging can fully resolve the accuracy of STOCs as biosensors for intracellular $Ca^{2+}$ activity.

#### *7.2.3.2 Future Implications*

As suggested previously, STOCs can become a powerful diagnostic tool in assessing the intracellular $Ca^{2+}$ status of a cell. Definitely more research in correlating intracellular $Ca^{2+}$ status with STOC activity needs to be done in order to fully validate its accuracy as a biosensor. In intestinal smooth muscle cells that show prominent STOC activity, which represents active intracellular $Ca^{2+}$ cycling, these cells can represent a special population of SMCs that require such an internal oscillator, such as pacemaker SMCs generating spiking action potentials. Again further research into the roles of actively cycling intracellular $Ca^{2+}$ stores in smooth muscle cells and its effects in excitability is needed to investigate this hypothesis.

## 7.3 A Simple Model of GI Motility

The intrinsic properties of the "players" in GI motility are important in identifying their roles. It is common to think of smooth muscle cells solely as effectors of contraction (Huizinga, 1991; Ward *et al.* 1991). My research has shown that there are different populations of smooth muscle cells with different ionic currents, suggesting different functions. Also, a population of smooth muscles cells were shown to have very active intracellular $Ca^{2+}$ stores, as reflected by robust STOC activity. ICC have been shown to

be auto-rhythmic and contractile, not unlike certain isolated smooth muscle cells but with definite differences. With these properties, certain roles for these cells can be implied. The roles that smooth muscle cells and ICC take are important in defining their function(s) in GI motility.

### *7.3.1 Possible Additional Roles of SMC*

Two main hypotheses can be used to explain the observation of different populations of smooth muscle cells within the muscularis externae:

1. The different populations reflect adaptations to their function and location; for example, smooth muscle cells next to neuronal varicosities have specialized and adapted to express more receptors, and thus altered their ionic current profile to be more excitable.
2. The different populations are really subtypes of different smooth muscle cells present in the muscularis externae. This deliberate specialization would be there to force distinct patterns of excitation and propagation.

It is well known that smooth muscle cells are plastic and can alter their morphology according to their surrounding conditions to express either a contractile or synthetic phenotype (Chamley Campbell *et al.* 1979). Over the course of short term culture, whole cell ionic current profiles were found not to change over time, suggesting that smooth muscle cells retain their unique properties when shifting morphologies.

In our current state of knowledge, smooth muscle cells appear very complex, with multiple signal transduction pathways and intracellular $Ca^{2+}$ stores. The first possibility suggests that the generic smooth muscle cell is, indeed, very complex and would require a complex system for cell regulation. Because of the similarities between different smooth muscle cells, organized motility would require outside systems, such as ICC and/or nerves. The second possibility suggests that the complex different properties are likely to be carried by specialized subtypes such that each subtype has a relatively simple but distinct character. Makhlouf et al. has already suggested specific differences between longitudinal and circular smooth muscle tissue (Makhlouf & Murthy, 1998). The composition of the intestinal tissue of different specialized cells would determine the motility characteristics of that segment. Other investigators have observed region differences in smooth muscle properties (Maehara *et al.* 1994; Okamoto *et al.* 1997). The specialization of an intestinal segment demands that it contributes more significantly to the organization and initiation of motility than if smooth muscle was similar within the thickness as well as between segments.

Currently, the intestinal smooth muscle cells are considered to be the end effector leading to contraction. Thus, the roles of initiators, propagators, integrators, and transducers of excitatory and inhibitory signals should be present in all smooth muscle cells. Alternatively, if smooth muscle cells show specialization into subtypes, there are "specialized" cells that have a specific intracellular organization that can be shown by analyzing each cell separately. There will be specific cells that would function as initiators, propagators, integrators, and transducers. The characteristics of motility would,

therefore, depend on the properties of specific cells and their organization and interactions.

### *7.3.2 Possible Additional Roles of ICC*

The most obvious role for ICC is to be the initiators of pacemaker slow wave activity. Slow wave activity has been shown to provide directional and coordinated peristaltic activity (Der-Silaphet *et al.* 1997). Neuronal circuitry has been shown to be important providing the forward inhibition and backward excitation crucial to peristalsis. An important question arises: are the ICC networks a redundant system for providing directionality and coordination in the intestine, or are they part of a synergistic system? An important observation is that there is usually more than one network of ICC within the same thickness of intestinal tissue; such as the ICC network located at the deep muscular plexus of the small intestine and the ICC network at the myenteric plexus of the colon. Also, ICC are always found to have close contact with enteric nerves, suggesting a possible role as an intermediary in neurotransmission to smooth muscle (Daniel & Berezin, 1992; Daniel & Fox-Threlkeld, 1993; Sanders, 1996). Alternatively, ICC can behave as a feedback system from smooth muscle to enteric nerves and vice versa. ICC have been shown to be capable of generating extracellular messengers (NO, others?) (Burns *et al.* 1996) as well as having intercellular communication with smooth muscle cells with gap junctions (Berezin *et al.* 1988). The slow wave depolarization may be important in determining the direction and degree of intercellular communication because gap junctions can be sensitive to transcellular voltages (Bennett & Verselis, 1992).

Histologically, ICC are ideal as stretch receptors in that they cover the length and circumference of the tubular gut and are one cell layer thick. Individual ICC have been shown to be contractile and excitable (see Chapter 2). Therefore, stretch across the intestinal walls can potentially activate ICC to provide feedback, either through production of NO or other messengers, or through ICC contacts to affect both neurons and/or smooth muscle. Gap junctional contacts with ICC and smooth muscle has been observed to be rectifying (Farraway & Huizinga, 1993). Collectively, it is likely that ICC have more than one role in the GI system.

### *7.3.3 Ionic Basis of Pacemaker Slow Wave Activity*

The two main electrical activities in the intestine are spiking action potentials and slow wave activity. The origin of the spiking action potentials and slow wave activity can be traced back to smooth muscle and ICC, respectively. Both these cells have been examined by various electrophysiological methods, including patch clamp, such that it is possible to assign ionic conductances responsible for these electrical activities.

The spiking action potentials have been seen in isolated longitudinal and circular smooth muscle segments, as well as in isolated smooth muscle cells (Huizinga, 1991). Recently, the spiking action potential activity was examined with a combination of whole cell patch clamp and real time $Ca^{2+}$ imaging in single ileal smooth muscle cells (Kohda *et al.*, 1997). This study showed spiking action potentials involve the activation of L-type $Ca^{2+}$ channels and $Ca^{2+}$-activated K channels, but little involvement from CICR. The triggering of spiking activity is voltage based, such that once the membrane potential

surpasses a critical voltage threshold, the smooth muscle cell will generate spiking activity. Alteration of the voltage threshold, either by modifying the L-type $Ca^{2+}$ channels by phosphorylation or other intracellular signaling event, would lead to different characteristics of spiking activity. For example, if the voltage threshold is lowered toward the resting membrane potential, spiking activity can occur simply from small depolarizations from EPSPs or by random membrane potential fluctuations. If the voltage threshold is sufficiently high (away from the resting membrane potential), spiking activity can only occur if there is a significant depolarization, such as a slow wave event. This model for periodic smooth muscle spiking activation was demonstrated in Figure 2-11. Overall, the current data establishes that spiking activity is generated by ionic conductances present in smooth muscle and that spiking activity is an intrinsic property of smooth muscle.

The slow waves have been shown to originate from pacemaker ICC and its ionic basis has been speculated on (Chapter 2 & 3; Barajas-Lopez, 1989; Koh *et al.*, 1998). The slow waves seen in intact tissue appear to be made up of two components – an LCCB sensitive component and an LCCB-insensitive component (Huizinga, 1991). The LCCB sensitive component includes part of the slow wave upstroke as well as the plateau. In the presence of LCCB, only the "initiation" part of the slow wave is expressed.

The "initiation" slow wave can be seen clearly in isolated ICC and is generated by an active inward "pacemaker" current that is not voltage sensitive. It appears that the repolarization of the "initiation" slow wave does not rely on activation of $K^+$ currents, but simply on termination of the "pacemaker" current (Chapter 2). The triggering of the

"pacemaker" current is dependent on normal intracellular $Ca^{2+}$ cycling and metabolism, suggesting an intracellular metabolic "clock" is responsible for rhythmicity and frequency of slow waves.

The plateau potential does not appear to be voltage sensitive but requires the company of the "initiation" slow wave to be present. An inward rectifying non-specific current has been seen in isolated smooth muscle cells that is not voltage-sensitive but triggered by an unknown intracellular mechanism (Jon Lee, unpublished results). This inward current resembles cholinergic-activated non-selective inward current seen in gastric smooth muscle cells (Sims, 1992). The appearance of this cholinergic-activated inward current is associated with smooth muscle cell contraction. My personal observations on this non-specific inward current is similar in noticing this inward current is associated with smooth muscle cell contraction and that the reversal potential is roughly at –30 to –40 mV. Upon the activation of this non-specific inward current, the membrane potential will be clamped at ~–30 to -40 mV (Jon Lee, unpublished results), roughly the plateau potential seen in intact tissue. The main determinant in plateau duration will simply be the termination of this non-specific current in smooth muscle. The plateau duration can be influenced by activation of certain $K^+$ conductances, such as $K_{Ca}$, but they will the indirect influences to the termination of the plateau (Huizinga, 1991).

My speculations of the series of ionic events that occur during a slow wave event with superimposed spiking activity can be summarized as follows:

1) The "initiation" slow wave is triggered by a currently unknown metabolic clock in ICC.
2) The "initiation" slow wave is propagated through ICC couplings with smooth muscle and other ICC.
3) The "initiation" slow wave triggers smooth muscle to generate the plateau potential.
4) The plateau potential brings the smooth muscle membrane potential past the critical voltage threshold for spiking activity. Thus, spiking activity is triggered on top of the plateau.
5) The plateau potential terminates and brings the membrane potential back to its resting levels.

The outward $K^+$ currents are important in waveform-shaping and modifying excitability at different stages of the slow wave event, as suggested for the heart myocardium (Escande, 1993). Therefore, manipulation of $K^+$ currents by pharmacological or other means provides subtle means to affect slow wave and spiking activity.

It is undeniable that the ionic conductances in the intestinal musculature are responsible for the spiking and slow wave activities seen. The coordination of these activities are crucial in determining functional G.I. motility. Influences that modify either slow wave or spiking activity, such as the enteric nervous inputs or humoral factors, could be alternative systems that coordinate motility on top of the intrinsic myogenic motility mechanisms as determined by the intestinal smooth muscle and ICC.

### *7.3.4 Schematic Organization of G.I. Motility*

With the possible roles of smooth muscle and ICC defined, it is possible to construct a simple model for the organization and control of motility in the gut. The enteric nervous system is, of course, an important and crucial link with the central nervous system and the GI system. For this model, the end target is the smooth muscle of the muscularis externae. The enteric nervous system connection to this target has been suggested to be both parallel and serial innervation (Sanders, 1996). Although there is a plethora of receptors and transduction mechanisms to receive enteric neurotransmitters, there does not appear to be enough knowledge about the communication from smooth muscle to enteric nerves innervating the muscularis externae (Costa & Brookes, 1994). ICC are intercalated between nerve terminals and smooth muscle syncytium, which is an ideal position to transduce signals from nerves to smooth muscle, as well as signals from smooth muscle to nerves (Smith *et al.* 1989; Berezin *et al.* 1990; Berezin *et al.* 1990).

The following diagram illustrates this relationship:

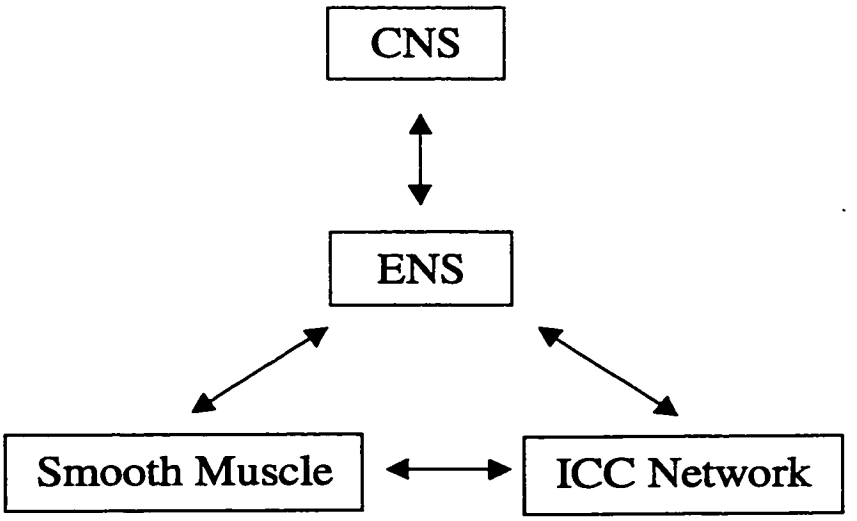


Figure 7-1 Schematic diagram of the inter-relations involved with GI motility.

The hybrid serial and parallel innervation, and possibly duplex communication is necessary to provide feedback to the enteric nervous system. To engage an activity as complex as peristalsis, feedback information would be needed not only from the mucosal/submucosal afferents, but possibly directly from the end target (muscularis externae) also.

## 7.4 Final Comments

While all objectives have been fulfilled by the results presented in this thesis, it has opened new questions into the fundamental basis of motility. While ICC have been

receiving a lot of attention lately, smooth muscle definitely deserves a second look. Both ICC and smooth muscle have revealed themselves to be much more complex than originally thought. It is hoped that this thesis will help in understanding the fundamental building blocks of intrinsic motility and be poised in promoting the integration of regulatory influences to arrive, at last, to a fuller understanding of gastrointestinal motility.

## 7.5 Bibliography for Introduction and Discussion

ALVAREZ, W. C. (1948). *An introduction to gastroenterology*. New York: Paul B. Hoeber Inc.

BARAJAS-LOPEZ, C., DEN HERTOG, A. & HUIZINGA, J. D. (1989). Ionic basis of pacemaker generation in dog colonic smooth muscle. *Journal of Physiology - London* **416**, 385-402.

BENHAM, C. D. & BOLTON, T. B. (1986). Spontaneous transient outward currents in single visceral and vascular smooth muscle cells of the rabbit. *Journal of Physiology - London* **381**, 385-406.

BENNETT, M. V. & VERSELIS, V. K. (1992). Biophysics of gap junctions. [Review]. *Seminars in Cell Biology* **3**, 29-47.

BEREZIN, I., DANIEL, E. E. & HUIZINGA, J. D. (1990). Structural characterization of interstitial cells of Cajal in myenteric plexus and circular muscle of canine colon. *Canadian Journal of Physiology & Pharmacology* **68**, 1419-1431.

BEREZIN, I., HUIZINGA, J. D. & DANIEL, E. E. (1988). Interstitial cells of Cajal in the canine colon: a special communication network at the inner border of the circular muscle. *Journal of Comparative Neurology* **273**, 42-51.

BEREZIN, I., HUIZINGA, J. D., FARRAWAY, L. & DANIEL, E. E. (1990). Innervation of interstitial cells of Cajal by vasoactive intestinal polypeptide containing nerves in canine colon. *Canadian Journal of Physiology & Pharmacology* **68**, 922-932.

BITAR, K. N., BRADFORD, P. G., PUTNEY, J. W.,JR. & MAKHLOUF, G. M. (1986). Stoichiometry of contraction and Ca2+ mobilization by inositol 1, 4,5-trisphosphate in isolated gastric smooth muscle cells. *Journal of Biological Chemistry* **261**, 16591-16596.

BITAR, K. N., BURGESS, G. M., PUTNEY, J. W.,JR. & MAKHLOUF, G. M. (1986). Source of activator calcium in isolated guinea pig and human gastric muscle cells. *American Journal of Physiology* **250**, Pt 1):G280-6.

BURNS, A. J., LOMAX, A. E., TORIHASHI, S., SANDERS, K. M. & WARD, S. M. (1996). Interstitial cells of Cajal mediate inhibitory neurotransmission in the stomach. *Proc Natl Acad Sci U S A* **93**, 12008-12013.

CAJAL, S. R. Y. (1893). Sur les ganglions et plexus nerveux d'intestin. *Societie Biologique de Paris* **5**, 217-223.

CAJAL, S. R. Y. (1911). *Histologie du system nerveux de l'homme et des vertebres.* Paris: Maloine.

CHAMLEY CAMPBELL, J., CAMPBELL, G. R. & ROSS, R. (1979). The smooth muscle cell in culture. *Physiological Reviews* **59**, 1-61.

COSTA, M. & BROOKES, S. J. (1994). The enteric nervous system. [Review]. *American Journal of Gastroenterology* **94**, S129-37.

DANIEL, E. E. & BEREZIN, I. (1992). Interstitial cells of Cajal: are they major players in control of gastrointestinal motility? *Journal of Gastrointestinal Motility* **4**, 1-24.

DANIEL, E. E. & FOX-THRELKELD, J. E. T. (1993). VIP release from small intestinal neurons: Its modulation by multiple neuropeptides: Association with motility changes and functional role. *Biomedical Research* **13**, 195-200.

DER-SILAPHET, T. D., HUIZINGA, J. D., MALYSZ, J., ARSENAULT, A. L. & HAGEL, S. (1997). Interstitial cells of Cajal direct normal propulsive contractile activity in the small intestine. *Gastroenterology* revision submitted

DURDLE, N. G., KINGMA, Y. J., BOWES, K. L. & CHAMBERS, M. M. (1983). Origin of slow waves in the canine colon. *Gastroenterology* **84**, 375-382.

ESCANDE, D. & HENRY, P. (1993). Potassium channels as pharmacological targets in cardiovascular medicine. [Review]. *European Heart Journal* **14**, Suppl B:2-9.

FARRAWAY, L. & HUIZINGA, J. D. (1993). Heterogeneity of metabolic and electrical communication within the colonic musculature. *Journal of Gastrointestinal Motility* **5**, 190(Abstract)

FAUSSONE PELLEGRINI, M. S. (1985). Ultrastructural peculiarities of the inner portion of the circular layer of the colon. II. Research on the mouse. *Acta Anat.(Basel)* **122**, 187-192.

FAUSSONE PELLEGRINI, M. S. & CORTESINI, C. (1984). Ultrastructural peculiarities of the inner portion of the circular layer of colon. I. Research in the human. *Acta.Anat.(Basel).* **120**, 185-189.

FRY, G. N., DEVINE, C. E. & BURNSTOCK, G. (1977). Freeze-fracture studies of nexuses between smooth muscle cells. Close relationship to sarcoplasmic reticulum. *Journal of Cell Biology* **72**, 26-34.

FURNESS, J. B. & COSTA, M. (1980). Types of nerves in the enteric nervous system. *Neuroscience* **5**, 1-20.

GABELLA, G. (1974). Special muscle cells and their innervation in the mammalian small intestine. *Cell & Tissue Research* **153**, 63-77.

GABELLA, G. (1989). Structure of intestinal musculature. In *Motility and Circulation*, ed. AMERICAN PHYSIOLOGICAL SOCIETY, pp. 103Oxford University Press.

GABELLA, G. & BLUNDELL, D. (1981). Gap junctions of the muscles of the small and large intestine. *Cell & Tissue Research* **219**, 469-488.

HUIZINGA, J. D., THUNEBERG, L., VANDERWINDEN, J.M. & RUMESSEN, J.J. (1997). Interstitial cells of Cajal as pharmacological targets for gastrointestinal motility disorders. *Trends in Pharmacological Sciences* **18(10)**, 393-403

HUIZINGA, J. D., THUNEBERG, L., KLUPPEL, M., MALYSZ, J., MIKKELSEN, H. B. & BERNSTEIN, A. (1995). The W/kit gene required for interstitial cells of Cajal and for intestinal pacemaker activity. *Nature* 373, 347-349.

HUIZINGA, J. D. (1991). Action potentials in gastrointestinal smooth muscle. *Canadian Journal of Physiology & Pharmacology* **Vol 69 No.8**, 1133-1142.

HUIZINGA, J. D. & CHOW, E. (1988). Electrotonic current spread in colonic smooth muscle. *American Journal of Physiology* **254**, G702-G710.

JIMENEZ, M., CAYABYAB, F. S., VERGARA, P. & DANIEL, E. E. (1996). Heterogeneity in electrical activity of the canine ileal circular muscle: interaction of two pacemakers. *Neurogastroenterol.Motil.* **8**, 339-349.

KATASE, T. & TOMITA, T. (1971). Na participation in the recovery from K-contracture in the guinea-pig taenia coli. *Journal of Physiology - London* **218**, 48P

KOHDA, M., KOMORI, S., UNNO, T. & OHASHI, H. (1997). Characterization of action potential-triggered [Ca2+]i transients in single smooth muscle cells of guinea-pig ileum. *British.Journal.of.Pharmacology* **122**, 477-486.

KOH, S. D., SANDERS, K. M. & WARD, S. M. (1998). Spontaneous electrical rhythmicity in cultured interstitial cells of Cajal from the murine small intestine. *Journal of Physiology - London* **513(1)**, 203-213.

LANGTON, P., WARD, S. M., CARL, A., NORELL, M. A. & SANDERS, K. M. (1989). Spontaneous electrical activity of interstitial cells of Cajal isolated from canine proximal colon. *Proceedings of the National Academy of Sciences U.S.A.* **86**, 7280-7284.

LEE, H. K. & SANDERS, K. M. (1993). Comparison of ionic currents from interstitial cells and smooth muscle cells of canine colon. *Journal of Physiology - London* **460**, 135-152.

LIU, L. W. C. & HUIZINGA, J. D. (1994). Canine colonic circular muscle generates action potentials without the pacemaker component. *Canadian Journal of Physiology & Pharmacology* **72(1)**, 70-81.

LIU, L. W. C., RUO, R. & HUIZINGA, J. D. (1997). Circular muscle lamellae of canine colon are electrically isolated functional units. *Canadian Journal of Physiology & Pharmacology* **75**, 112-119.

MAEHARA, T., FUJITA, A., SUTHAMNATPONG, N., TAKEUCHI, T. & HATA, F. (1994). Differences in relaxant effects of cyclic GMP on skinned muscle preparations from the proximal and distal colon of rats. *European Journal of Pharmacology* **261**, 163-170.

MAKHLOUF, G. M. & MURTHY, K. S. (1998). Signal transduction in gastrointestinal smooth muscle. [Review] [92 refs]. *Cellular Signalling 1997 May-Jun;9(3-4):269-76* 269-276.

MALYSZ, J., RICHARDSON, D., FARRAWAY, L., CHRISTEN, M. O. & HUIZINGA, J. D. (1995). Initiation of slow wave type action potentials in the mouse small intestine involves a non-L-type calcium channel. *Neurogastroenterol. Mot.* **7**, 272(Abstract)

MIKKELSEN, H. B., HUIZINGA, J. D., THUNEBERG, L. & RUMESSEN, J. J. (1993). Immunohistochemical localization of a gap junction protein (connexin 43) in the muscularis externa of murine, canine and human intestine. *Cell & Tissue Research* **274**, 249-246.

MIKKELSEN, H. B., MALYSZ, J., HUIZINGA, J. D. & THUNEBERG, L. (1997). Action potential generation, Kit immunoreactivity and morphology of *Sl* mutant mouse small intestine. *Neurogastroenterol. Mot.* in press

NELSON, M. T., CHENG, H., RUBART, M., SANTANA, L. F., BONEV, A. D., KNOT, H. J. & LEDERER, W. J. (1995). Relaxation of arterial smooth muscle by calcium sparks. *Science* **270**, 633-637.

NOACK, T., DEITMER, P. & LAMMEL, E. (1992). Characterization of membrane currents in single smooth muscle cells from the guinea-pig gastric antrum. *Journal of Physiology - London* **451**, 387-417.

OHYA, Y., KITAMURA, K. & KURIYAMA, H. (1987). Cellular calcium regulates outward currents in rabbit intestinal smooth muscle cell. *American Journal of Physiology* **252**, C401-C410.

OKAMOTO, H., INOUE, K., KAMISAKI, T., TAKAHASHI, K. & SATO, M. (1997). Regional differences in calcium sensitivity in the guinea-pig intestine. *Journal of Pharmacy & Pharmacology* **49**, 981-984.

OSINSKI, M. A. & BASS, P. (1995). Myenteric denervation of rat jejunum alters calcium responsiveness of intestinal smooth muscle. *Gastroenterology* **108**, 1629-1636.

RAEYMAEKERS, L., WUYTACK, F., BATRA, S. & CASTEELS, R. (1977). A comparative study of the calcium accumulation by mitochondria and microsomes isolated from the smooth muscle of the guinea-pig taenia coli. *Pflugers Arch.* **368**, 217-223.

RUMESSEN, J. J., MIKKELSEN, H. B., QVORTRUP, K. & THUNEBERG, L. (1993). Ultrastructure of interstitial cells of Cajal in circular muscle of human small intestine. *Gastroenterology* **104**, 343-350.

RUMESSEN, J. J. & THUNEBERG, L. (1991). Interstitial cells of Cajal in human small intestine. Ultrastructural identification and organization between the main smooth muscle layers. *Gastroenterology* **100**, 1417-1431.

RUSKO, J., BOLTON, T. B., AARONSON, P. & BAUER, V. (1990). Effects of phenylephrine in single isolated smooth muscle cells of rabbit and guinea pig taenia caeci. *European Journal of Pharmacology* **184**, 325-328.

SANDERS, K. M. (1996). A case for interstitial cells of Cajal as pacemakers and mediators of neurotransmission in the gastrointestinal tract. [Review]. *Gastroenterology* **111**, 492-515.

SANDERS, K. M., STEVENS, R., BURKE, E. & WARD, S. W. (1990). Slow waves actively propagate at submucosal surface of circular layer in canine colon. *American Journal of Physiology* **259**, G258-G263.

SERIO, R., HUIZINGA, J. D., BARAJAS-LOPEZ, C. & DANIEL, E. E. (1990). Interstitial cells of Cajal and slow wave generation in canine colonic circular muscle. *Journal of the Autonomic Nervous System* **30 Suppl**, S141-S143.

SIMS, S. M. (1992). Cholinergic activation of a non-selective cation current in canine gastric smooth muscle is associated with contraction. *Journal of Physiology - London* **449**, 377-398.

SMITH, T. K., REED, J. B. & SANDERS, K. M. (1987). Interaction of two electrical pacemakers in muscularis of canine proximal colon. *American Journal of Physiology* **252**, C290-C299.

SMITH, T. K., REED, J. B. & SANDERS, K. M. (1989). Electrical pacemakers of canine proximal colon are functionally innervated by inhibitory motor neurons. *American Journal of Physiology* **256**, C466-C477.

THUNEBERG, L., JOHANSEN, V., RUMESSEN, J. J. & ANDERSEN, B. G. (1983). Interstitial Cells of Cajal: Selective Uptake of Methylene Blue Inhibits Slow Wave Activity. In *Gastrointestinal Motility*, ed. ROMAN, C. pp. 495-502. Lancaster: MTP Press Limited.

THUNEBERG, L., RUMESSEN, J. J. & MIKKELSEN, H. B. (1982). Interstitial cells of Cajal - an intestinal impulse generation and conduction system? *Scandinavian Journal of Gastroenterology - Supplement* **71**, 143-144.

TOKUTOMI, N., MAEDA, H., TOKUTOMI, Y., SATO, D., SUGITA, M., NISHIKAWA, S., NISHIKAWA, S. I., NAKAO, J., IMAMURA, T. & NISHI, K. (1995). Rhythmic $Cl^-$ current and physiological roles of the intestinal c-kit positive cells. *Pflügers Archiv - European Journal of Physiology* **431**, 169-177.

WARD, S. M., KELLER, R. G. & SANDERS, K. M. (1991). Structure and organization of electrical activity of canine distal colon. *American Journal of Physiology* **260**, G724-G735.

WARD, S. M. & SANDERS, K. M. (1990). Pacemaker activity in septal structures of canine colonic circular muscle. *American Journal of Physiology* **259**, G264-G273.

ZHOLOS, A. V., BAIDAN, L. V. & SHUBA, M. F. (1991). Properties of the late transient outward current in isolated intestinal smooth muscle cells of the guinea-pig. *Journal of Physiology - London* **443**, 555-574.

## 7.6 Publications


1. THOMSEN, L., T.L. ROBINSON, J.C.F. LEE, L. FARRAWAY, M.J.G. HUGHES, D.W. ANDREWS, AND J.D. HUIZINGA. Interstitial cells of Cajal generate a rhythmic pacemaker current. *Nat.Med.* 4: 848-851, 1998. (Chapter 3)
2. LEE, J.C.F., L. THUNEBERG, I. BEREZIN, AND J.D. HUIZINGA. The generation of slow waves in membrane potential is an intrinsic property of interstitial cells of Cajal. *Am.J.Physiol.* 1999. In Press. (Chapter 2)
3. LEE, J.C.F., C. BARAJAS-LÓPEZ, AND J.D. HUIZINGA. Characterization of transient outward currents in smooth muscle cells of the mouse small intestine. *Am.J.Physiol.* Submitted. (Chapter 5)
4. MOLLEMAN, A., S. SIMS, J.C.F. LEE, AND J.D. HUIZINGA. Ion channels involved in gastrointestinal action potential generation. In: *Pacemaker Activity and Intercellular Communication*, edited by J.D. Huizinga. CRC Press: Baton Rouge, 1995, p. 223-236.
5. HUIZINGA, J.D., L.W.C. LIU, J. MALYSZ, J.C.F. LEE, S. DAS, AND L. FARRAWAY. Interstitial cells of Cajal as pacemaker cells of the gut. In: *Smooth muscle excitation*, edited by T. Bolton and T. Tomita. Academic Press Ltd., 1996, p. 427-435.
6. LEE J.C.F. AND J.D. HUIZINGA. Smooth muscle heterogeneity in the mouse small intestine. *Can.J.Phys.Pharm.* Submitted. (Chapter 4)